SPACE, TELECOMMUNICATIONS AND RADIOSCIENCE LABORATORY

STARLAB
DEPARTMENT OF ELECTRICAL ENGINEERING
STANFORD UNIVERSITY • STANFORD, CA 94305

Diurnal Variations of Globally Measured ELF/VLF Radio Noise

by

D. A. Chrissan
A. C. Fraser-Smith

Technical Report D177-2

July 1997

Sponsored by
The Office of Naval Research
through
Grants No. N00014-92-J-1576 and No. N00014-93-1-1073

UNCLASSIFIED

SECURITY CLASSIFICATION OF THIS PAGE *(When Data Entered)*

REPORT DOCUMENTATION PAGE

READ INSTRUCTIONS BEFORE COMPLETING FORM

1. REPORT NUMBER: D 177-2	2. GOVT ACCESSION NO.
3. RECIPIENT'S CATALOG NUMBER	
4. TITLE *(and Subtitle)*: Diurnal Variations of Globally Measured ELF/VLF Radio Noise	5. TYPE OF REPORT & PERIOD COVERED: TECHNICAL
	6. PERFORMING ORG. REPORT NUMBER
7. AUTHOR(s): D.A. CHRISSAN and A.C. FRASER-SMITH	8. CONTRACT OR GRANT NUMBER(s): GRANT No. N00014-92-J-1576 GRANT No. N00014-93-1-1073
9. PERFORMING ORGANIZATION NAME AND ADDRESS: SPACE, TELECOMMUNICATIONS AND RADIOSCIENCE LAB. DURAND BUILDING, STANFORD UNIVERSITY, 94305-9515	10. PROGRAM ELEMENT, PROJECT, TASK AREA & WORK UNIT NUMBERS
11. CONTROLLING OFFICE NAME AND ADDRESS: OFFICE OF NAVAL RESEARCH, CODE 321SR 800 QUINCY STREET ARLINGTON, VA 22217	12. REPORT DATE: JULY 1997
	13. NUMBER OF PAGES
14. MONITORING AGENCY NAME & ADDRESS*(if different from Controlling Office)*	15. SECURITY CLASS. *(of this report)*: UNCLASSIFIED
	15a. DECLASSIFICATION/DOWNGRADING SCHEDULE

16. DISTRIBUTION STATEMENT *(of this Report)*

DISTRIBUTION UNLIMITED, APPROVED FOR PUBLIC RELEASE AND SALE.

17. DISTRIBUTION STATEMENT *(of the abstract entered in Block 20, if different from Report)*

18. SUPPLEMENTARY NOTES

19. KEY WORDS *(Continue on reverse side if necessary and identify by block number)*

ELF NOISE	GLOBAL NOISE MEASUREMENTS	HISS
VLF NOISE	RADIO NOISE MEASUREMENTS	
SFERICS	LONG-TERM NOISE MEASUREMENTS	
CHORUS	SEASONAL VARIATIONS	

20. ABSTRACT *(Continue on reverse side if necessary and identify by block number)*

THE SPACE, TELECOMMUNICATIONS AND RADIOSCIENCE (STAR) LABORATORY AT STANFORD HAS BEEN CONDUCTING A GLOBAL SURVEY OF EXTREMELY-LOW FREQUENCY (ELF) AND VERY-LOW FREQUENCY (VLF) RADIO NOISE SINCE FEBRUARY 1985. EIGHT MEASUREMENT STATIONS AROUND THE WORLD RECORD THE INSTANTANEOUS NOISE AMPLITUDE IN EACH OF SIXTEEN NARROW FREQUENCY BANDS IN THE 10 HZ - 32 KHZ FREQUENCY RANGE, AND THIS REPORT PRESENTS CALCULATIONS OF THE LONG-TERM DIURNAL VARIATIONS OF THESE AMPLITUDES FOR THE FOUR STATIONS WITH THE LONGEST TIMES OF OPERATION.

(over)

DD FORM 1 JAN 73 1473 EDITION OF 1 NOV 65 IS OBSOLETE
S/N 0102-LF-014-6601

UNCLASSIFIED

SECURITY CLASSIFICATION OF THIS PAGE *(When Data Entered)*

FOR A GIVEN MONTH AND STATION, THE DIURNAL VARIATIONS OF ALL THE DAYS IN THAT MONTH ARE AVERAGED TOGETHER, THEN THE RESULTING MONTHLY DIURNAL VARIATIONS ARE AVERAGED BY MONTH OVER SUBSEQUENT YEARS. THESE CALCULATIONS PROVIDE THE LONG-TERM AVERAGES OF THE DIURNAL VARIATIONS OF ELF/VLF NOISE FOR EACH MONTH AND CHANNEL AND AT EACH LOCATION. SINCE THE PRINCIPAL SOURCE OF ELF/VLF RADIO NOISE IS LIGHTNING IN THUNDERSTORMS, AND THE VARIOUS THUNDERSTORM CENTERS AROUND THE GLOBE HAVE SPECIFIC DIURNAL SIGNATURES, THESE DATA HELP DETERMINE SOURCE LOCATIONS OF THE SFERICS THAT CONTRIBUTE TO A GIVEN STATION'S RECEIVED RADIO NOISE. IN ADDITION, SINCE THE PLOTS ARE BY MONTH, THEY AID IN TRACKING THE GLOBAL SHIFTS IN SOURCE DISTRIBUTION THROUGHOUT THE YEAR.

Diurnal Variations of Globally Measured ELF/VLF Radio Noise

by

D. A. Chrissan and A. C. Fraser-Smith

Technical Report D177-2

July 1997

Sponsored by

The Office of Naval Research

Grants No. N00014-92-J-1576 and No. N00014-93-1-1073

Abstract

The Space, Telecommunications and Radioscience (STAR) Laboratory at Stanford has been conducting a global survey of extremely-low frequency (ELF) and very-low frequency (VLF) radio noise since February 1985. Eight measurement stations around the world record the instantaneous noise amplitude in each of sixteen narrow frequency bands in the 10 Hz – 32 kHz frequency range, and this report presents calculations of the long-term diurnal variations of these amplitudes for the four stations with the longest times of operation.

For a given month and station, the diurnal variations of all the days in that month are averaged together, then the resulting monthly diurnal variations are averaged by month over subsequent years. These calculations provide the long-term averages of the diurnal variations of ELF/VLF noise for each month and channel at each location. Since the principal source of ELF/VLF radio noise is lightning in thunderstorms, and the various thunderstorm centers around the globe have specific diurnal signatures, these data help determine source locations of the sferics that contribute to a given station's received radio noise. In addition, since the plots are by month, they aid in tracking the global shifts in source distribution throughout the year.

Contents

1 Introduction

During the years 1985-1986, eight ELF/VLF (10 Hz – 32 kHz) radio noise measurement systems, or radiometers, were installed at a variety of high-latitude and mid-latitude sites in an effort to fill large gaps in the information available on radio noise in this frequency range. Most of the stations operated much longer than original program expectations, and this longevity allows us to examine diurnal trends over the course of many years. A number of other ELF/VLF measurement systems have been implemented in the past, but this is the only system of its kind in terms of its geographic coverage and continuity of simultaneous data collection.

The radiometers were primarily developed to obtain new information in support of defense communications and radio navigation systems, and to this end the data have been used to develop long range ELF/VLF noise prediction models [*Warber and Field,* 1995]. However, the data have also found use in geophysical and environmental analyses, such as to study polar region events (auroral hiss and polar chorus) and the effects of solar particle events [*Fraser-Smith and Turtle,* 1993], to define the natural background noise levels at power line frequencies for comparison with those levels created by man-made power generation and distribution systems around the world [*Fraser-Smith and Bowen,* 1992], and to relate long term variations in ELF/VLF noise to seasonal weather patterns and global climate change [*Füllekrug and Fraser-Smith,* 1997].

It is this last context in which we present the data in this paper. Radio noise at ELF/VLF frequencies is caused primarily by lightning occurring throughout the world, so the noise levels can be used to study global climate change and the propagation characteristics of the electromagnetic impulses, or sferics, radiated by the various lightning sources. Four of the radiometers — Arrival Heights, Antarctica (AH; 77.8°S, 193.3°W); Dunedin, New Zealand (DU; 45.8°S, 189.5°W); Søndrestromfjørd, Greenland (SS; 67.0°N, 50.1°W); and Stanford, California (SU; 37.4°N, 122.2°W) — have provided enough good, long term data to justify a long-term diurnal variation analysis. Fortunately these four stations cover mid- and high-latitude locations in both the northern and southern hemispheres. The other four stations (Grafton, New Hampshire; Thule, Greenland; Kochi, Japan; and L'Aquila, Italy) were either in operation for too short a time, had too many data gaps, or were too contaminated by man-made interference to provide long term averages of naturally occurring noise. The systems at Stanford and Arrival Heights

are continuing to collect data; the former has been in operation for eleven years and the latter for twelve. They should be able to collect data beyond one solar cycle.

Diurnal variations of ELF/VLF radio noise are presented by month. For a given month and station, the diurnal variations of all the days in that month are averaged together for each year, then these resulting monthly diurnal variations are averaged by month over subsequent years. This results in one plot per station, month and channel, for a total of 768 individual plots. Since the principal source of ELF/VLF radio noise is lightning in thunderstorms [*Watt and Maxwell,* 1957], and the various thunderstorm centers around the globe have specific diurnal signatures, these data help determine source locations of the sferics that contribute to a given station's received radio noise. In addition, since the plots are by month, they aid in tracking the global shifts in source distribution throughout the year.

2 Radiometer System Description

A complete technical description of the radiometers used for the radio noise survey has been provided elsewhere [*Fraser-Smith and Helliwell,* 1985], so we give only an overview as it pertains to the data being presented. Each radiometer contains two receivers, one for the 10–400 Hz frequency range (which we designate ELF in this communication) and the other for the 400 Hz – 32 kHz frequency range (designated VLF). Each receiver has its own pair of crossed loop antennas, one oriented in the N-S geomagnetic direction and the other in the E-W geomagnetic direction. The ELF antennas are 1164 turn coils which are either buried or enclosed in order to prevent noise due to wind induced motion of the coils in the earth's magnetic field. The VLF antennas are single-turn triangular above-ground loops 18m wide and 9m high.

Time series recordings are made of both the ELF and VLF receiver outputs, but only for one minute every hour. In addition to these time series recordings, continuous data collection is obtained by monitoring the outputs of a bank of sixteen narrowband channel filters with center frequencies distributed roughly logarithmically across the 10 Hz – 32 kHz band. Each of the 32 filters (the N-S and E-W loops must be filtered separately) is a six pole Chebychev bandpass filter with a two sided bandwidth equal to five percent of the center frequency. The sixteen center frequencies and bandwidths are

Channel	Frequency	Bandwidth
1	10 Hz	0.5 Hz
2	30	1.5
3	80	4
4	135	6.75
5	275	13.75
6	380	19
7	500	25
8	750 Hz	37.5
9	1 kHz	50
10	1.5	75
11	2	100
12	3	150
13	4	200
14	8	400
15	10.2	510
16	32 kHz	1600 Hz

Table 1: Center frequencies and bandwidths for the 16 narrowband channels of the ELF/VLF radiometer.

contained in Table 1 – the first six are within the ELF receiver's frequency range and the last ten are within the VLF receiver's.

Each filter output is passed through an analog RMS detector which squares the input, performs a time average, and outputs the square root of the average. The RMS detector output is then sampled at a rate of ten times per second by an analog to digital converter and sent to a digital computer, which computes the root-sum-square of the N-S and E-W detector outputs to determine the RMS amplitude of the horizontal component of magnetic field for each channel. The analog to digital convertors have a useful dynamic range of 70 dB, but switchable gain amplifiers in the analog receiver circuitry increase the total system dynamic range to 100 dB.

In order to save digital tape space, the computer writes out only every tenth sample. However, it also stores the average and RMS values for each minute (600 samples), along with the minimum and maximum of the 600 values for that minute. The measurements reported here are derived from these one-minute average amplitudes.

3 ELF/VLF Noise Measurements

To provide a basic context for our ELF/VLF noise amplitude measurements, Figure 1 shows the one hour average noise amplitudes over the course of one month for one channel, the 10 Hz band measured at Arrival Heights during the month of June 1994. Each of the 720 points on this graph is an average of roughly 32,000 noise filter output samples (not 36,000 because of calibration periods). The data consist of both random and diurnal variations; they sometimes show occasional short duration impulses due to both man made and natural interference as well. The entire database contains thousands of these plots, one for each station, month and channel.

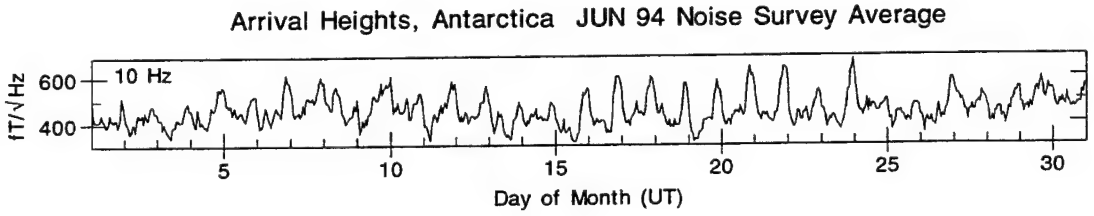

Figure 1: Noise averages in the 10 Hz frequency band recorded June, 1994, at Arrival Heights, Antarctica. Each of the 720 points on this plot is an average of one hour of data.

The unit $\mathrm{fT}/\sqrt{\mathrm{Hz}}$ is essentially the square root of power spectral density, obtained in this case by dividing the RMS filter amplitude output (in fT) by 0.707, the square root of the 0.5 Hz bandwidth for the 10 Hz channel filter. We present the data in fT because our system detects magnetic field. The vertical electric field component and/or the power of the incoming signal may be obtained using 377 Ω as the impedance of free space, but this is an approximation (albeit usually a good one) that assumes the impinging electromagnetic waves are planar. To convert to electric field under this assumption, the relation $B = \sqrt{\mu_0 \epsilon_0} E = E/c$ may be used to determine that 1fT is equivalent to $0.300 \mu\mathrm{V/m}$. If it is desired to relate magnetic field (or magnetic flux density) B to magnetic intensity H, the relation $B = \mu_0 H$ can be used to find that 1fT is equivalent to $7.958 \times 10^{-4} \mu\mathrm{A/m}$.

Determining the diurnal variations of natural radio noise over the course of many years requires three steps: (1) each day is divided into 12 two hour time blocks, the first being 00:00-01:59 UT and the last being 22:00-23:59 UT, (2) for each time block, all the days of a given month during a given year are averaged together, and (3) all the years are then averaged together by month, resulting in an overall diurnal variation for each month at each station and for each of the sixteen frequency bands.

We wish to include only natural radio noise, so it is necessary to eliminate data corrupted by instrumentation problems, physical movement of the coils or man-made interference. Down-time and instrumentation problems are either reported by the system itself or detected by examining the data in the form of Figure 1. Sometimes individual channels are eliminated if hardware failures in those channels are detected; other times all the ELF or VLF channels must be removed. Another problem occurs occasionally: huge increases in levels of the ELF channels due to movement of the coils from local construction or agriculture, in which case the ELF channels only are neglected. The end result is that some months have a reduced number of samples and other months are missing altogether; however, there are no cases where this has a significant effect on the diurnal variations presented. It is of note that the 10.2 kHz band at each station is contaminated to some degree by Omega navigation signals. In addition, the 32 kHz band at Stanford is known to be contaminated by man-made noise.

4 Data Analysis

Figures 2 to 97 collectively show diurnal variations of the noise level for all months and channels at the four different stations. The error bars indicate the standard deviations from year to year, *i.e.*, small error bars indicate little variation from one year to the next in the diurnal cycle of a particular month. Note that the error bars are largely unrelated to the standard deviation of individual noise samples, which can be quite large; they are also unrelated to the standard deviation of the total average, which is minute since each point on these plots is an average of many thousands of sample values. Also note that each individual graph has its own scale.

Changes in average noise levels from year to year for each month are removed from the error bar calculations, since otherwise they would artifically enlarge the diurnal variation error bars. The normalization is performed in

three parts: (1) for each month and year, a noise average for the entire month is computed to produce a single value, (2) for each month, the resulting values from (1) for the different years are averaged together to give one total average reference value per month, and (3) all the data are normalized (by subtracting the difference between the corresponding values from parts (1) and (2)) such that differences in total monthly averages from year to year are removed, *i.e.*, each total monthly average now equals that month's reference value. Thus the error bars are truly an indication of the variation of the diurnal cycle. In most cases the error bars are small compared to their respective data, indicating little variation of diurnal cycles from year to year.

Every year for which a station collected valid data is included in the seasonal variation computation. For Arrival Heights, the years 1985 to 1994 are included; Dunedin includes 1986 to 1990; Søndrestrøm includes 1986 to 1991 and 1993; Stanford includes 1986 to 1993.

Large diurnal variations are seen in most of the frequency channels at most of the stations, but the phases of these diurnal variations can depend strongly on month, frequency, and especially station. Variation by station is primarily due to the diurnal signature of global lightning, for which it is known that lightning over North America peaks at roughly 00 UT, lightning over South America peaks at roughly 20 UT, lightning over Europe and Africa peaks at roughly 16 UT, and lightning over Southeast Asia peaks at roughly 08 UT [*Füllekrug and Fraser-Smith,* 1997, *Goodman and Christian,* 1993]. The differences in diurnal variations with respect to frequency can be attributed to different patterns in local and distant lightning, with the higher frequency variations being influenced more strongly by closer sources. Differences from month to month are due to seasonal variations of global lightning distributions, for which it is known that southern hemisphere locations are generally more active in the northern hemisphere winter and northern hemisphere locations are generally more active in the northern hemisphere summer [*Chrissan and Fraser-Smith,* 1996, *Goodman and Christian,* 1993].

In the range 1 – 3 kHz, at all the stations, the error bars are often too large relative to the data to extract a statistically significant diurnal variation. These frequency bands are within the range of the earth-ionosphere waveguide cutoff frequencies, where noise does not propagate far and the receiver predominantly picks up the fields from local sources. Radio noise falls off roughly as f^{-1} up to 2 – 3 kHz, rises up to 10 kHz, then decreases again throughout the VLF range [*Lanzerotti et al.,* 1990]. Propagation mode changes account for the 2 – 10 kHz effect, but otherwise radio noise propa-

gates with greater attenuation at higher frequencies so distant sources contribute less.

Arrival Heights (at $77.8°S$ latitude) sees roughly equal contributions from storms at all longitudes at the lowest frequencies. The lowest frequencies thus exhibit a diurnal pattern in phase with the overall worldwide distribution, a broad peak from 14-22 UT. From June to September, however, the peak shifts to roughly 22 UT, indicating a strong contribution from American storms [*Füllekrug and Fraser-Smith,* 1997]. The higher frequencies at Arrival heights have a broad peak near 12 UT, due to a greater influence from storms across Asia. (The Arrival Heights site is on the edge of the Antarctic continent closest to New Zealand.)

The Dunedin, New Zealand, data have relatively large error bars at the lowest frequencies except during the northern hemisphere summer, when a peak at 00 UT occurs, again indicating a strong contribution from American storms. Diurnal variations of the higher frequencies at Dunedin are in phase with those at Arrival Heights. These two southern hemisphere sites are affected both by the locality of southern hemisphere storm patterns (Dunedin from the Australian continent and Southeast Asia; Arrival Heights from all of the southern hemisphere) and by the greater quantity of lightning in the northern hemisphere [*Price and Rind,* 1994].

The lowest frequencies at Søndrestrøm have diurnal variations with the same phase as the worldwide diurnal distribution of lightning for every month. Above 275 Hz, however, the data exhibit a peak in the 00 UT time range. These results are consistent with Søndrestrøm's fairly high latitude and proximity to the North American continent.

At Stanford, the diurnal variations of the lowest frequencies are similar to those at Arrival Heights: a broad peak from 14-22 UT except during the northern hemisphere summer, when the peak shifts to roughly 22 UT and becomes sharper. Above 380 Hz, however, the Stanford data exhibit a broad maximum from 04-10 UT. This phenomenon is unaccounted for; we cannot find man-made interference in the raw data which would otherwise explain it.

5 Conclusion

We have presented the diurnal variations of ELF/VLF radio noise amplitudes as calculated from several years of data taken from four sites around the

world. The characteristics of the data can be attributed to natural variations in global storm patterns, and they do not appear to be influenced by man-made interference.

The diurnal variations presented in this report do not change significantly from year to year, but they do vary seasonally for some frequencies and stations. A lack of complete supporting information on the distribution of global lightning with respect to diurnal variation, month and location precludes us from determining a physical justification for every characteristic of the data; however, the data correlate well in general with known lightning distribution results. These data thus can be used to study the seasonal and diurnal changes in thunderstorm distribution patterns.

6 Acknowledgement

This research was sponsored by the Office of Naval Research through Grants No. N00014-92-J-1576 and No. N00014-93-1-1073. Logistic support for the measurements at Søndrestromfjørd, Greenland, and Arrival Heights, Antarctica, was provided by the National Science Foundation through NSF cooperative agreement ATM 88-22560, and NSF grants DPP-8720167 and OPP-9119552, respectively. We thank Paul R. McGill for his assistance in the project, Dr. J.D. Kelly of SRI international for facilitating the measurements at Søndrestromfjørd, and Dr. N.R. Thomson of the University of Otago for his help with the Dunedin measurements.

7 References

[*Chrissan and Fraser-Smith,* 1996] Chrissan, D., and A.C. Fraser-Smith, Seasonal variations of globally measured ELF/VLF radio noise, *Radio Sci., 31*(5), 1141-1152, 1996.

[*Chrissan and Fraser-Smith,* 1996] Chrissan, D., and A.C. Fraser-Smith, Seasonal variations of globally measured ELF/VLF radio noise, *Technical Report D177-1, Space, Telecommunications and Radioscience Laboratory,* Stanford Univ., Stanford, CA, 1996.

[*Fraser-Smith and Bowen,* 1992] Fraser-Smith, A.C., and M.M. Bowen, The natural background levels of 50/60 Hz radio noise, *IEEE Trans. Elecromagn. Compat., 34,* pp. 330–337, 1992.

[*Fraser-Smith and Helliwell,* 1985] Fraser-Smith, A.C., and R.A. Helliwell, The Stanford University ELF/VLF radiometer project: measurement of the global distribution of ELF/VLF electromagnetic noise, in *Proceedings of the 1985 Internat. Symp. on Electromag. Compatibility,* Wakefield, Mass., Aug. 1985.

[*Fraser-Smith and Turtle,* 1993] Fraser-Smith, A.C., and J.P. Turtle, ELF/VLF radio noise measurements at high latitudes during solar particle events, *AGARD Conf. Proc. No. 529,* pp. 16-1–16-8, May 1993.

[*Fraser-Smith et al.,* 1988] Fraser-Smith, A.C., R.A. Helliwell, B.R. Fortnam, P.R. McGill and C.C. Teague, A new global survey of ELF/VLF radio noise, Conf. on Effects of Electromagnetic Noise and Interference on Performance of Military Radio Communi-

cation Systems, Lisbon, Portugal, 26-30 October, 1987. Published in *AGARD Conf. Proc. No. 420,* pp. 4A-1–4A-7, 1988.

[*Füllekrug and Fraser-Smith,* 1997] Füllekrug,M., and A.C. Fraser-Smith, Global lightning and climate variability inferred from ELF magnetic field variations, to appear in *Geophys. Res. Letters,* 1997.

[*Goodman and Christian,* 1993] Goodman, S.J., and H.J. Christian, Global observations of lightning, in *Atlas of Satellite Observations Related to Global Change,* (R.J. Gurney, ed.), Cambridge University Press, New York, N.Y., 1993.

[*Lanzerotti et al.,* 1990] Lanzerotti, L.J., C.G. Maclennan and A.C. Fraser-Smith, Background magnetic spectra: $\sim 10^{-5}$ to $\sim 10^{5}$ Hz, *Geophysical Research Letters*, Vol. 17, No. 10, pp. 1593–1596, 1990.

[*Price and Rind,* 1992] Price, C., and D. Rind, Simulating global lightning distributions from satellite cloud data, in *Proceedings of the 9th Int. Conf. on Atmospheric Electricity,* St. Petersburg, Russia, pp. 327–330, 1992.

[*Price and Rind,* 1994] Price, C. , and D. Rind, Possible implications of global climate change on global lightning distributions and frequencies, *Journal of Geophysical Research,* Vol. 99, No. D5, pp. 10,823–10,831, 1994.

[*Warber and Field,* 1995] Warber, C.R., and E.C. Field, Jr., A long wave transverse electric-transverse

magnetic noise prediction model, *Radio Sci., 30*(3), 783–797, 1995.

[*Watt and Maxwell,* 1957] Watt, A.D., and E.L. Maxwell, Measured Statistical Characteristics of VLF Atmospheric Radio Noise, *Proc. of the IRE, 45*, 55–62, 1957.

8 Arrival Heights, Antarctica Diurnal Variation Figures

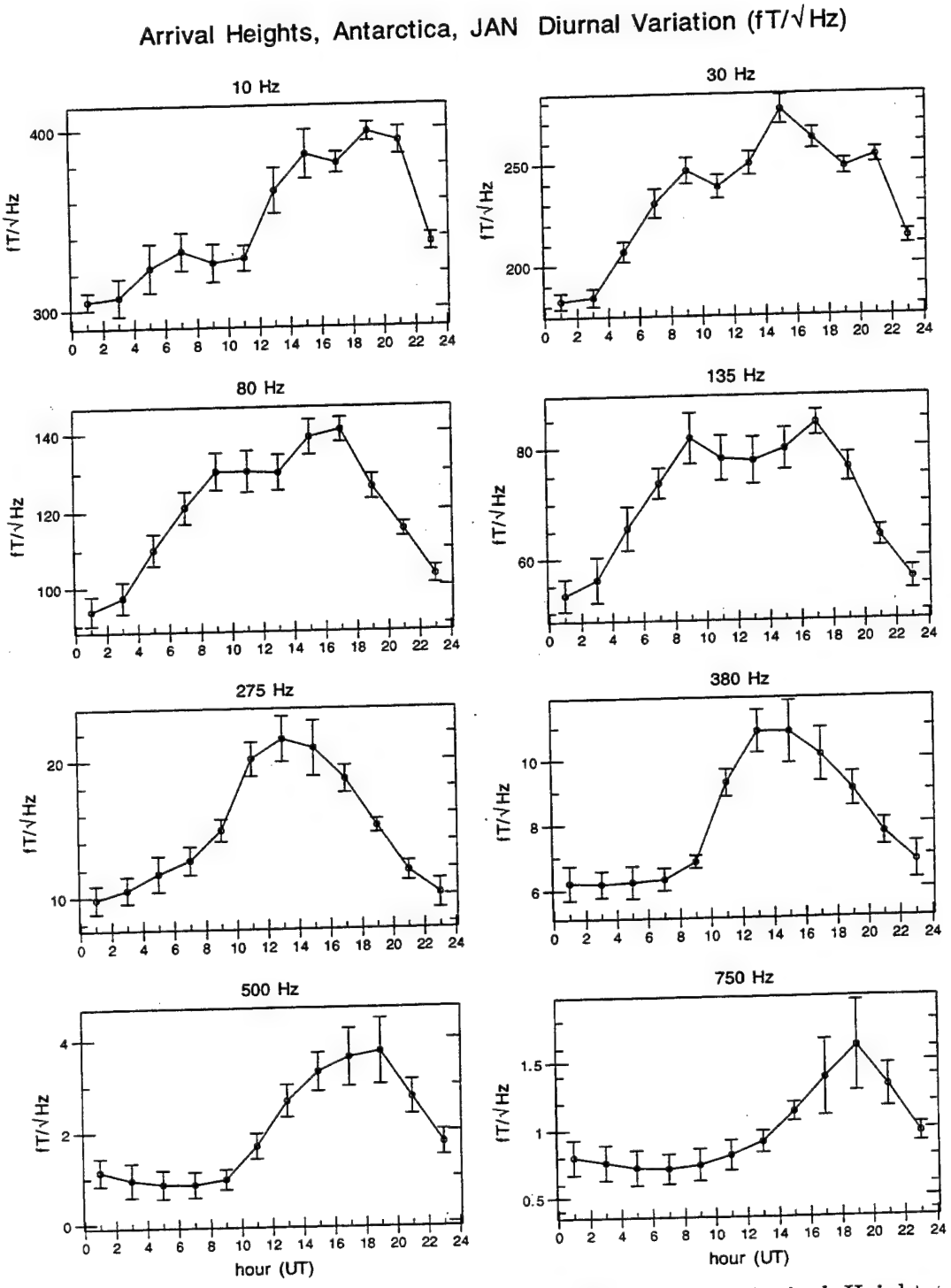

Figure 2: Diurnal variation of ELF/VLF radio noise at Arrival Heights, Antarctica, during the month of January for the eight lowest-frequency channels. The years 1985 to 1994 are included.

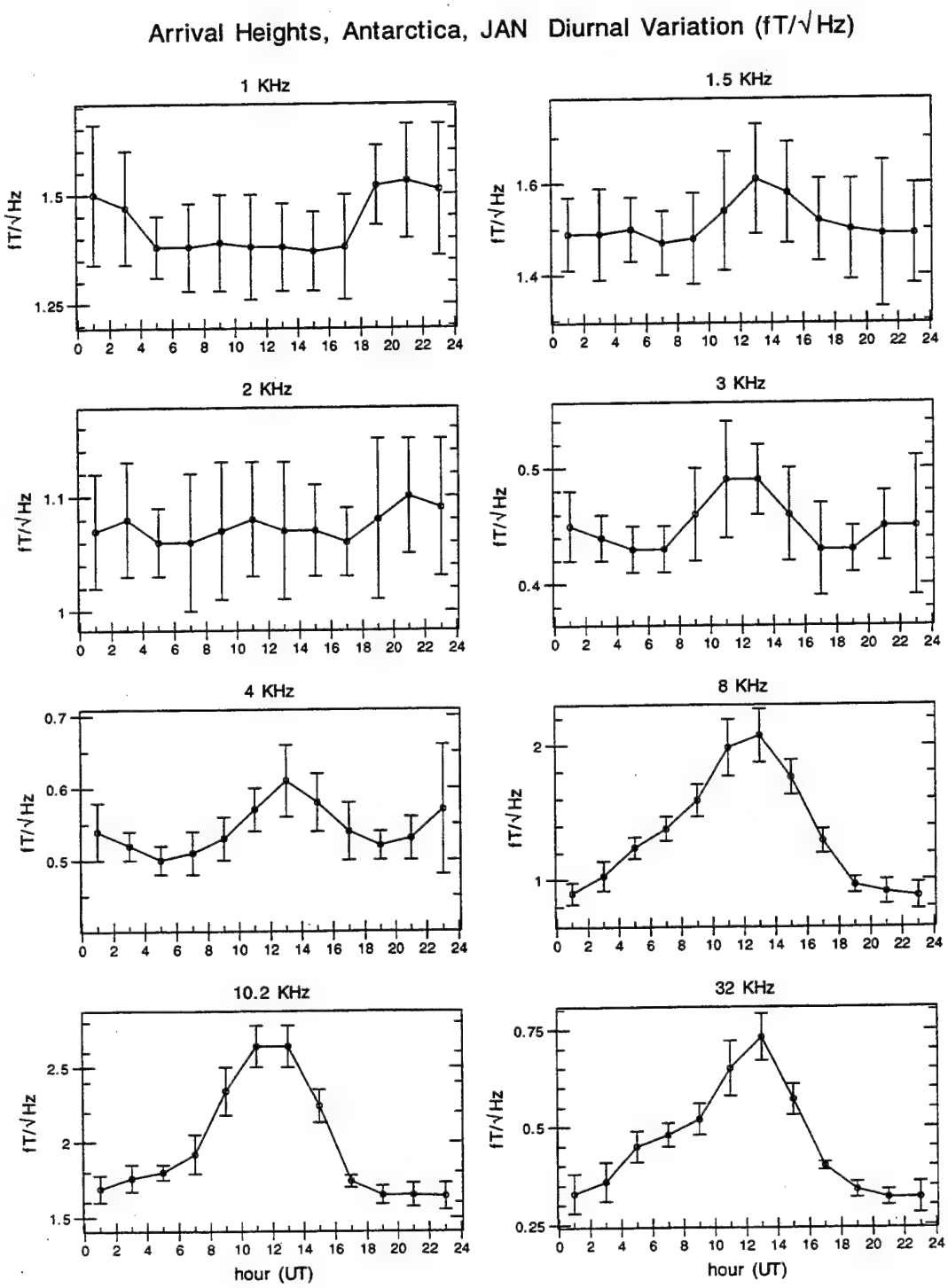

Figure 3: Diurnal variation of ELF/VLF radio noise at Arrival Heights, Antarctica, during the month of January for the eight highest-frequency channels. The years 1985 to 1994 are included.

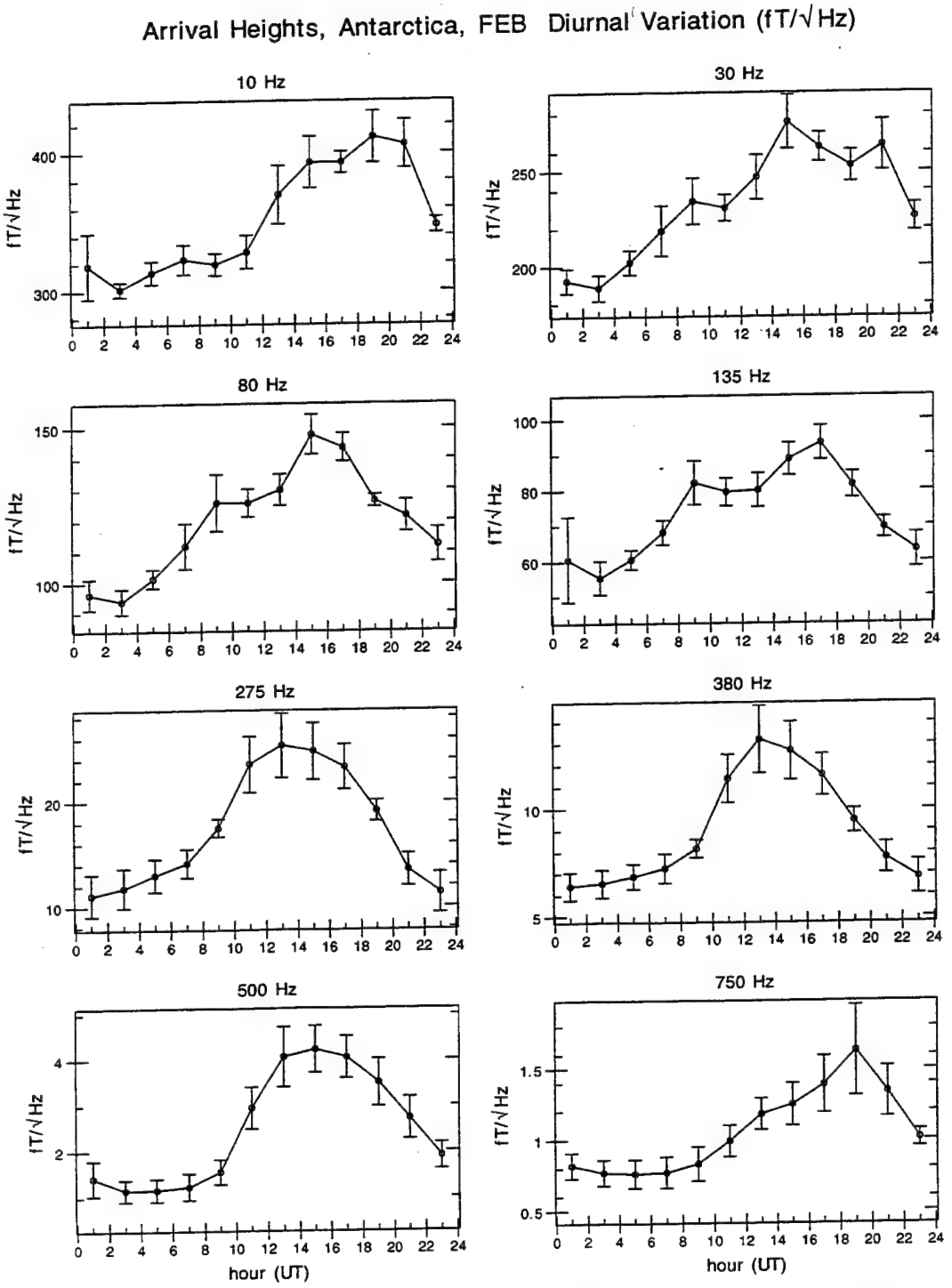

Figure 4: Diurnal variation of ELF/VLF radio noise at Arrival Heights, Antarctica, during the month of February for the eight lowest-frequency channels. The years 1985 to 1994 are included.

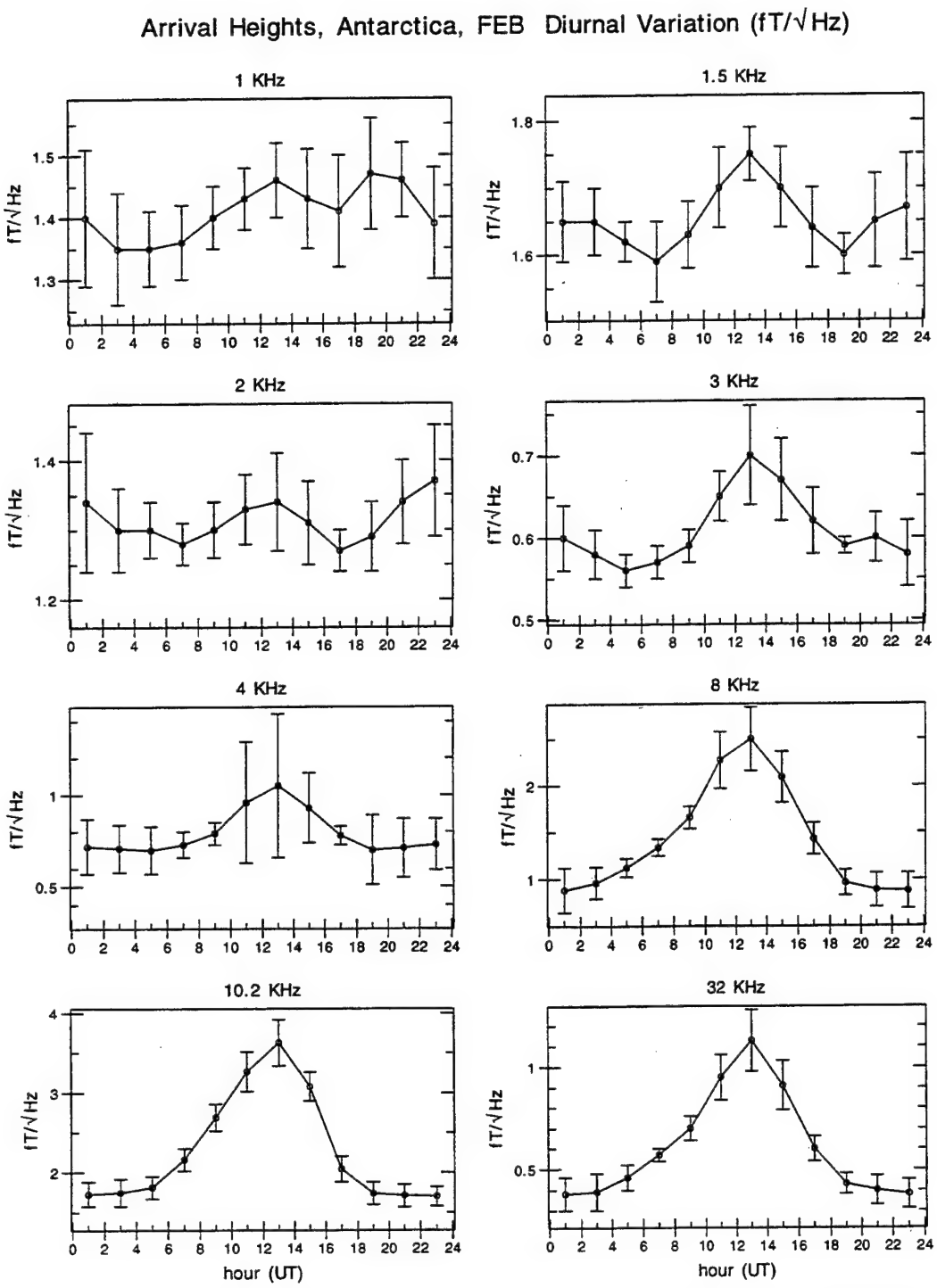

Figure 5: Diurnal variation of ELF/VLF radio noise at Arrival Heights, Antarctica, during the month of February for the eight highest-frequency channels. The years 1985 to 1994 are included.

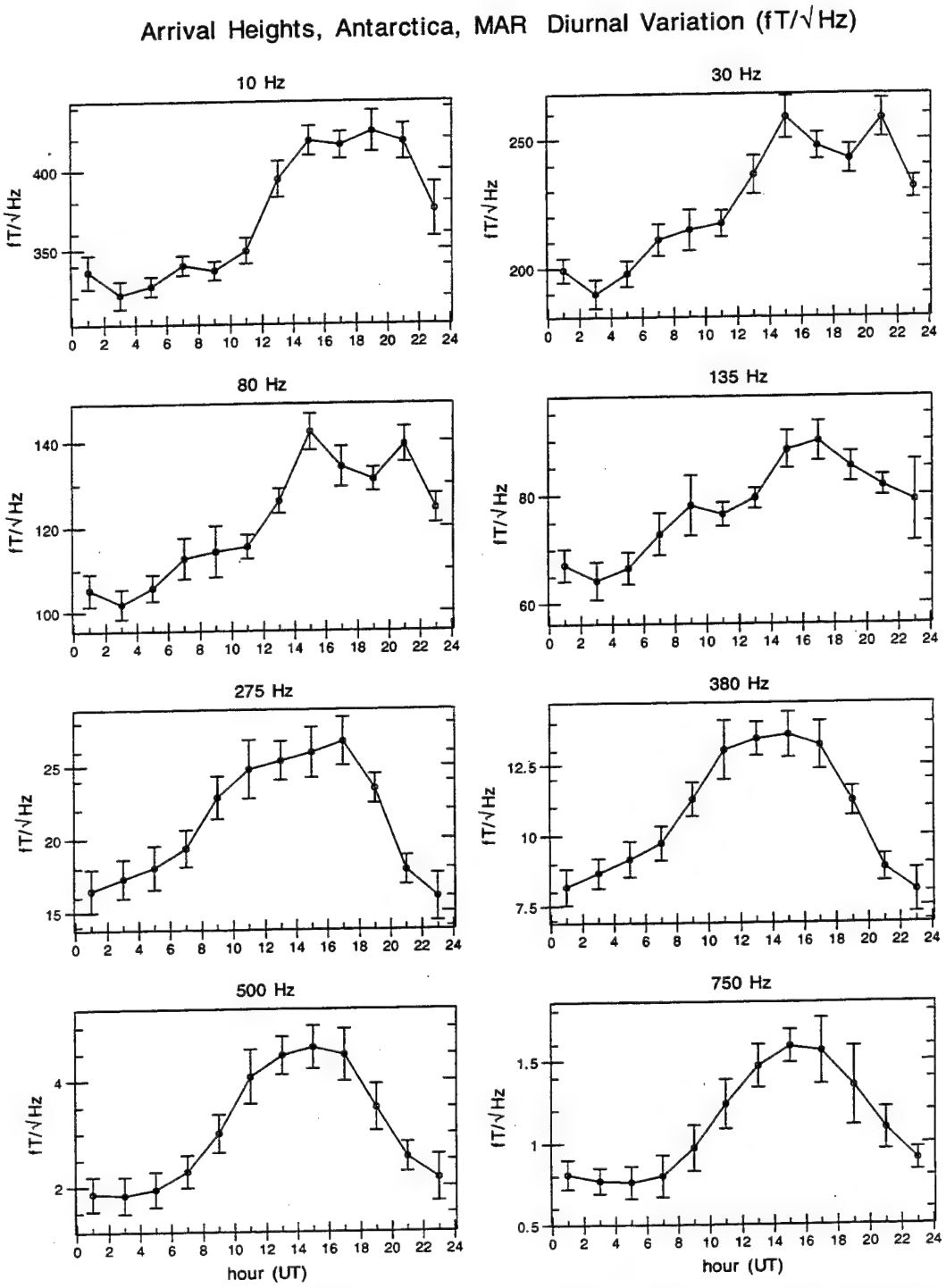

Figure 6: Diurnal variation of ELF/VLF radio noise at Arrival Heights, Antarctica, during the month of March for the eight lowest-frequency channels. The years 1985 to 1994 are included.

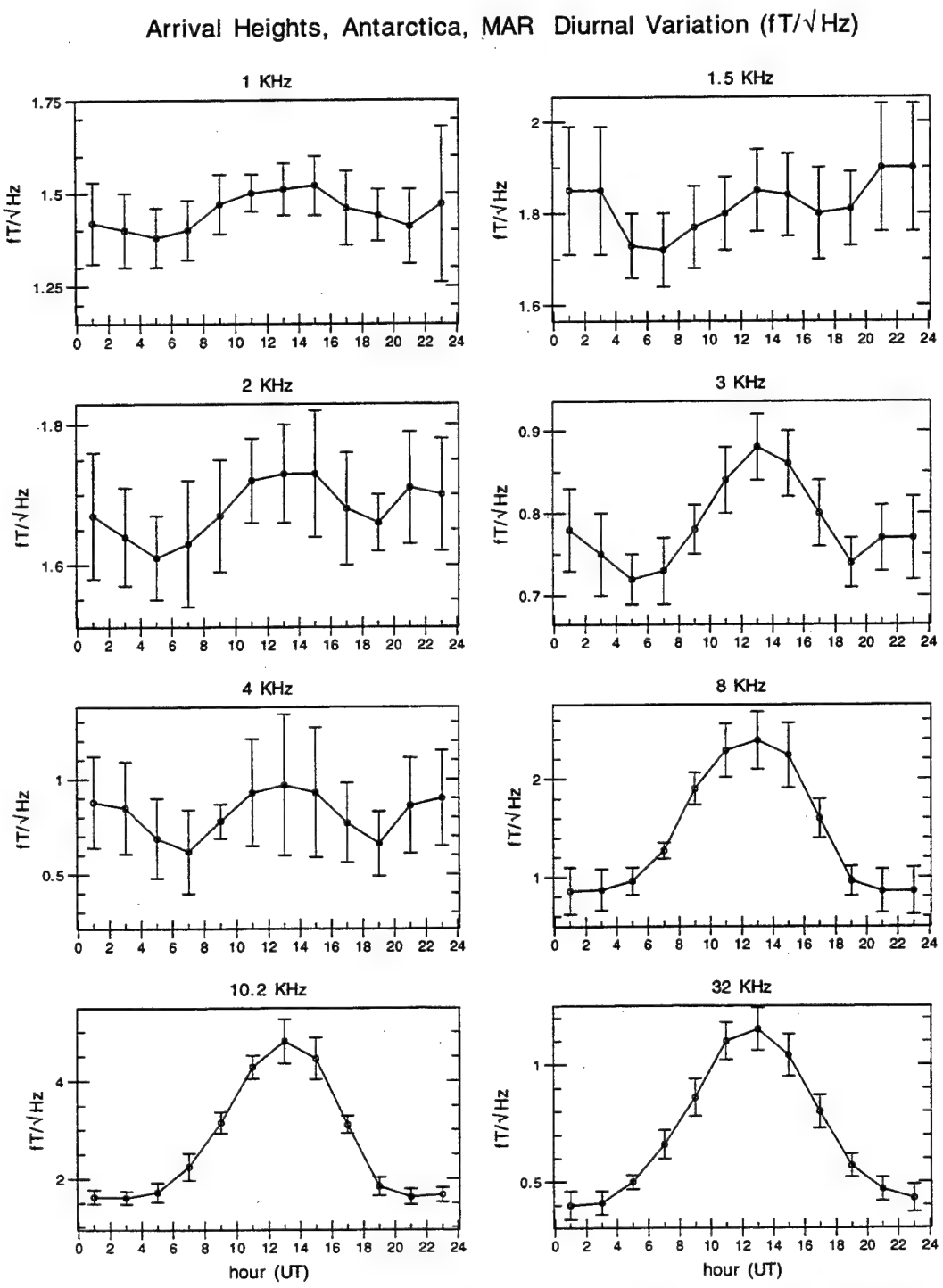

Figure 7: Diurnal variation of ELF/VLF radio noise at Arrival Heights, Antarctica, during the month of March for the eight highest-frequency channels. The years 1985 to 1994 are included.

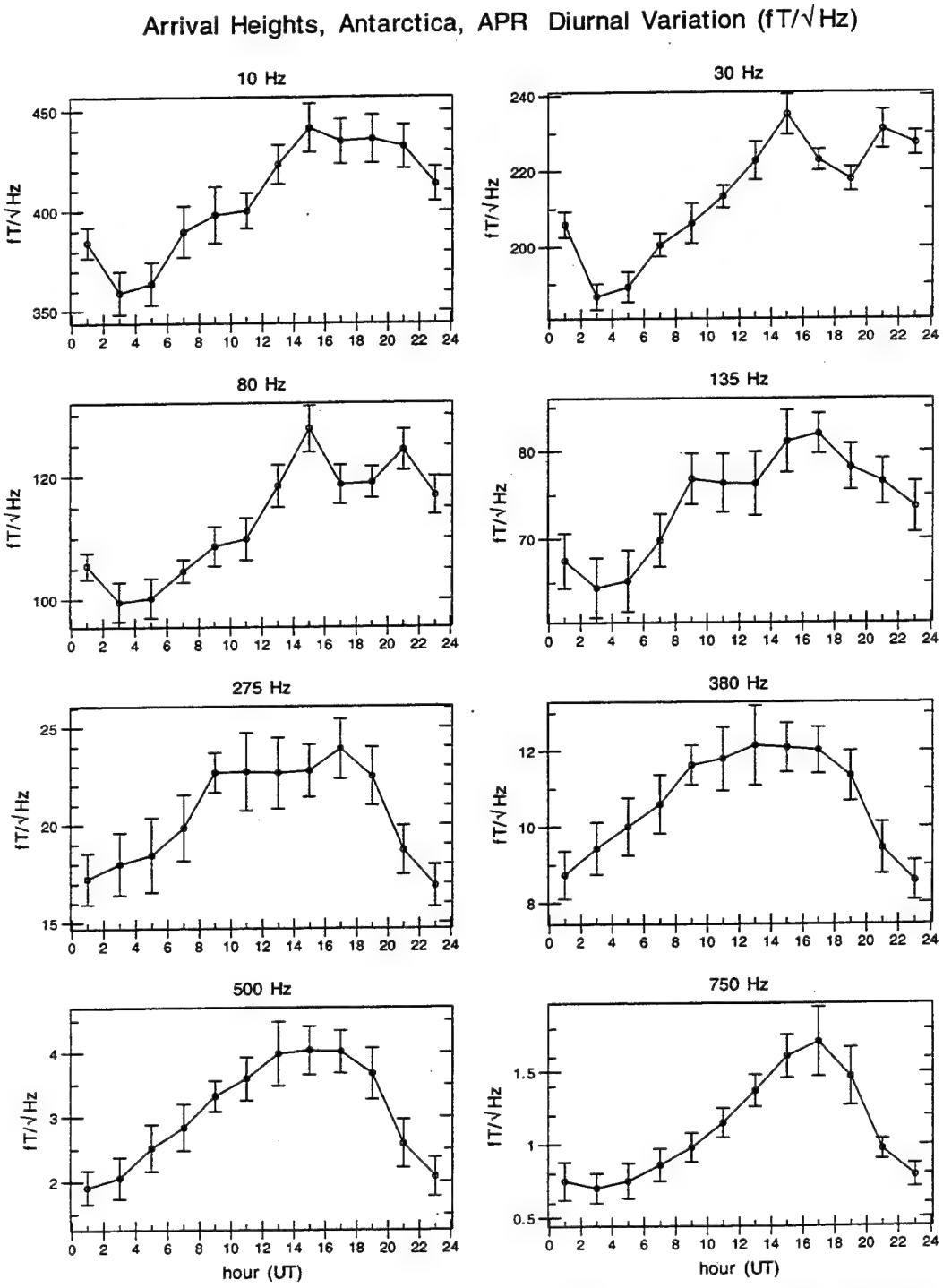

Figure 8: Diurnal variation of ELF/VLF radio noise at Arrival Heights, Antarctica, during the month of April for the eight lowest-frequency channels. The years 1985 to 1994 are included.

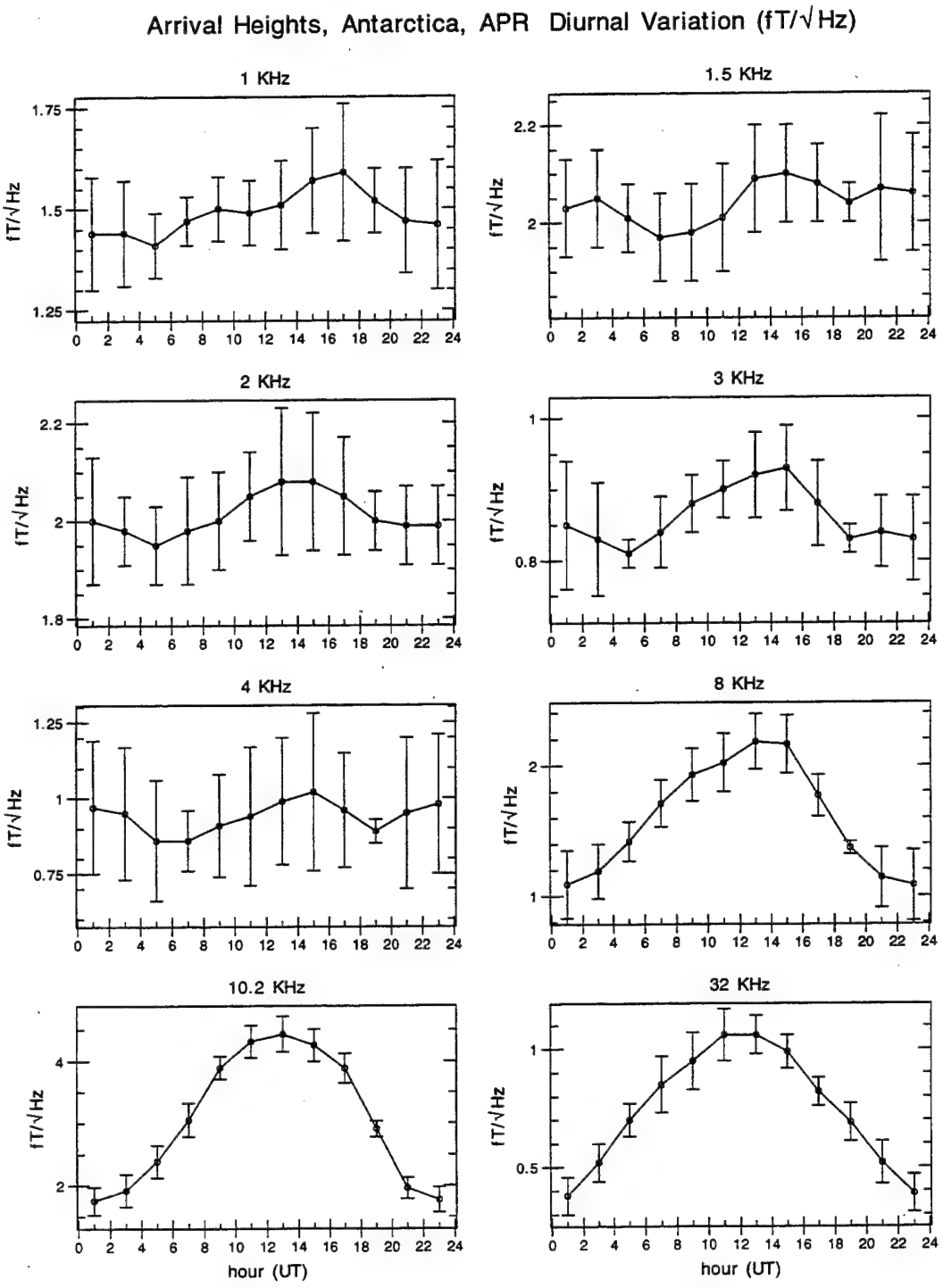

Figure 9: Diurnal variation of ELF/VLF radio noise at Arrival Heights, Antarctica, during the month of April for the eight highest-frequency channels. The years 1985 to 1994 are included.

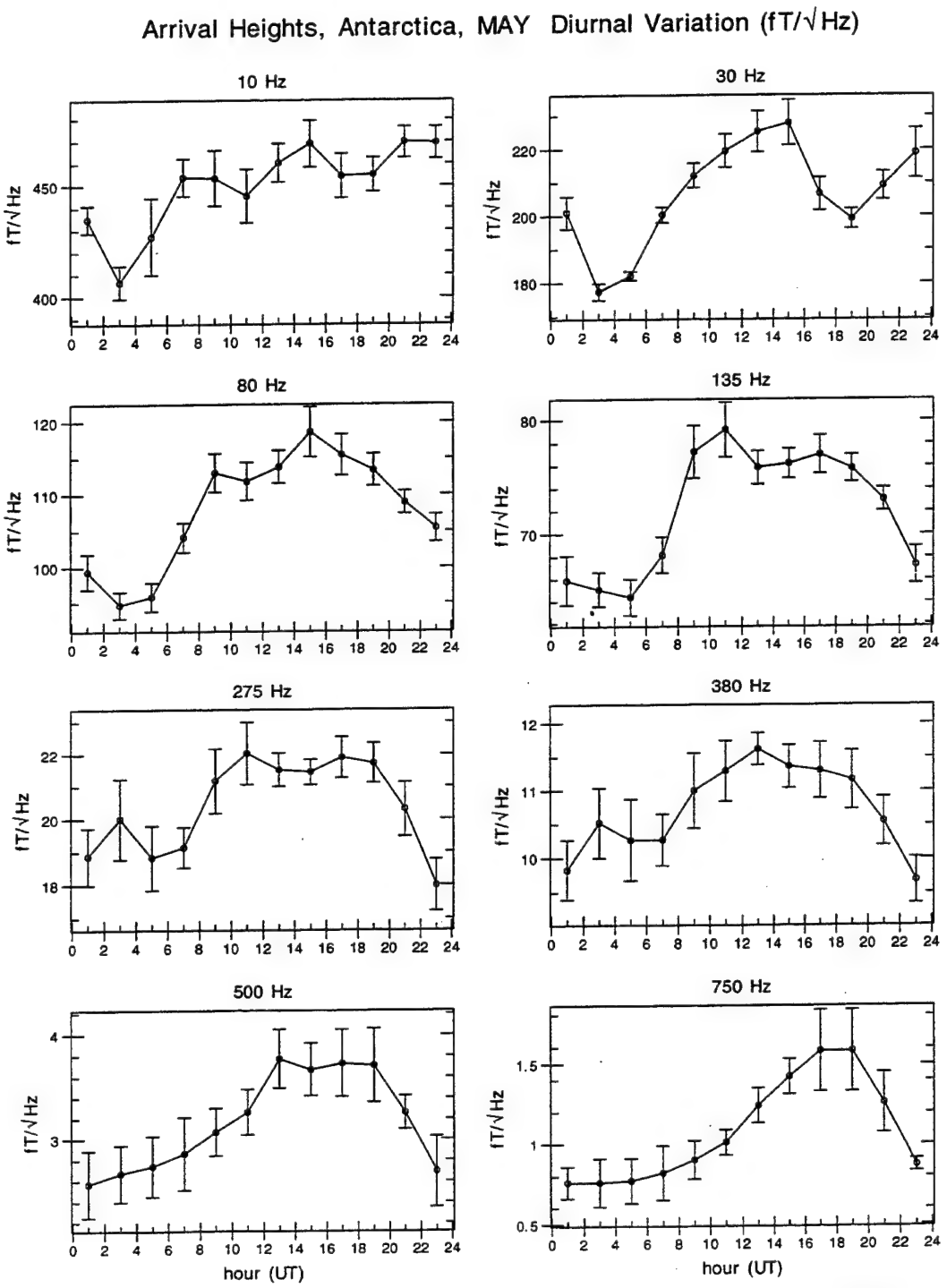

Figure 10: Diurnal variation of ELF/VLF radio noise at Arrival Heights, Antarctica, during the month of May for the eight lowest-frequency channels. The years 1985 to 1994 are included.

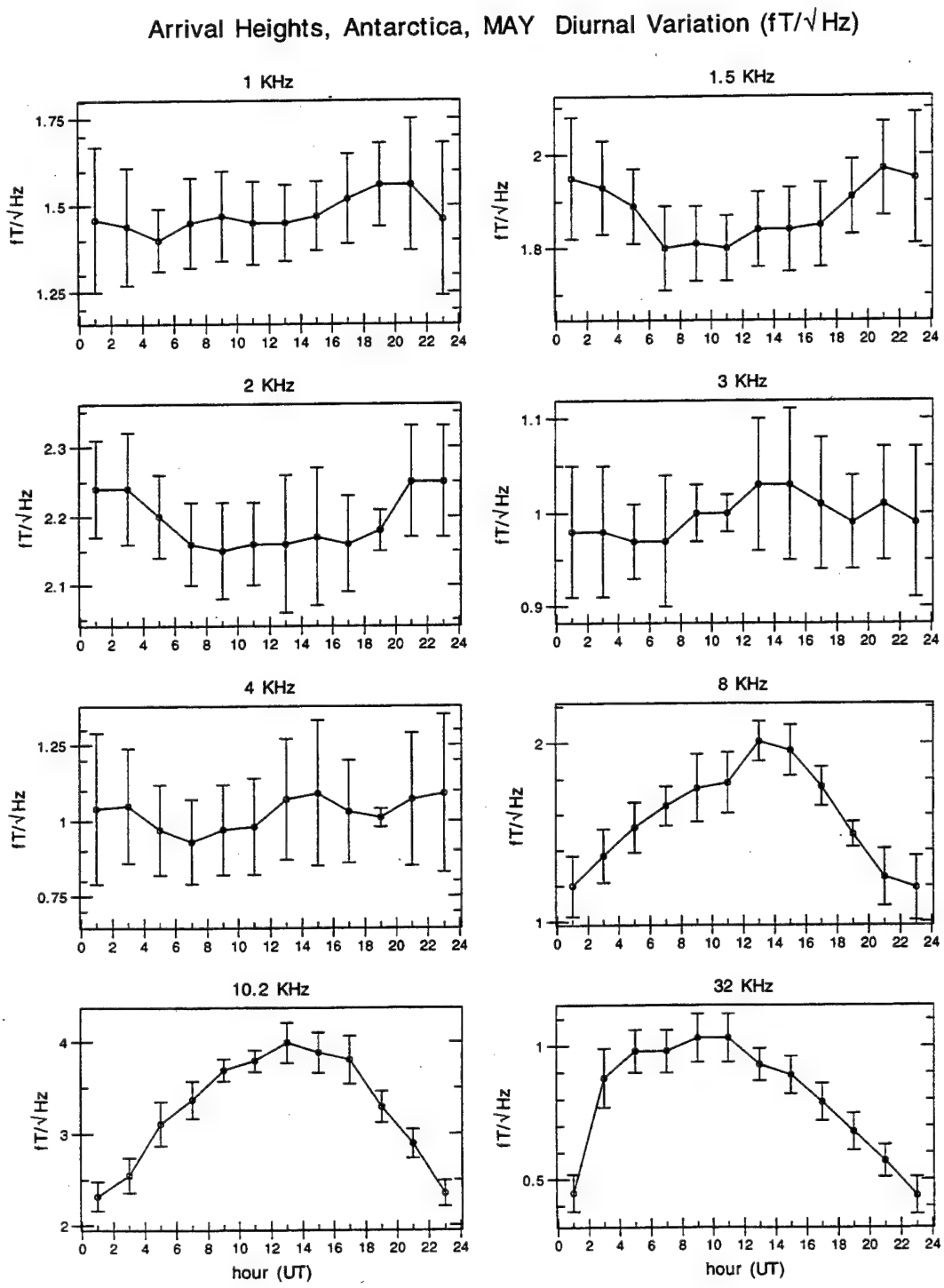

Figure 11: Diurnal variation of ELF/VLF radio noise at Arrival Heights, Antarctica, during the month of May for the eight highest-frequency channels. The years 1985 to 1994 are included.

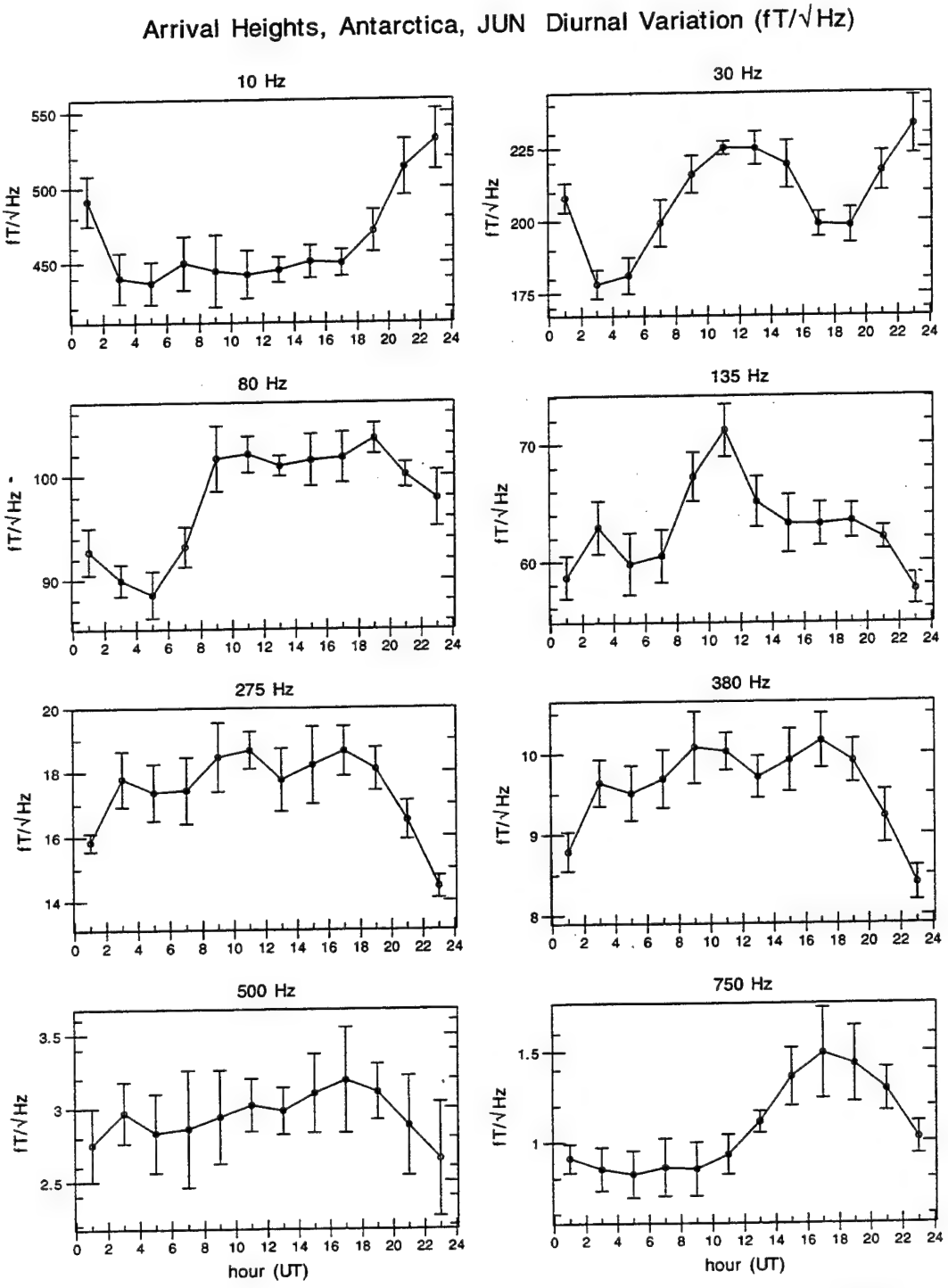

Figure 12: Diurnal variation of ELF/VLF radio noise at Arrival Heights, Antarctica, during the month of June for the eight lowest-frequency channels. The years 1985 to 1994 are included.

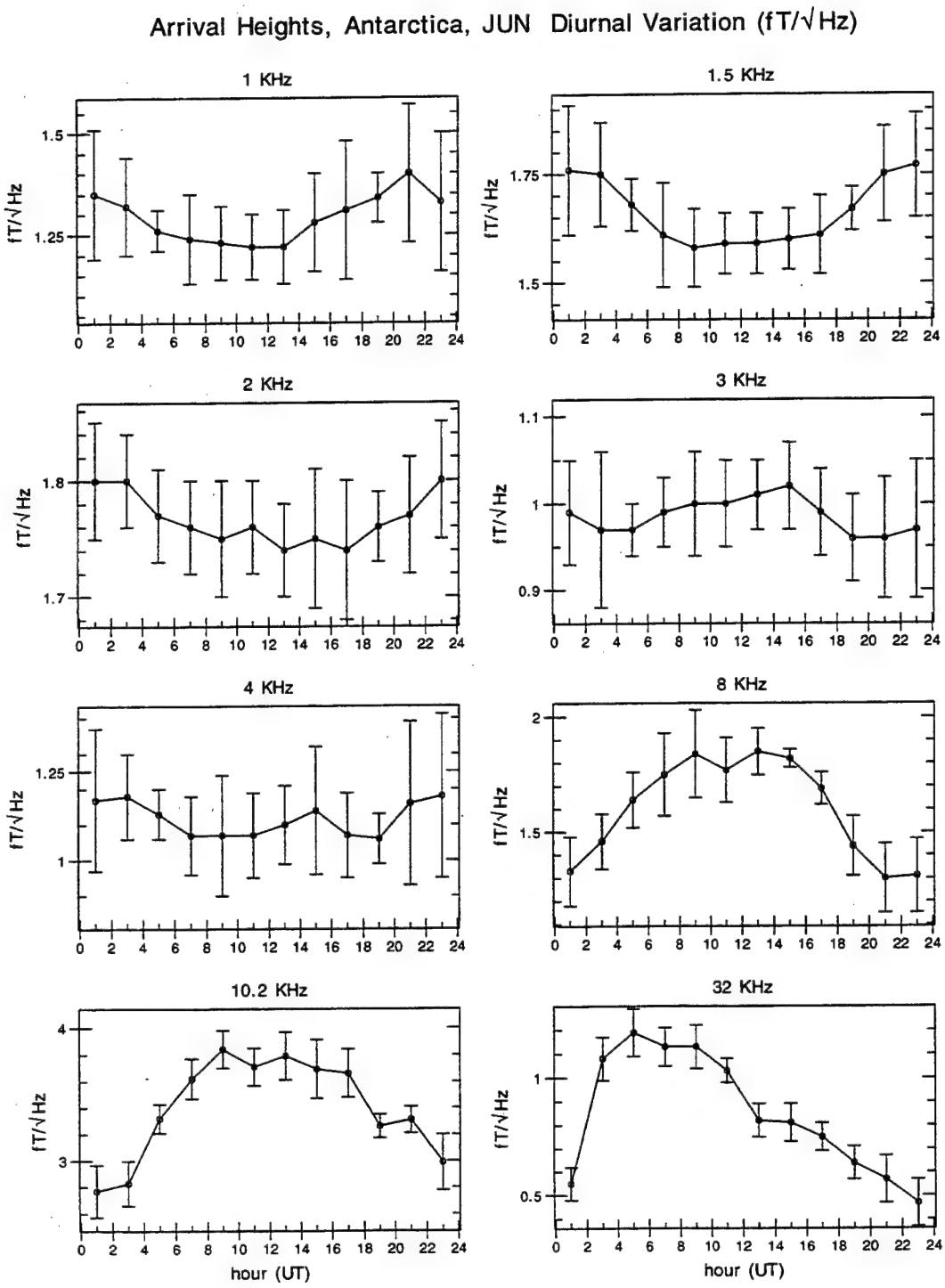

Figure 13: Diurnal variation of ELF/VLF radio noise at Arrival Heights, Antarctica, during the month of June for the eight highest-frequency channels. The years 1985 to 1994 are included.

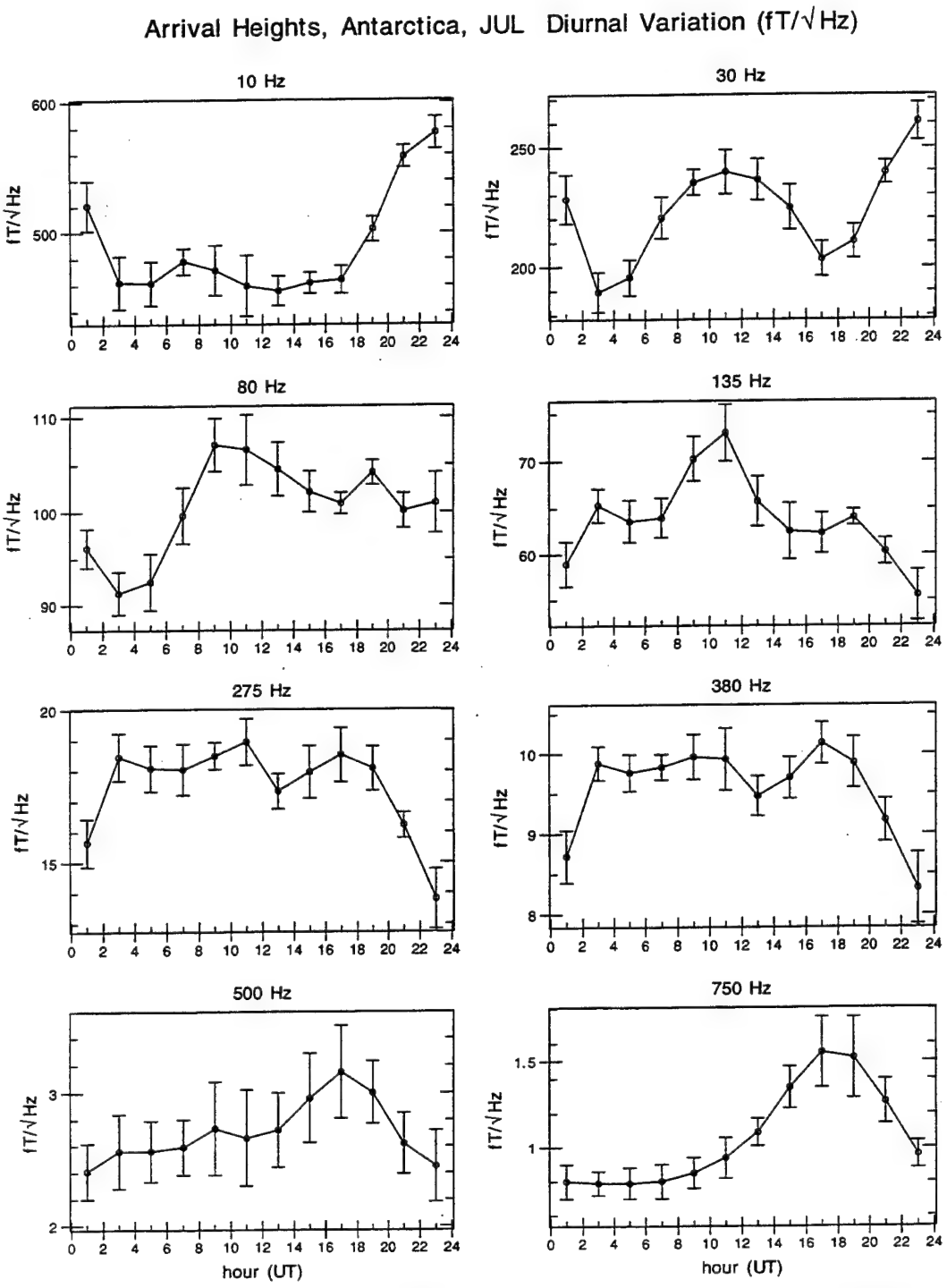

Figure 14: Diurnal variation of ELF/VLF radio noise at Arrival Heights, Antarctica, during the month of July for the eight lowest-frequency channels. The years 1985 to 1994 are included.

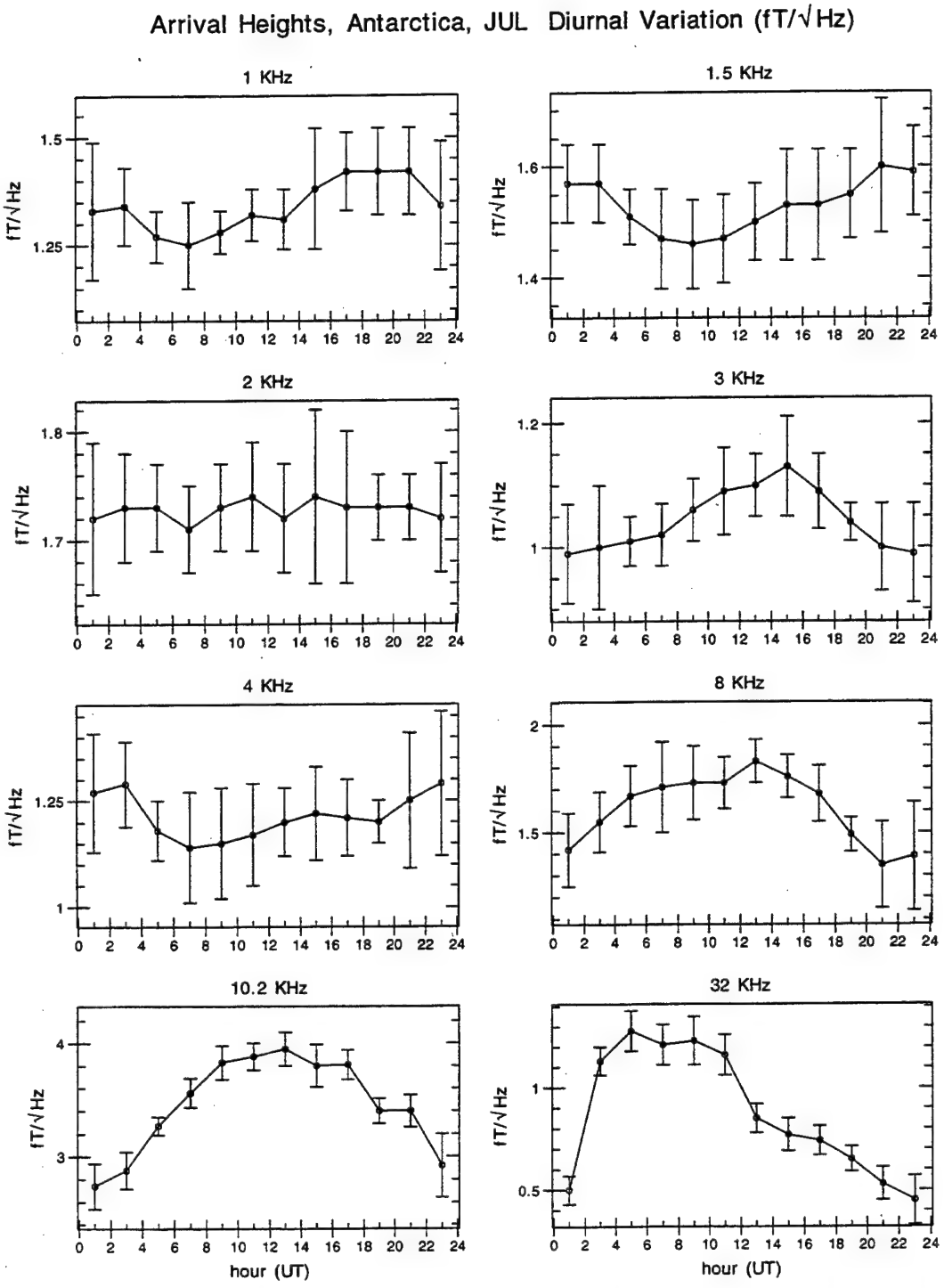

Figure 15: Diurnal variation of ELF/VLF radio noise at Arrival Heights, Antarctica, during the month of July for the eight highest-frequency channels. The years 1985 to 1994 are included.

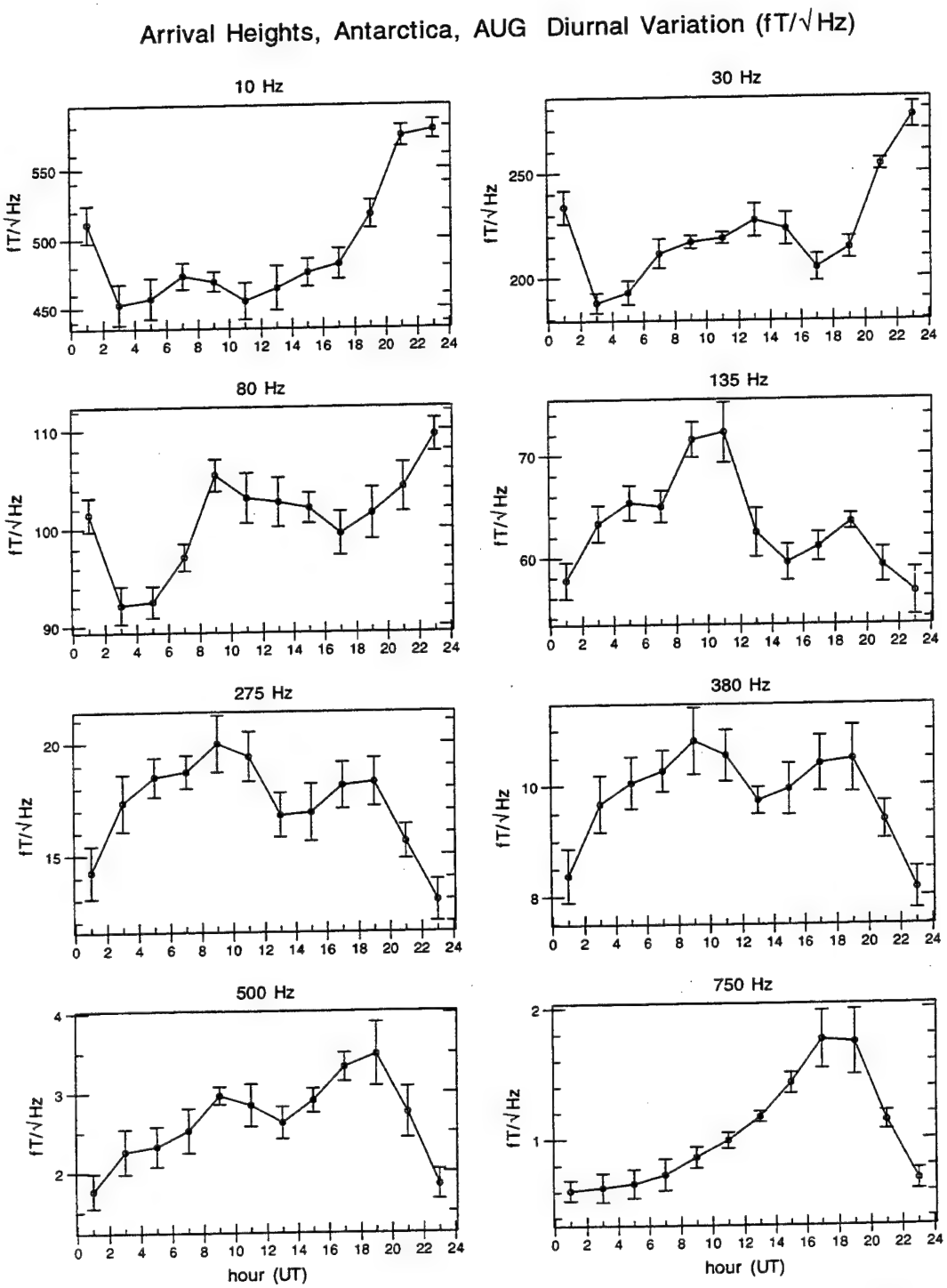

Figure 16: Diurnal variation of ELF/VLF radio noise at Arrival Heights, Antarctica, during the month of August for the eight lowest-frequency channels. The years 1985 to 1994 are included.

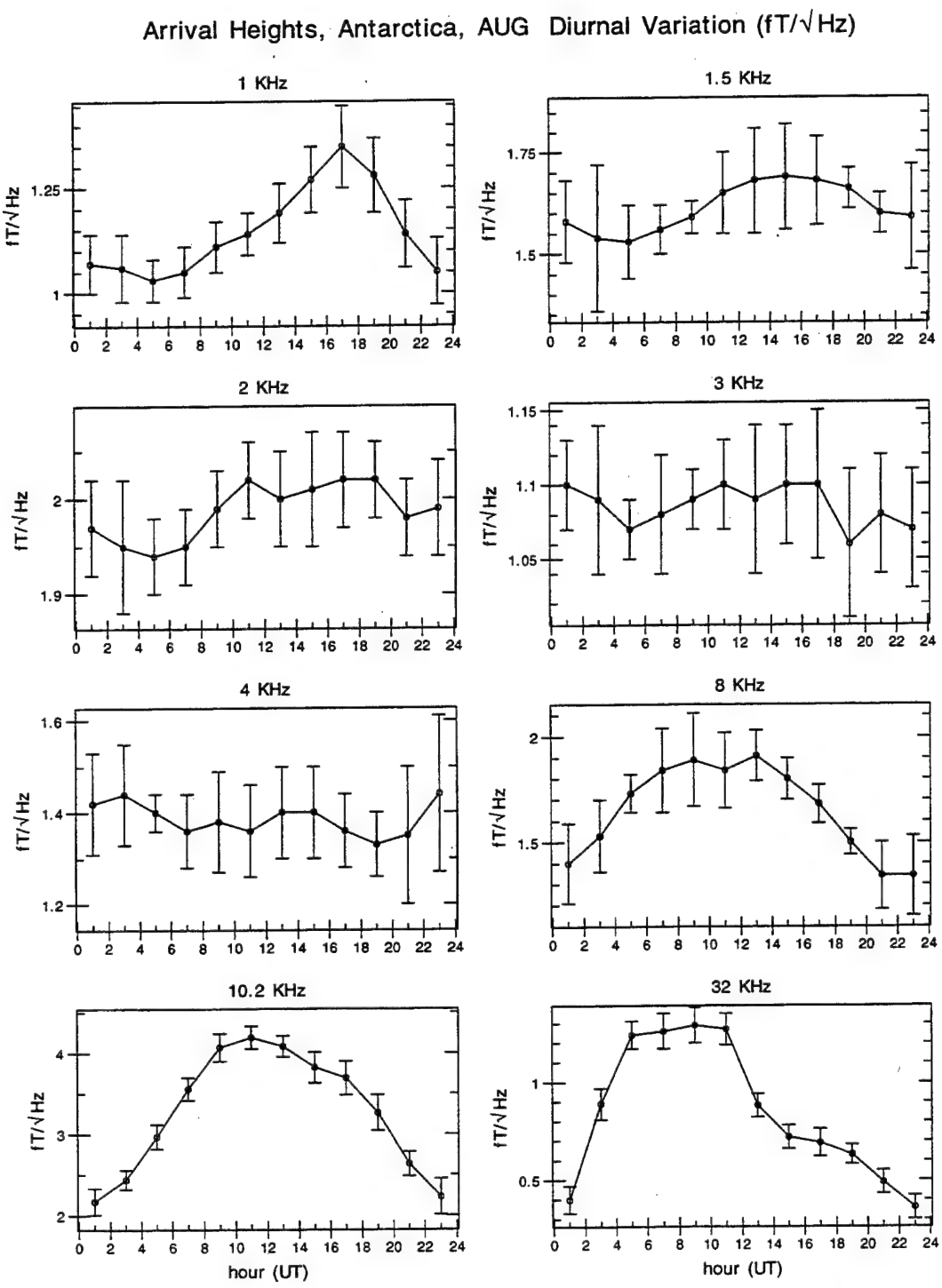

Figure 17: Diurnal variation of ELF/VLF radio noise at Arrival Heights, Antarctica, during the month of August for the eight highest-frequency channels. The years 1985 to 1994 are included.

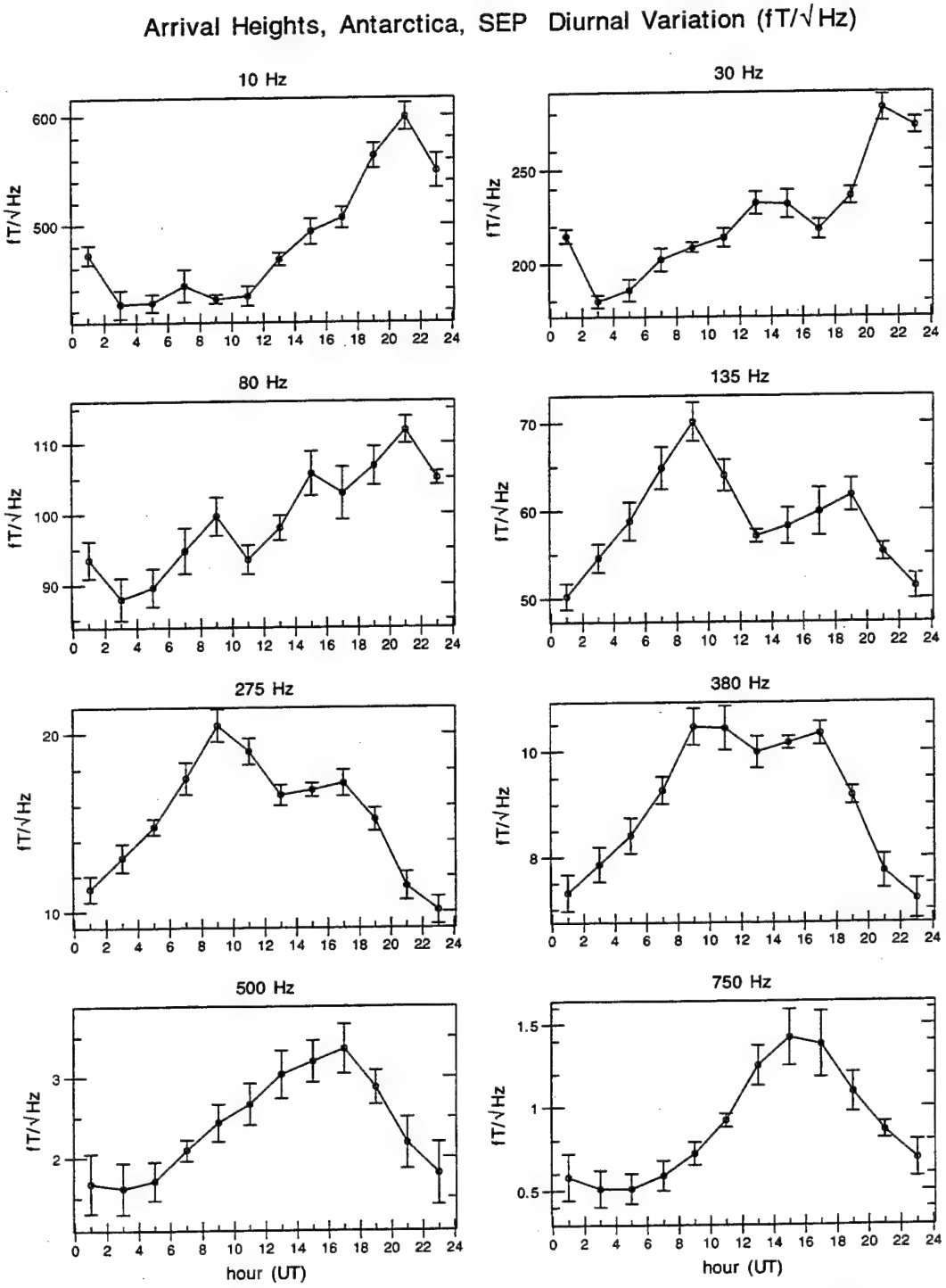

Figure 18: Diurnal variation of ELF/VLF radio noise at Arrival Heights, Antarctica, during the month of September for the eight lowest-frequency channels. The years 1985 to 1994 are included.

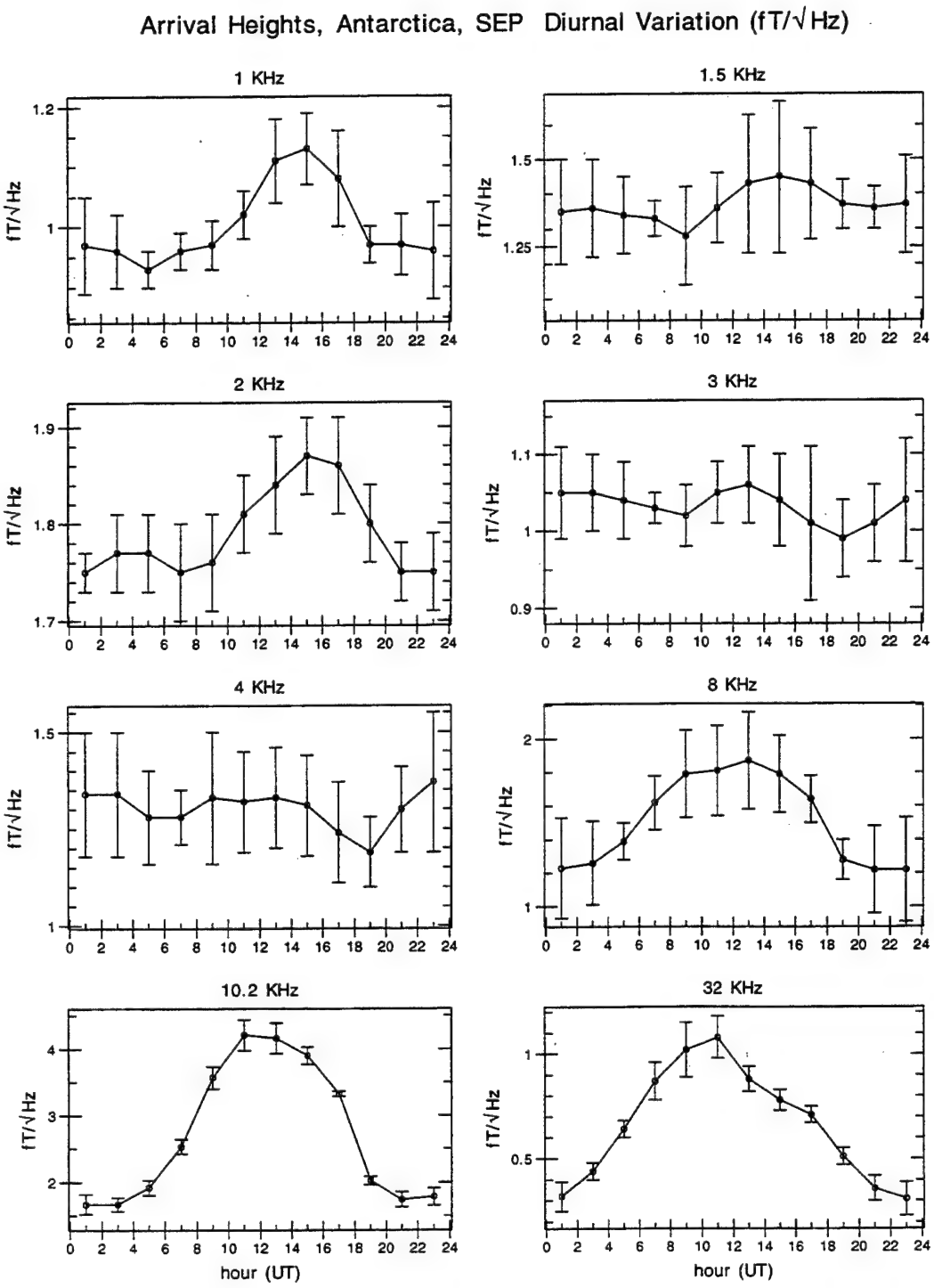

Figure 19: Diurnal variation of ELF/VLF radio noise at Arrival Heights, Antarctica, during the month of September for the eight highest-frequency channels. The years 1985 to 1994 are included.

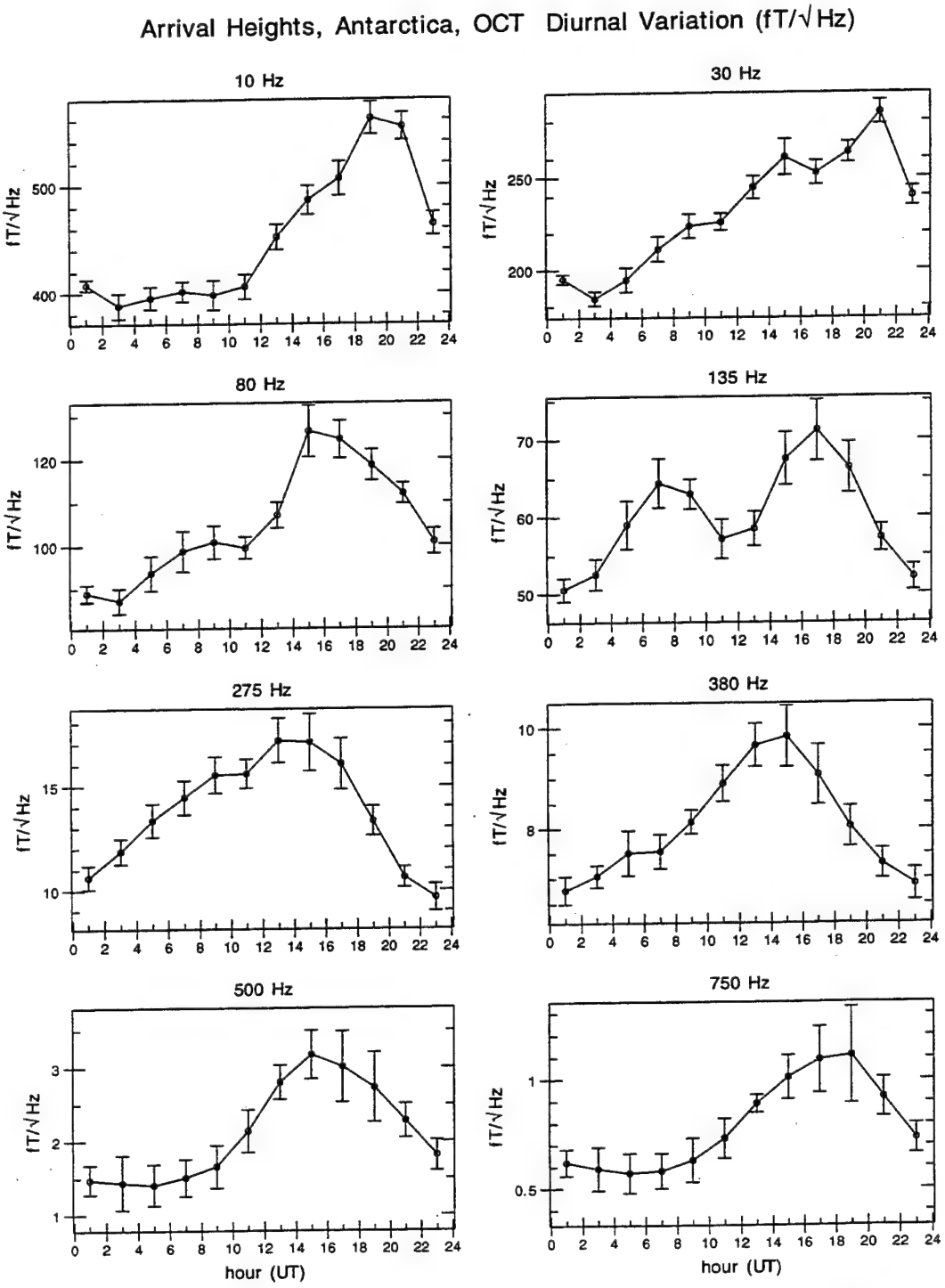

Figure 20: Diurnal variation of ELF/VLF radio noise at Arrival Heights, Antarctica, during the month of October for the eight lowest-frequency channels. The years 1985 to 1994 are included.

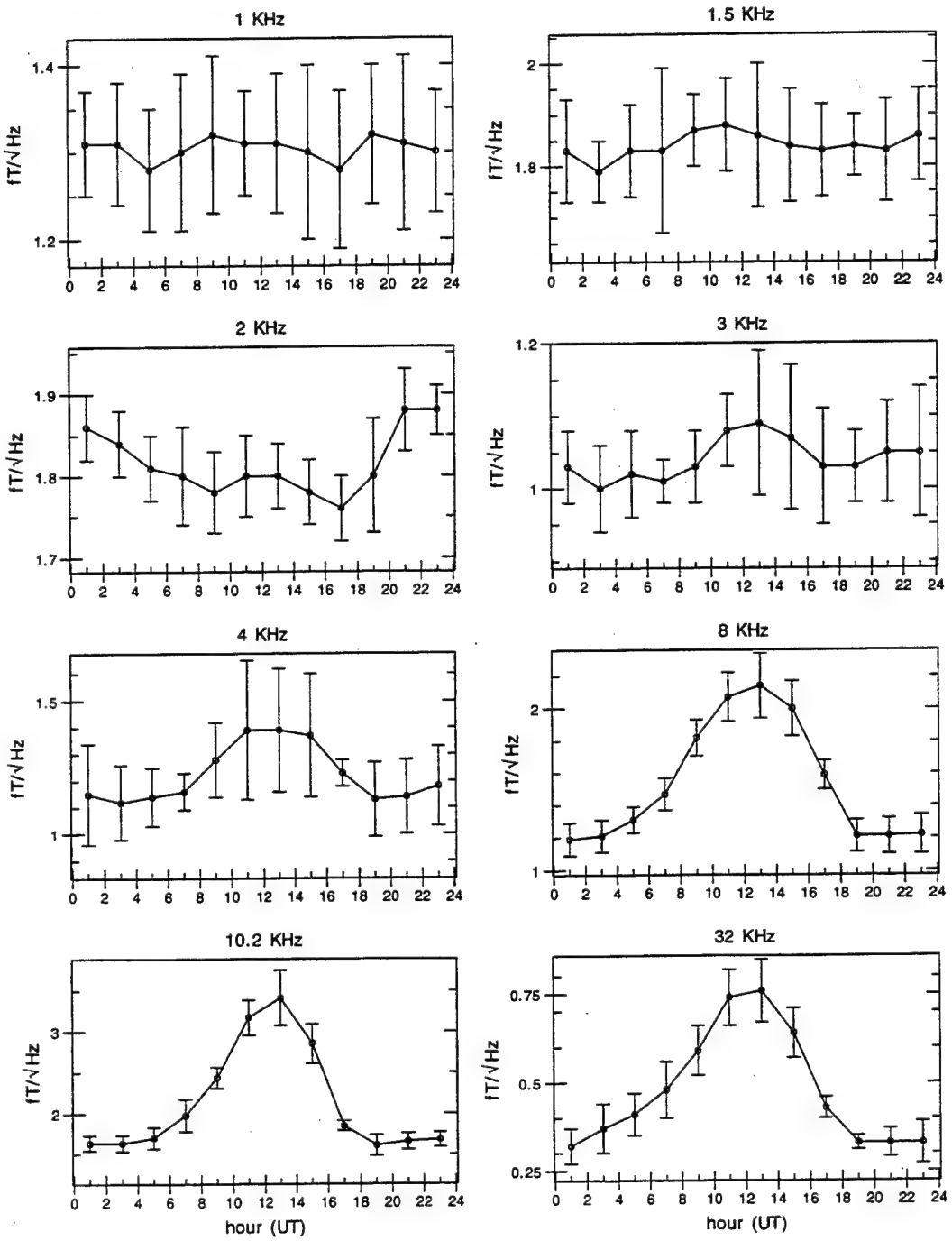

Figure 21: Diurnal variation of ELF/VLF radio noise at Arrival Heights, Antarctica, during the month of October for the eight highest-frequency channels. The years 1985 to 1994 are included.

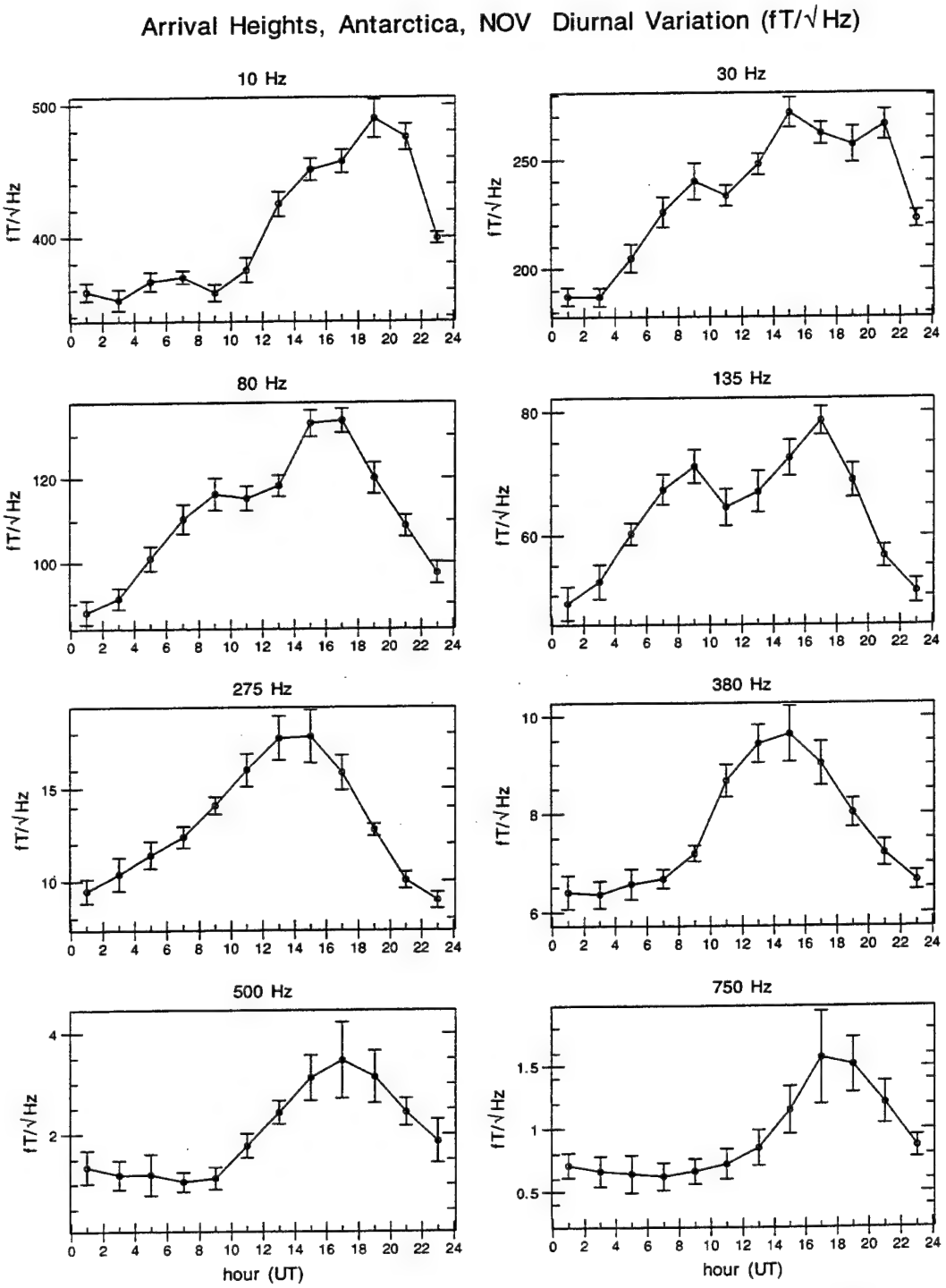

Figure 22: Diurnal variation of ELF/VLF radio noise at Arrival Heights, Antarctica, during the month of November for the eight lowest-frequency channels. The years 1985 to 1994 are included.

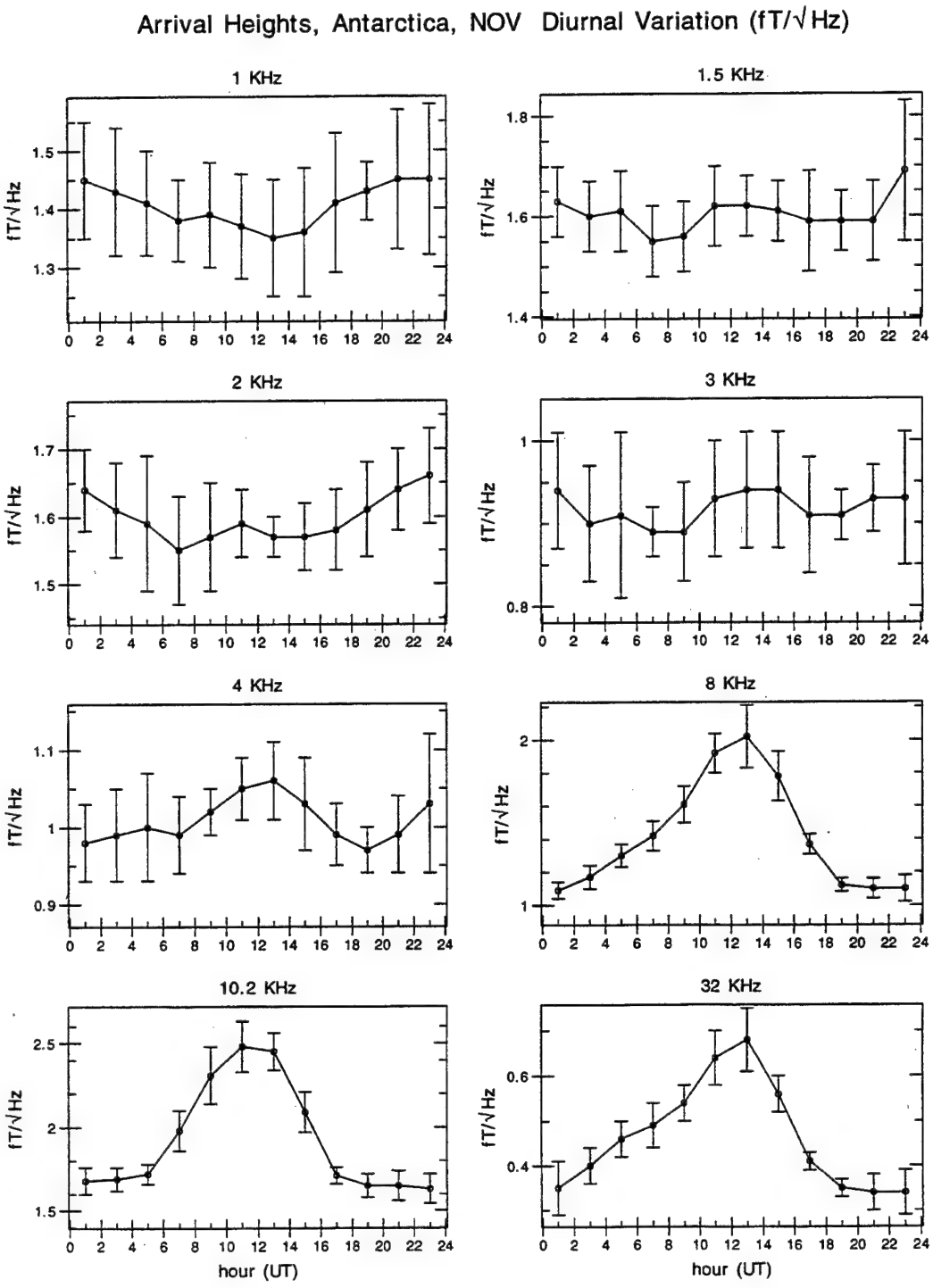

Figure 23: Diurnal variation of ELF/VLF radio noise at Arrival Heights, Antarctica, during the month of November for the eight highest-frequency channels. The years 1985 to 1994 are included.

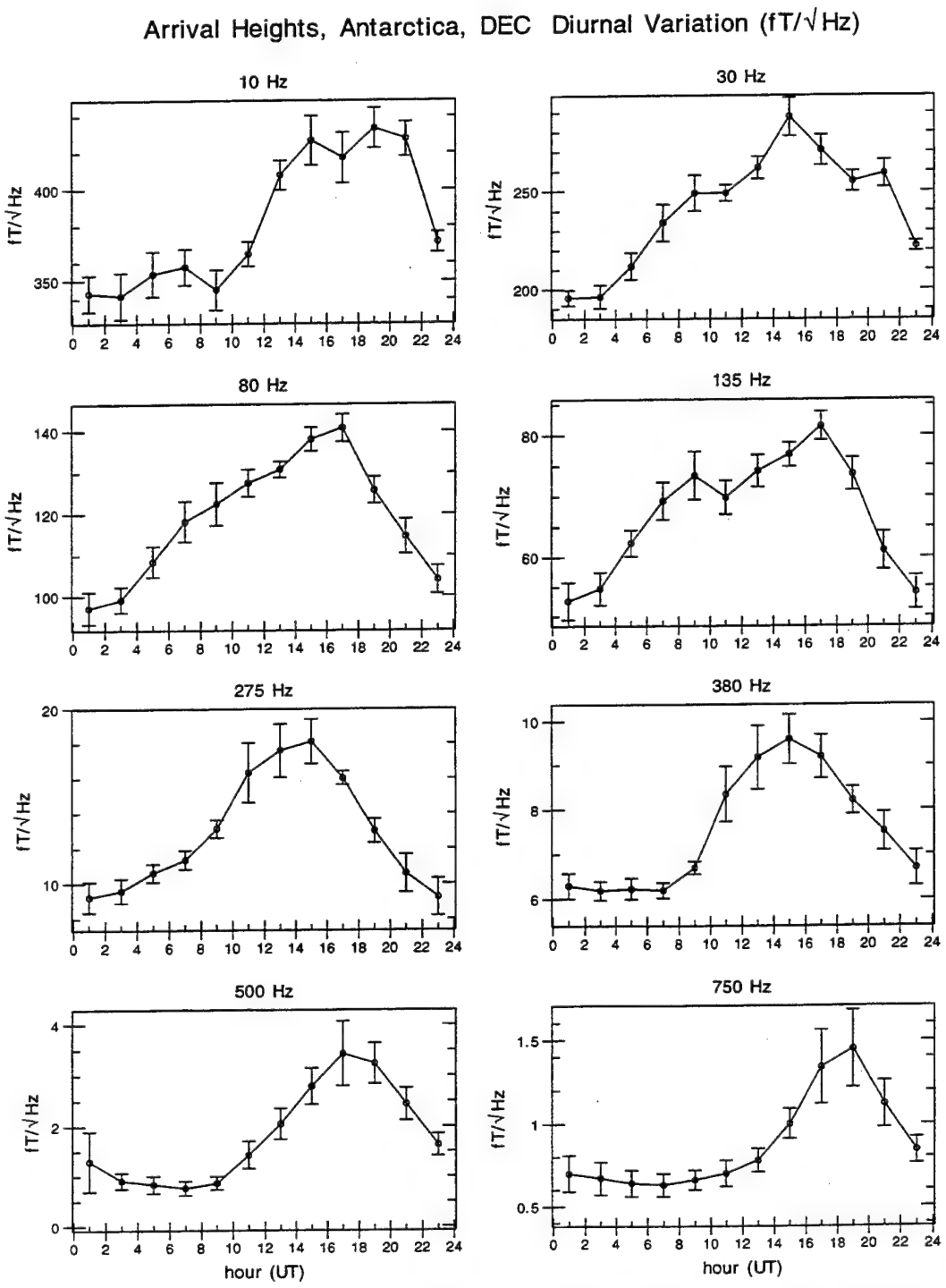

Figure 24: Diurnal variation of ELF/VLF radio noise at Arrival Heights, Antarctica, during the month of December for the eight lowest-frequency channels. The years 1985 to 1994 are included.

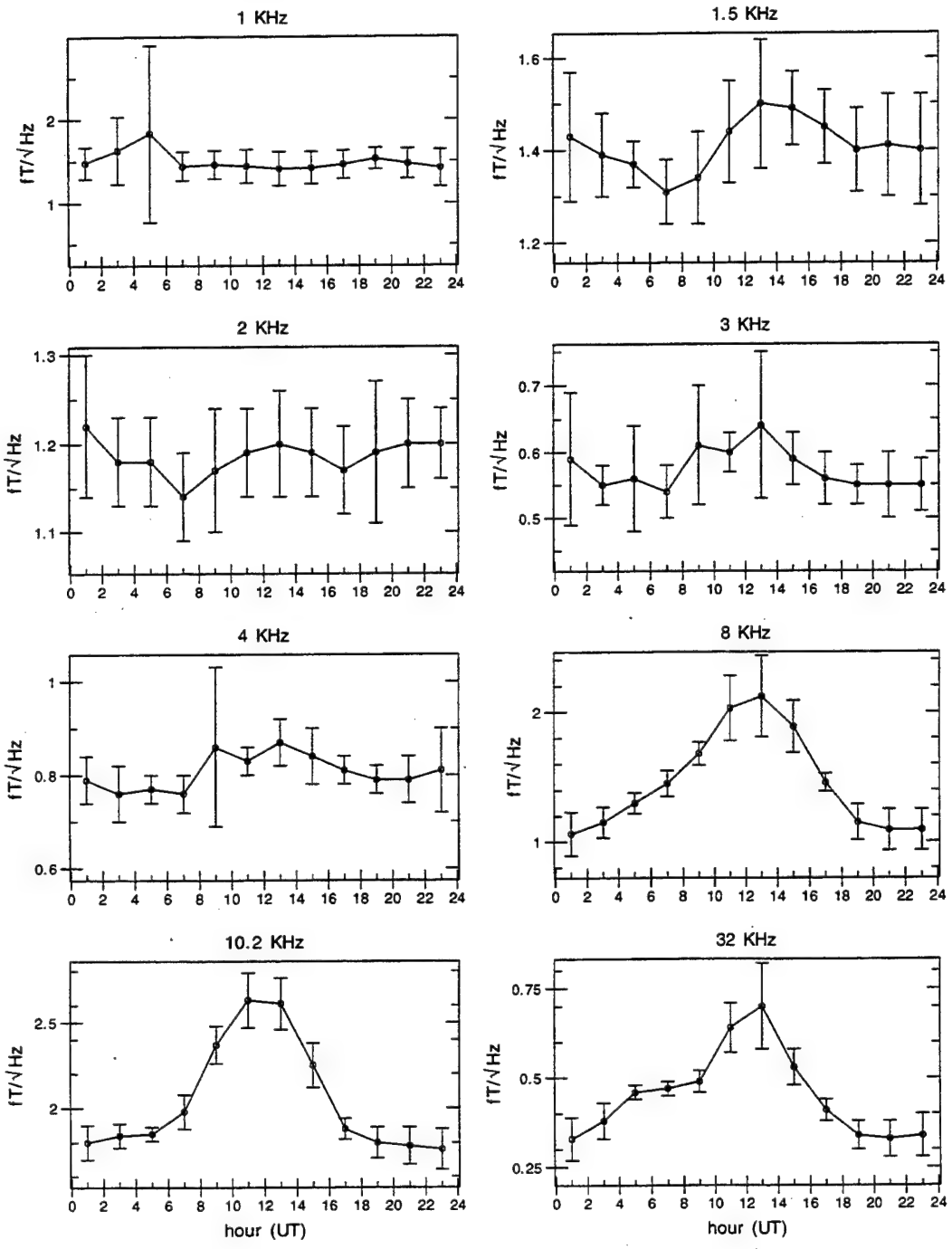

Figure 25: Diurnal variation of ELF/VLF radio noise at Arrival Heights, Antarctica, during the month of December for the eight highest-frequency channels. The years 1985 to 1994 are included.

9 Dunedin, New Zealand Diurnal Variation Figures

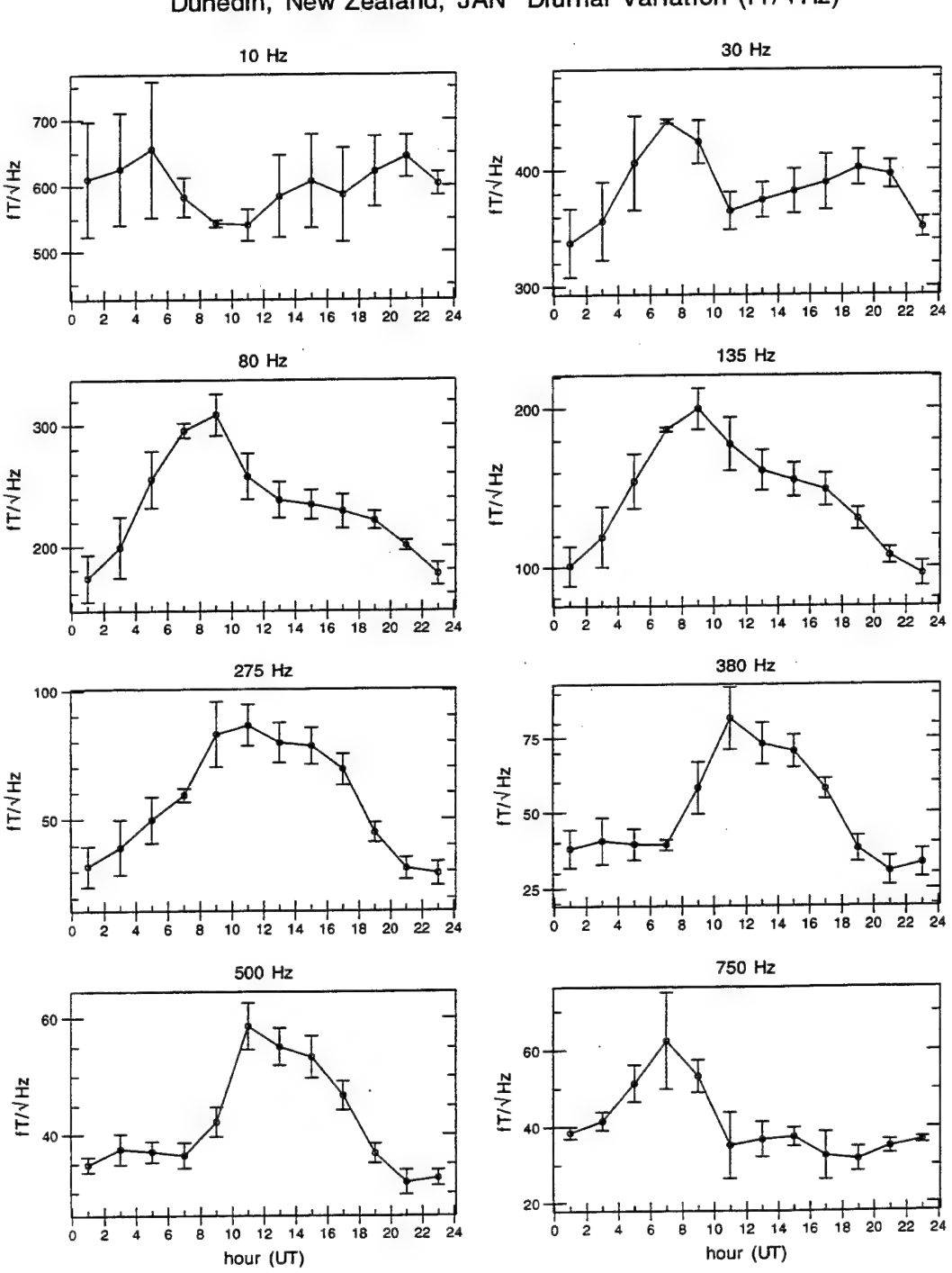

Figure 26: Diurnal variation of ELF/VLF radio noise at Dunedin, New Zealand, during the month of January for the eight lowest-frequency channels. The years 1986 to 1990 are included.

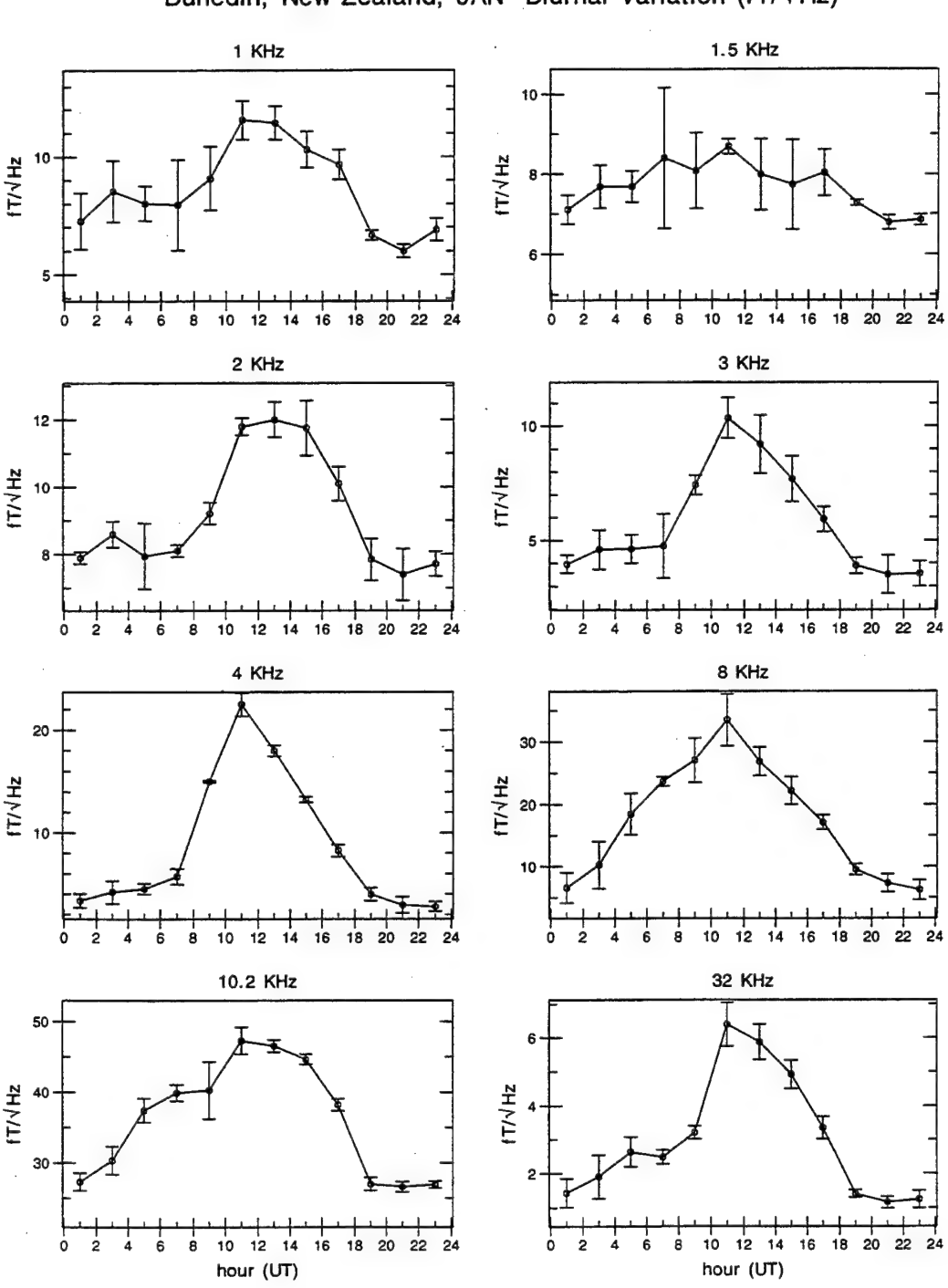

Figure 27: Diurnal variation of ELF/VLF radio noise at Dunedin, New Zealand, during the month of January for the eight highest-frequency channels. The years 1986 to 1990 are included.

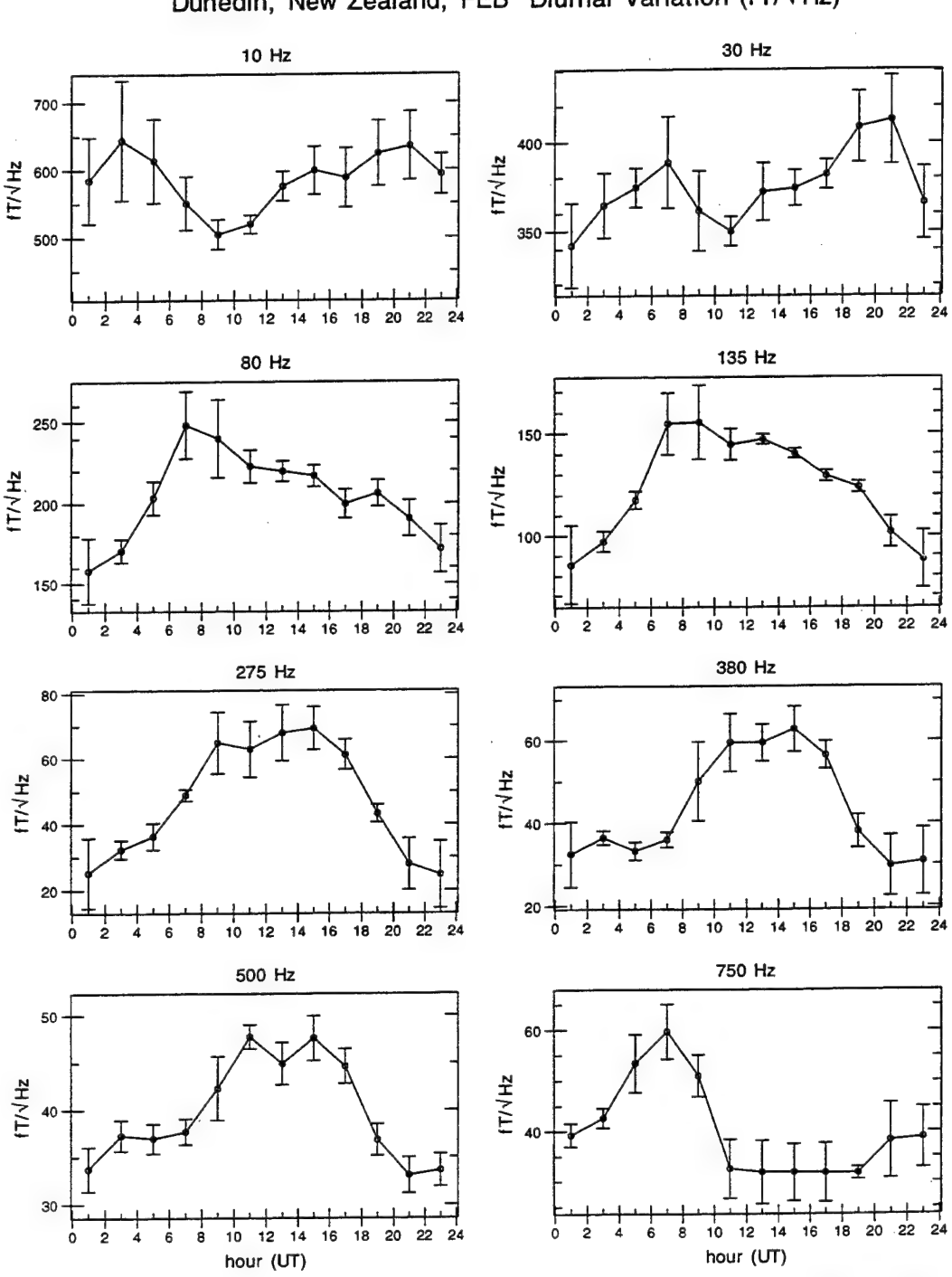

Figure 28: Diurnal variation of ELF/VLF radio noise at Dunedin, New Zealand, during the month of February for the eight lowest-frequency channels. The years 1986 to 1990 are included.

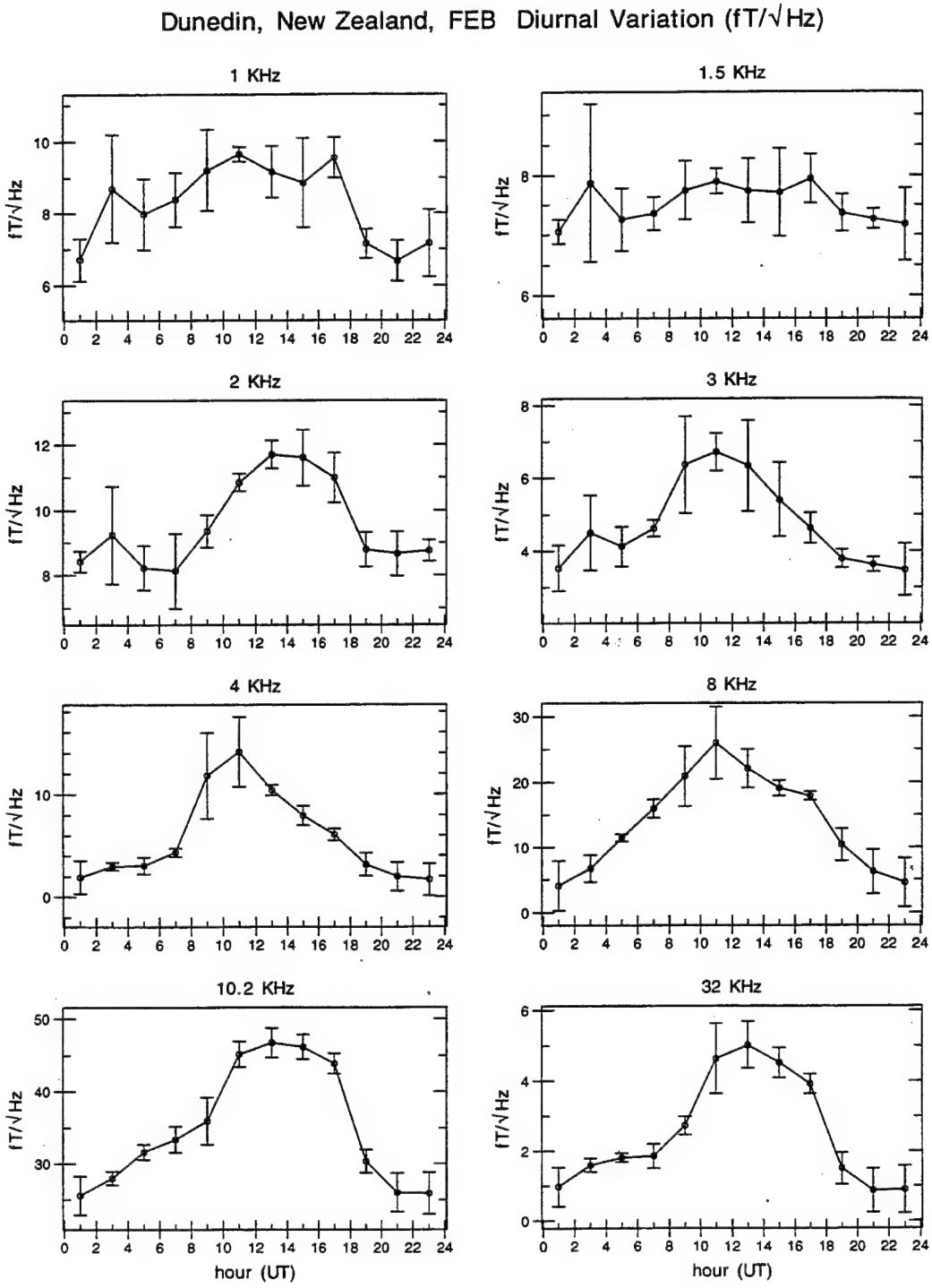

Figure 29: Diurnal variation of ELF/VLF radio noise at Dunedin, New Zealand, during the month of February for the eight highest-frequency channels. The years 1986 to 1990 are included.

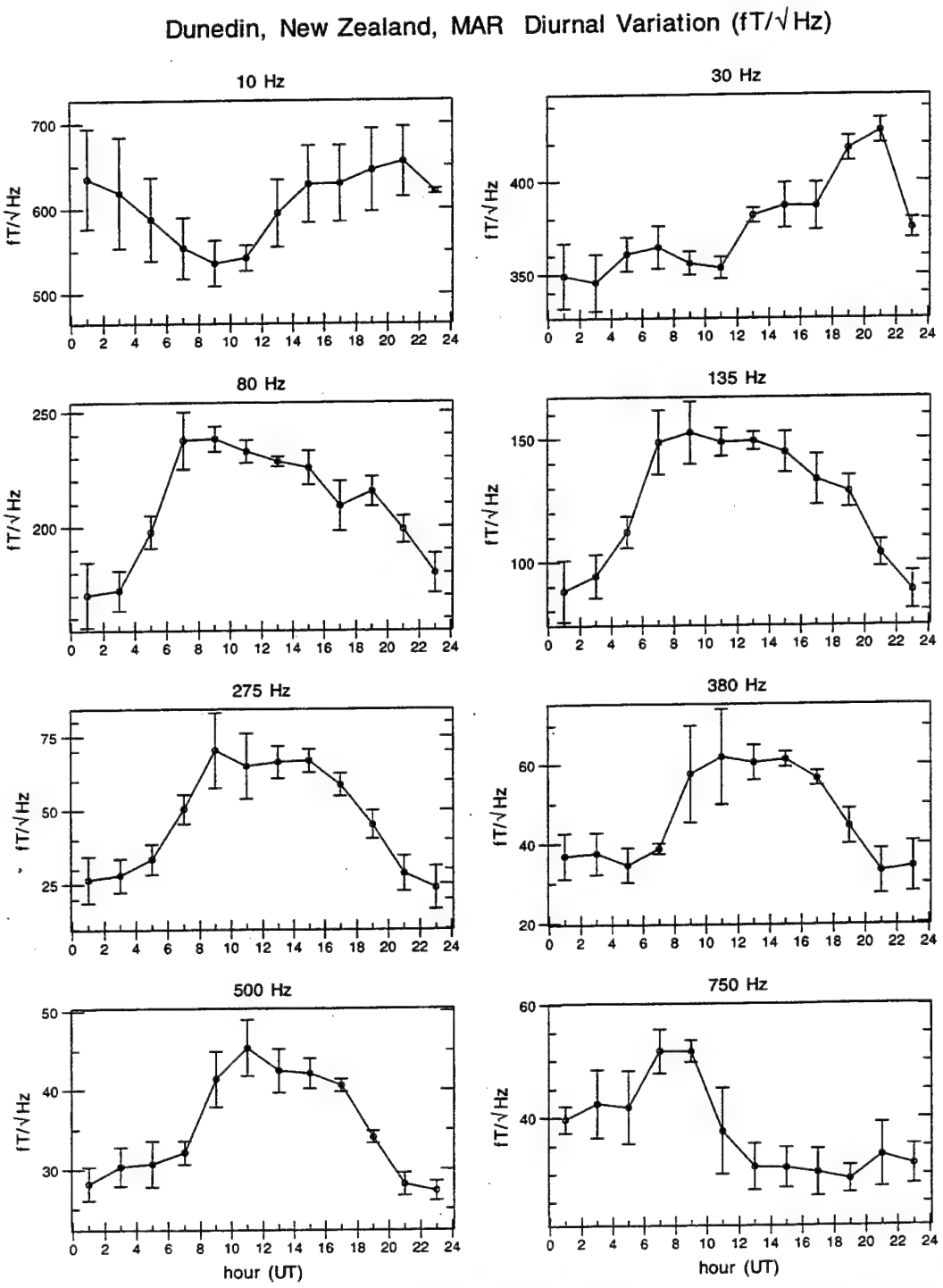

Figure 30: Diurnal variation of ELF/VLF radio noise at Dunedin, New Zealand, during the month of March for the eight lowest-frequency channels. The years 1986 to 1990 are included.

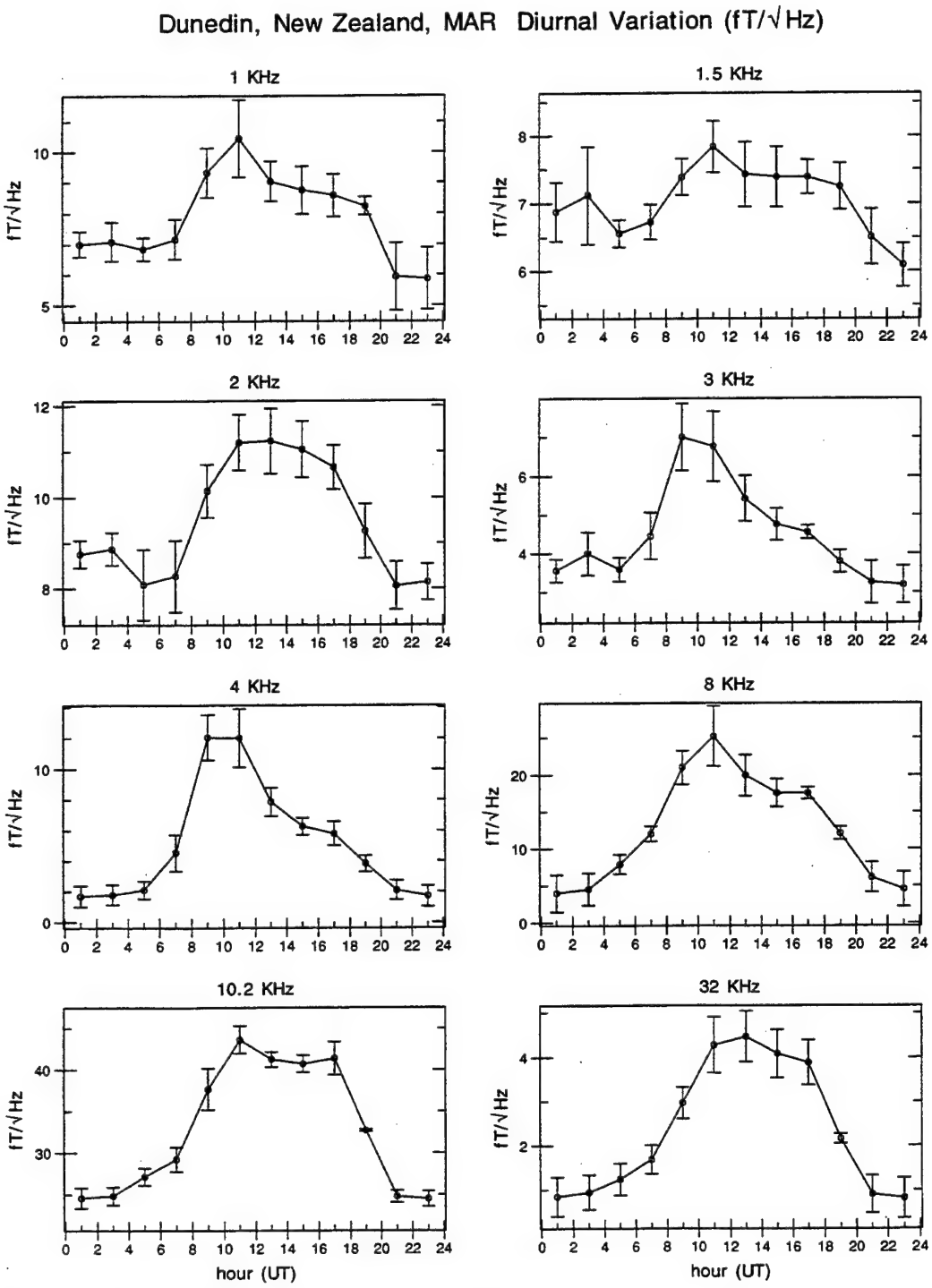

Figure 31: Diurnal variation of ELF/VLF radio noise at Dunedin, New Zealand, during the month of March for the eight highest-frequency channels. The years 1986 to 1990 are included.

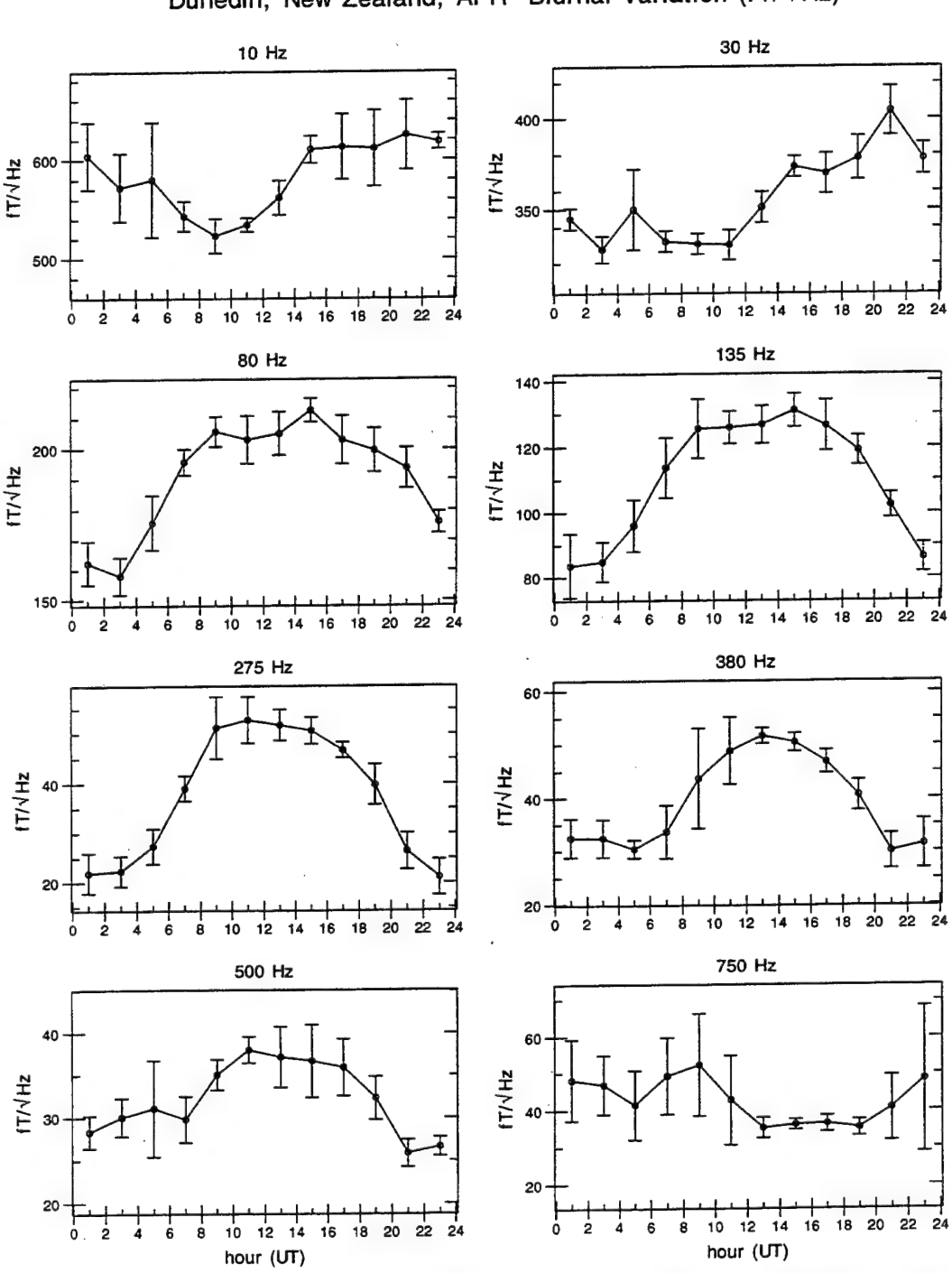

Figure 32: Diurnal variation of ELF/VLF radio noise at Dunedin, New Zealand, during the month of April for the eight lowest-frequency channels. The years 1986 to 1990 are included.

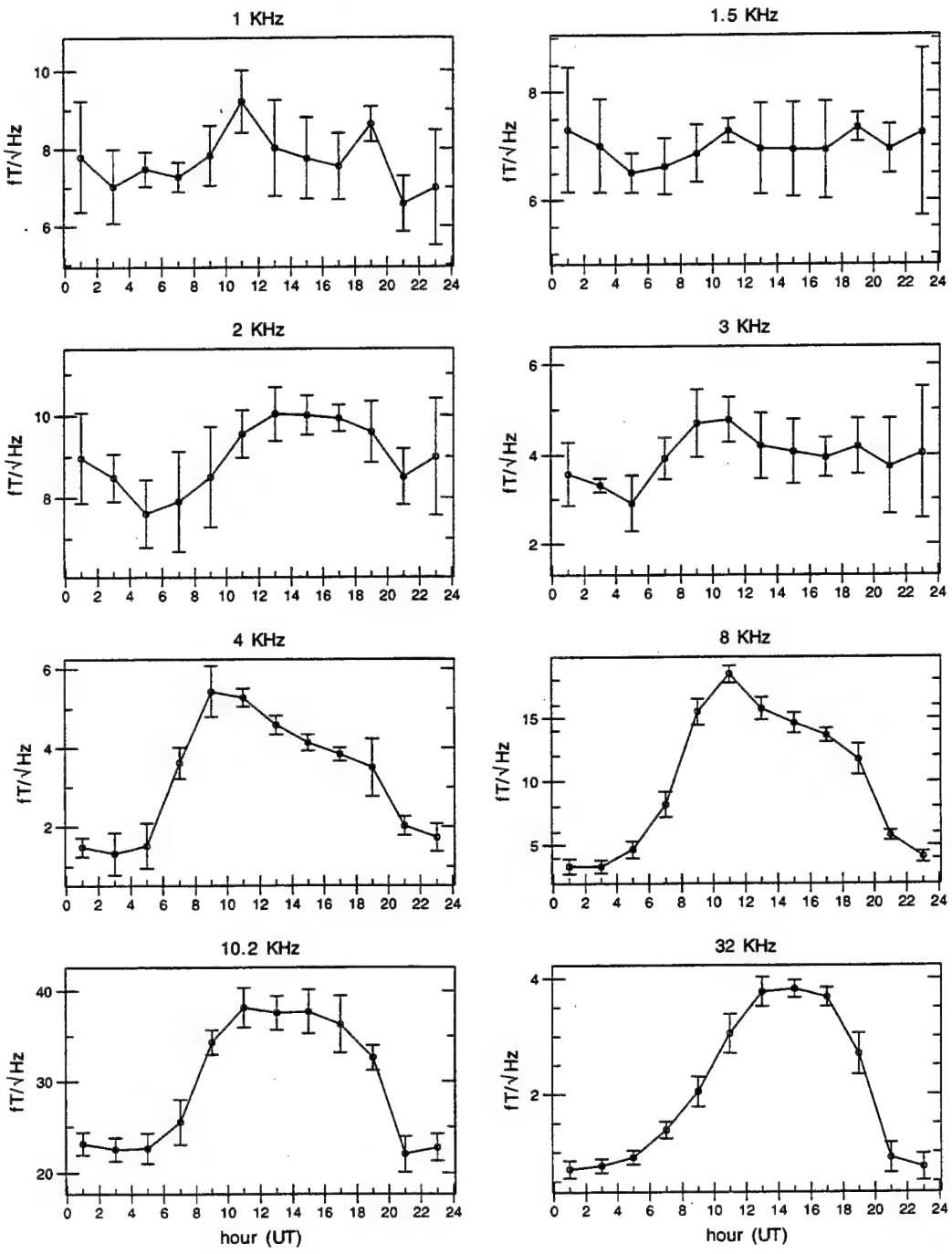

Figure 33: Diurnal variation of ELF/VLF radio noise at Dunedin, New Zealand, during the month of April for the eight highest-frequency channels. The years 1986 to 1990 are included.

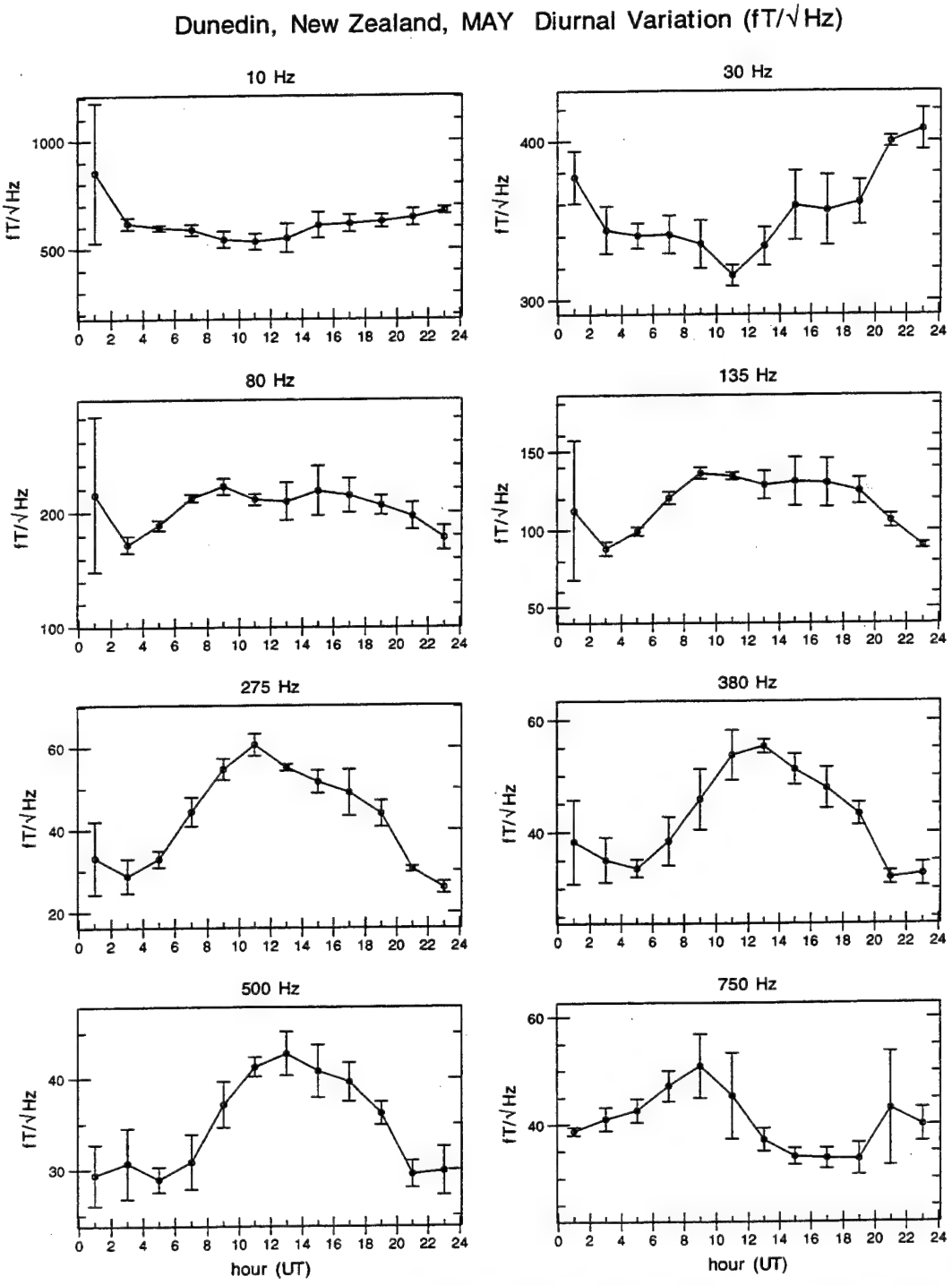

Figure 34: Diurnal variation of ELF/VLF radio noise at Dunedin, New Zealand, during the month of May for the eight lowest-frequency channels. The years 1986 to 1990 are included.

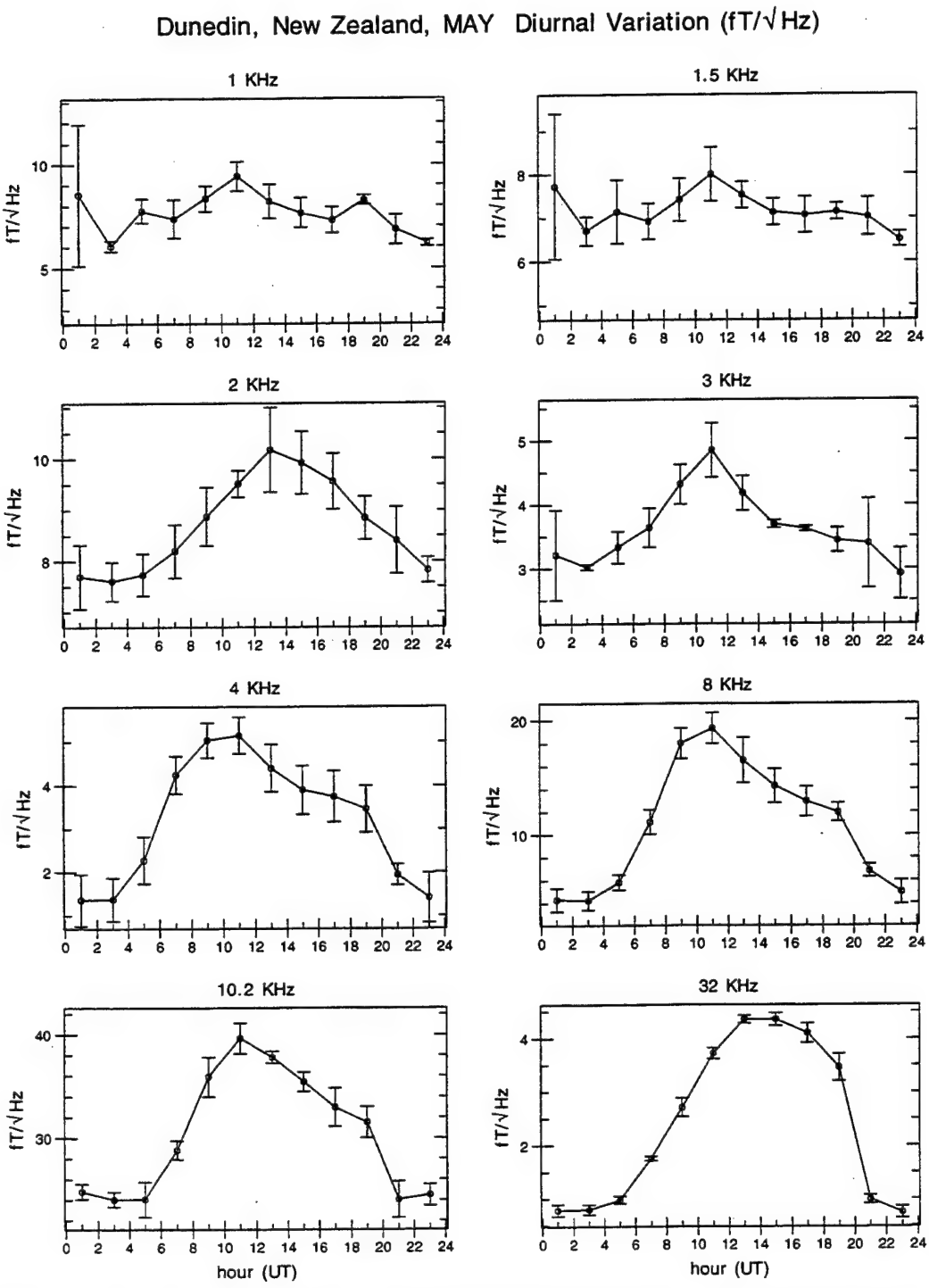

Figure 35: Diurnal variation of ELF/VLF radio noise at Dunedin, New Zealand, during the month of May for the eight highest-frequency channels. The years 1986 to 1990 are included.

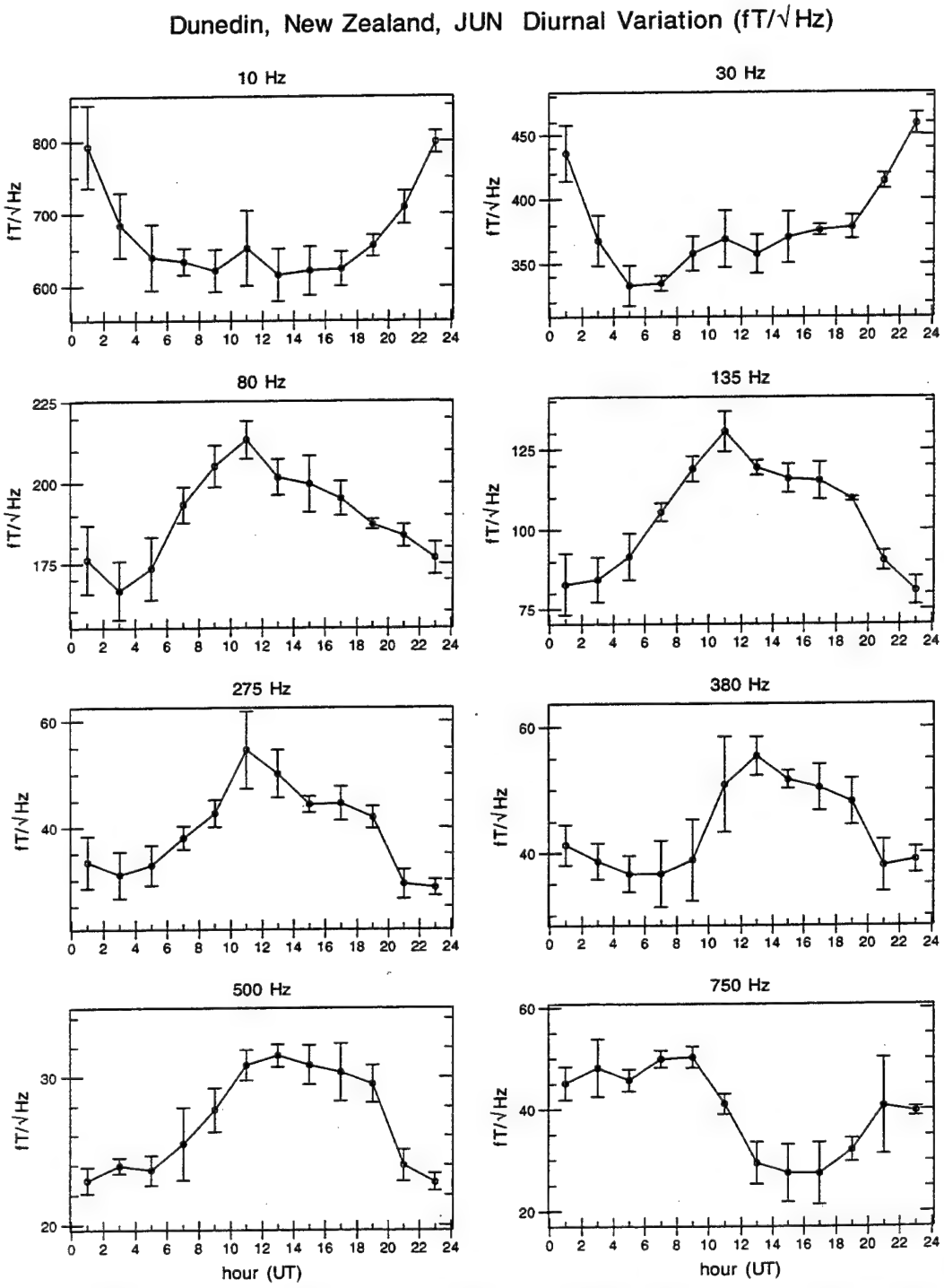

Figure 36: Diurnal variation of ELF/VLF radio noise at Dunedin, New Zealand, during the month of June for the eight lowest-frequency channels. The years 1986 to 1990 are included.

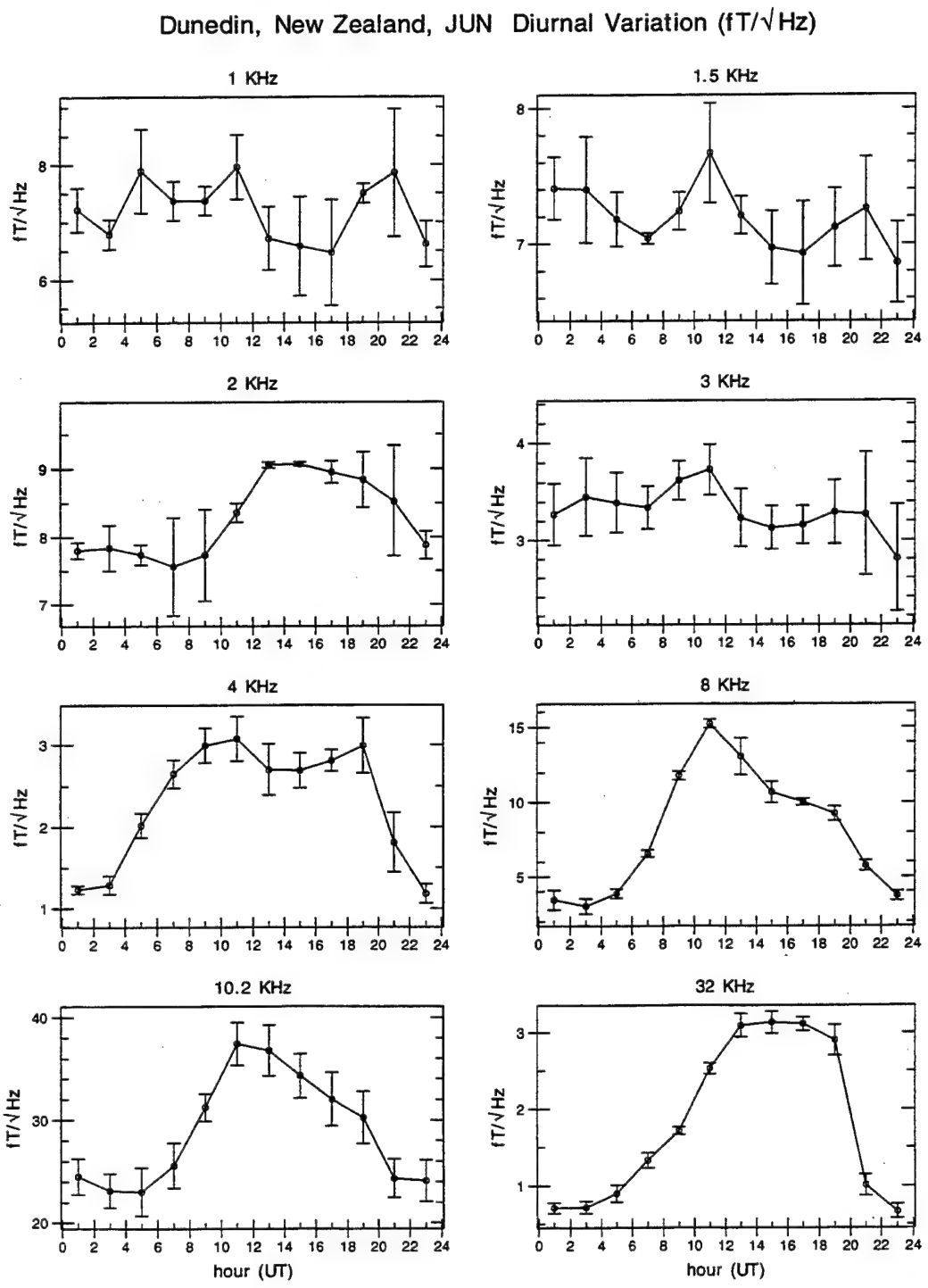

Figure 37: Diurnal variation of ELF/VLF radio noise at Dunedin, New Zealand, during the month of June for the eight highest-frequency channels. The years 1986 to 1990 are included.

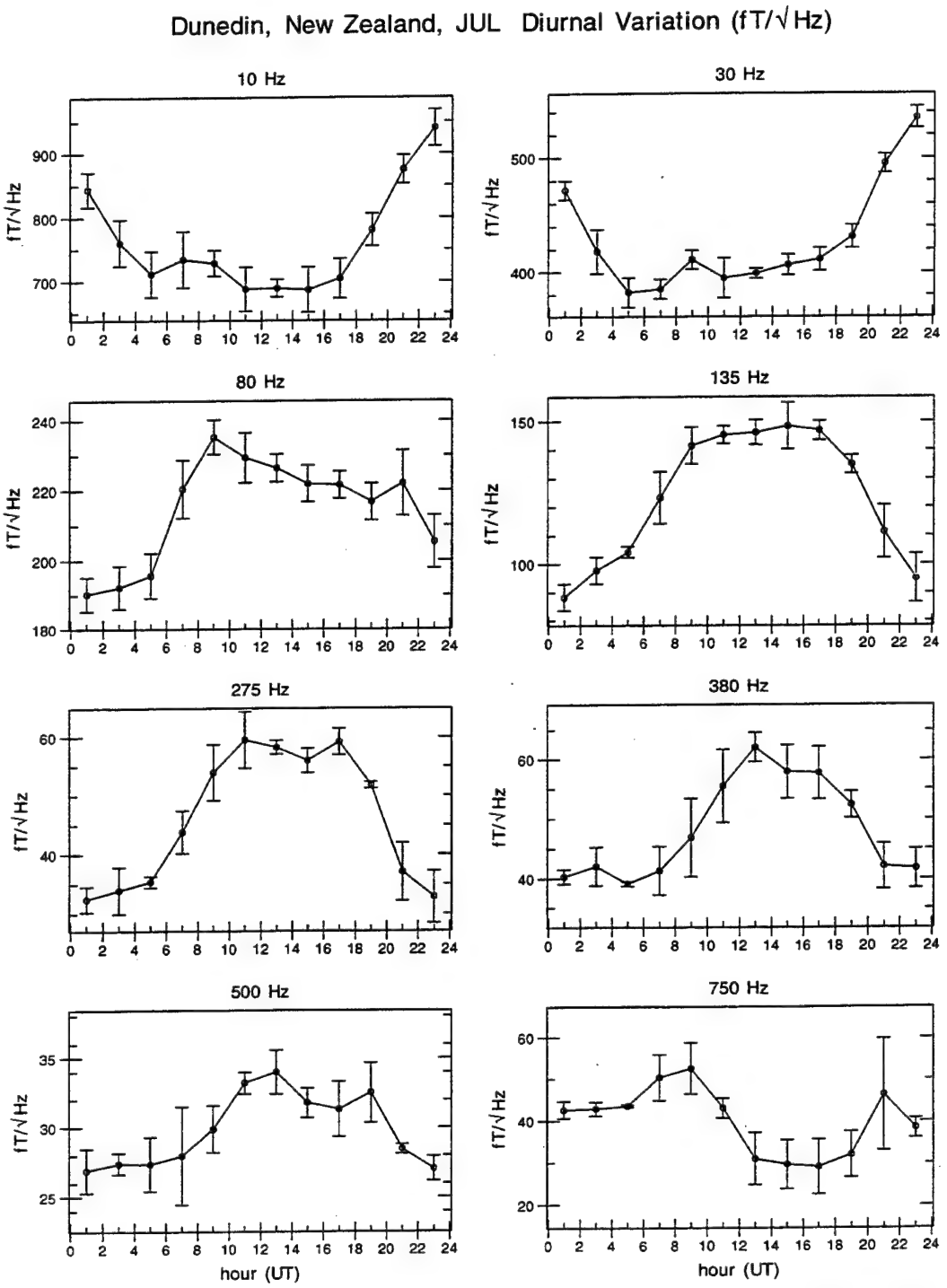

Figure 38: Diurnal variation of ELF/VLF radio noise at Dunedin, New Zealand, during the month of July for the eight lowest-frequency channels. The years 1986 to 1990 are included.

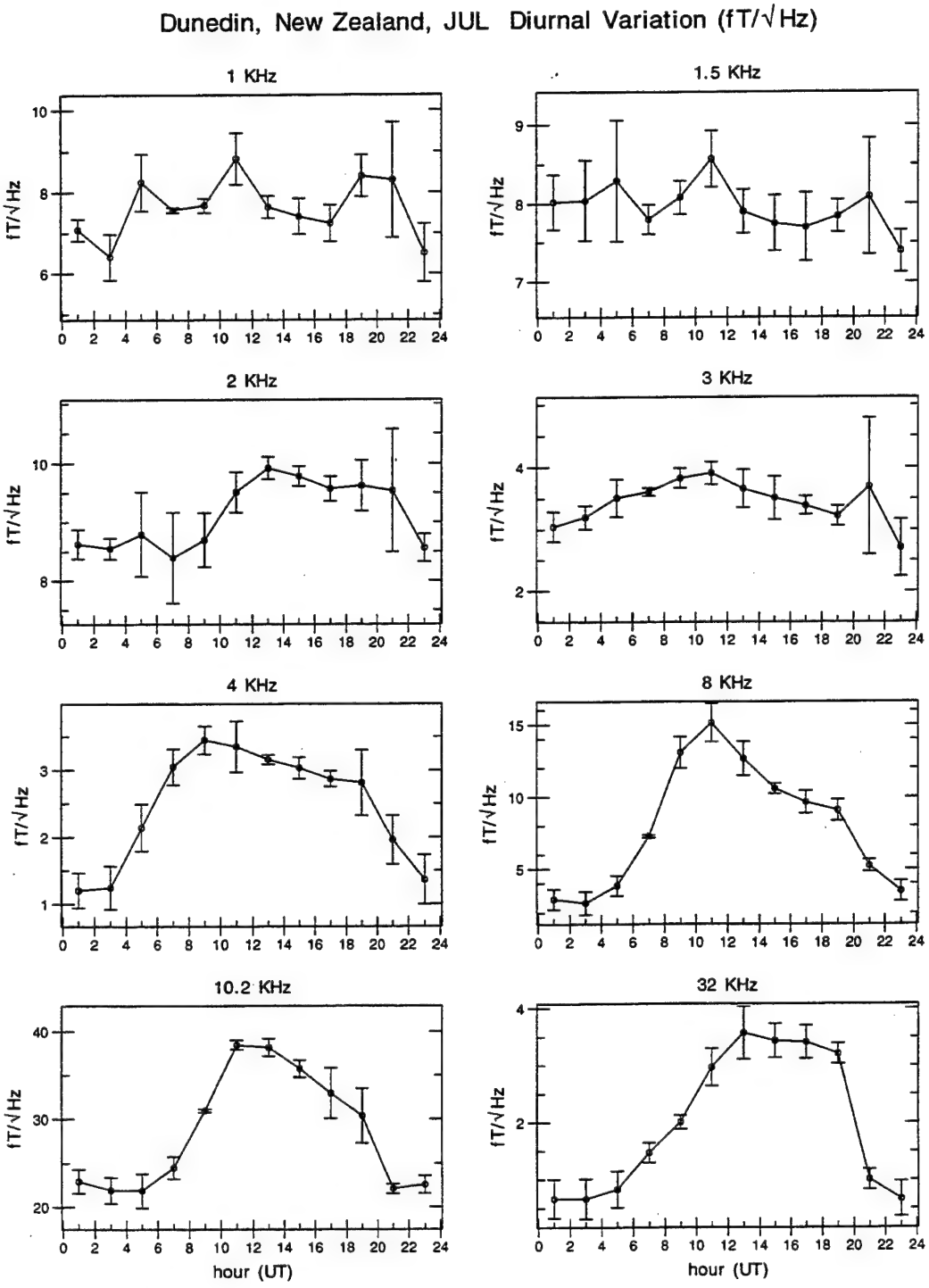

Figure 39: Diurnal variation of ELF/VLF radio noise at Dunedin, New Zealand, during the month of July for the eight highest-frequency channels. The years 1986 to 1990 are included.

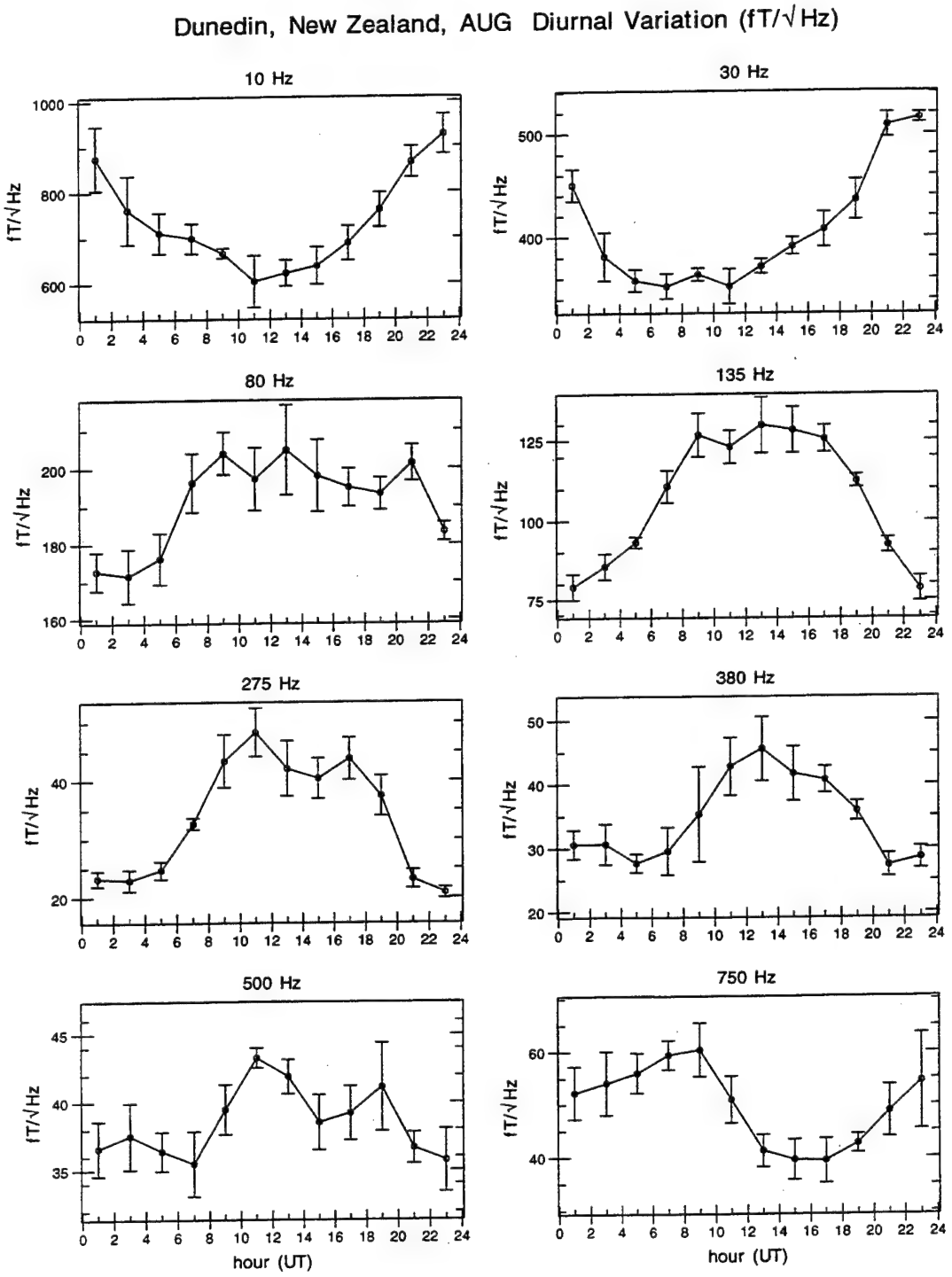

Figure 40: Diurnal variation of ELF/VLF radio noise at Dunedin, New Zealand, during the month of August for the eight lowest-frequency channels. The years 1986 to 1990 are included.

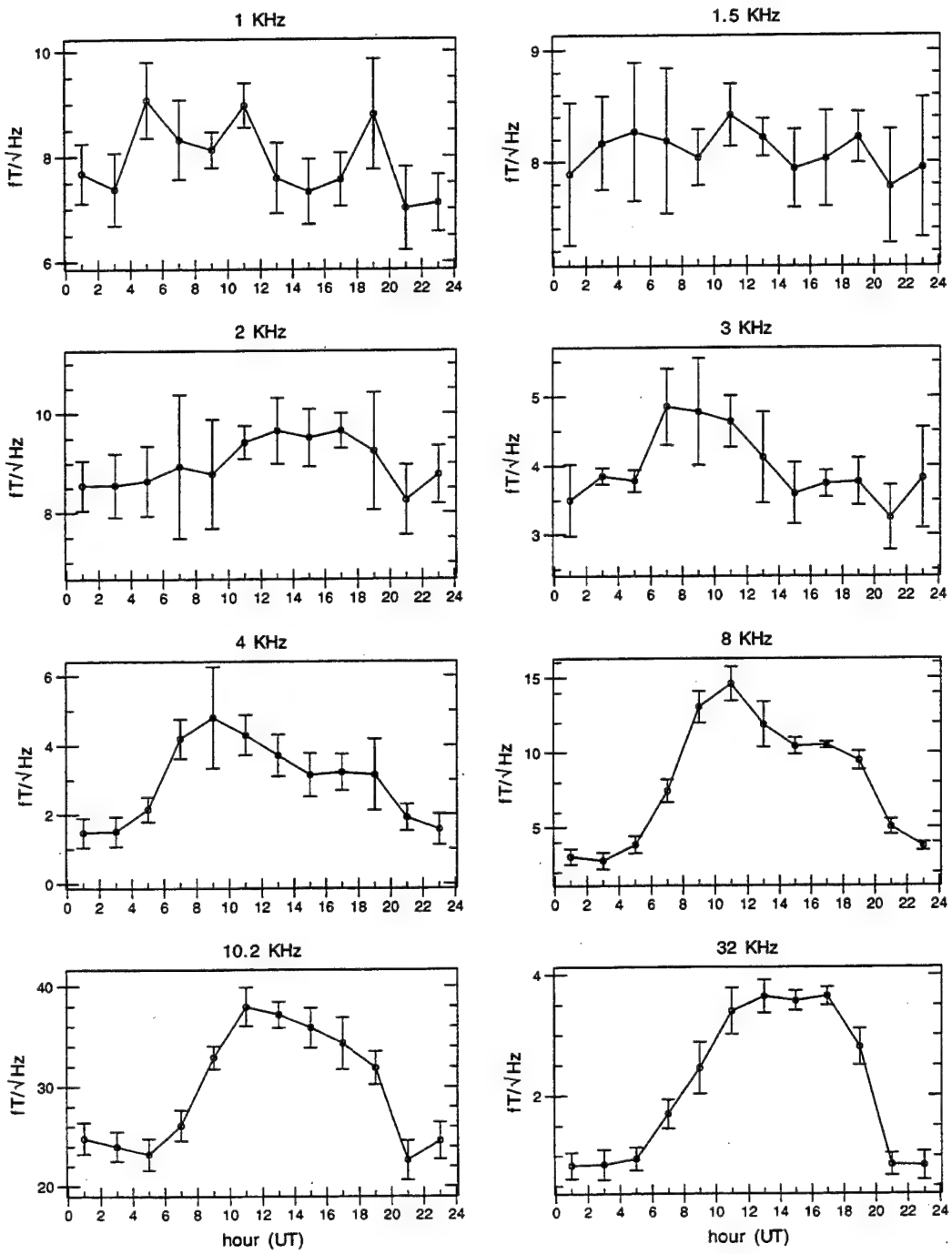

Figure 41: Diurnal variation of ELF/VLF radio noise at Dunedin, New Zealand, during the month of August for the eight highest-frequency channels. The years 1986 to 1990 are included.

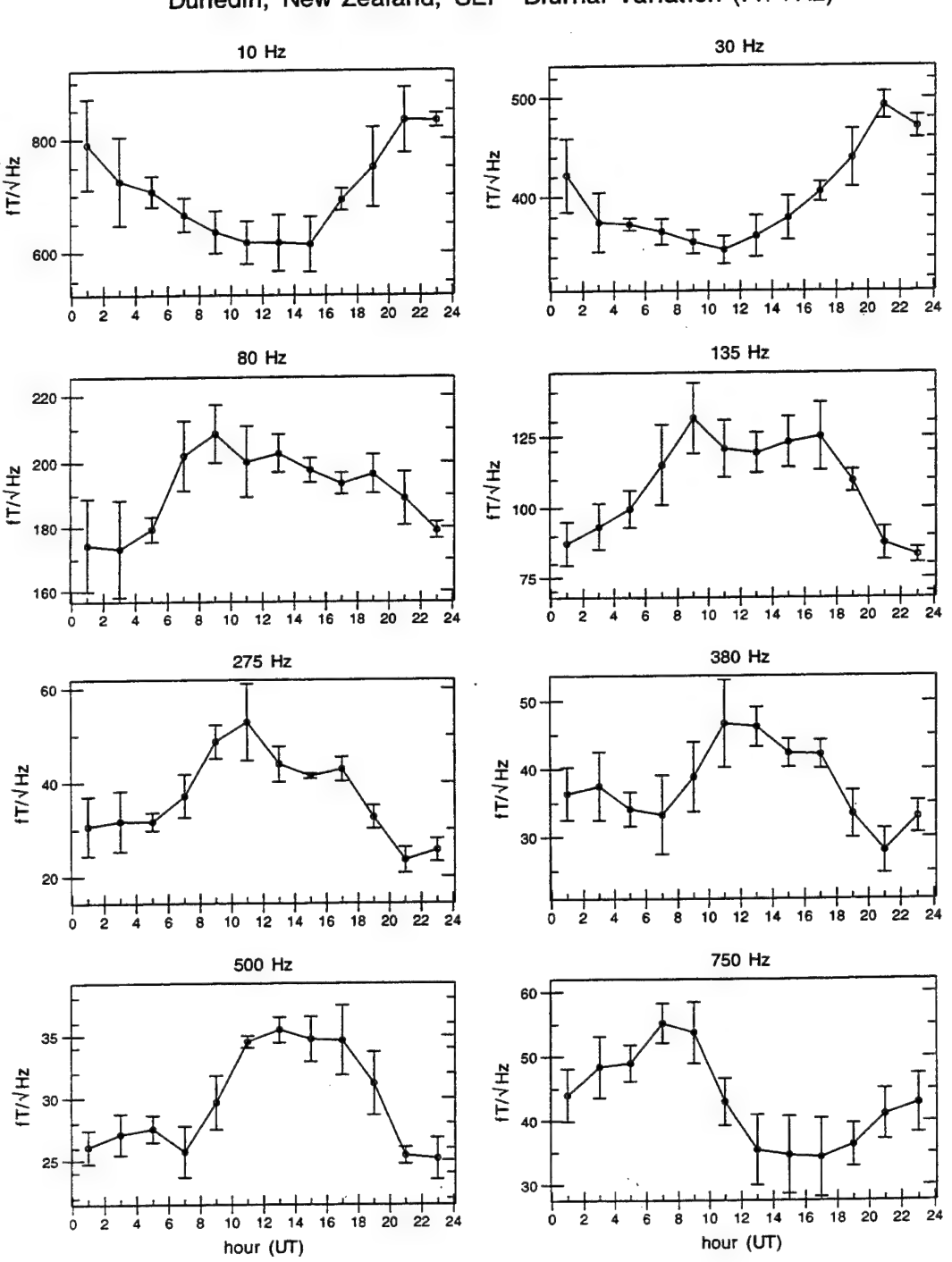

Figure 42: Diurnal variation of ELF/VLF radio noise at Dunedin, New Zealand, during the month of September for the eight lowest-frequency channels. The years 1986 to 1990 are included.

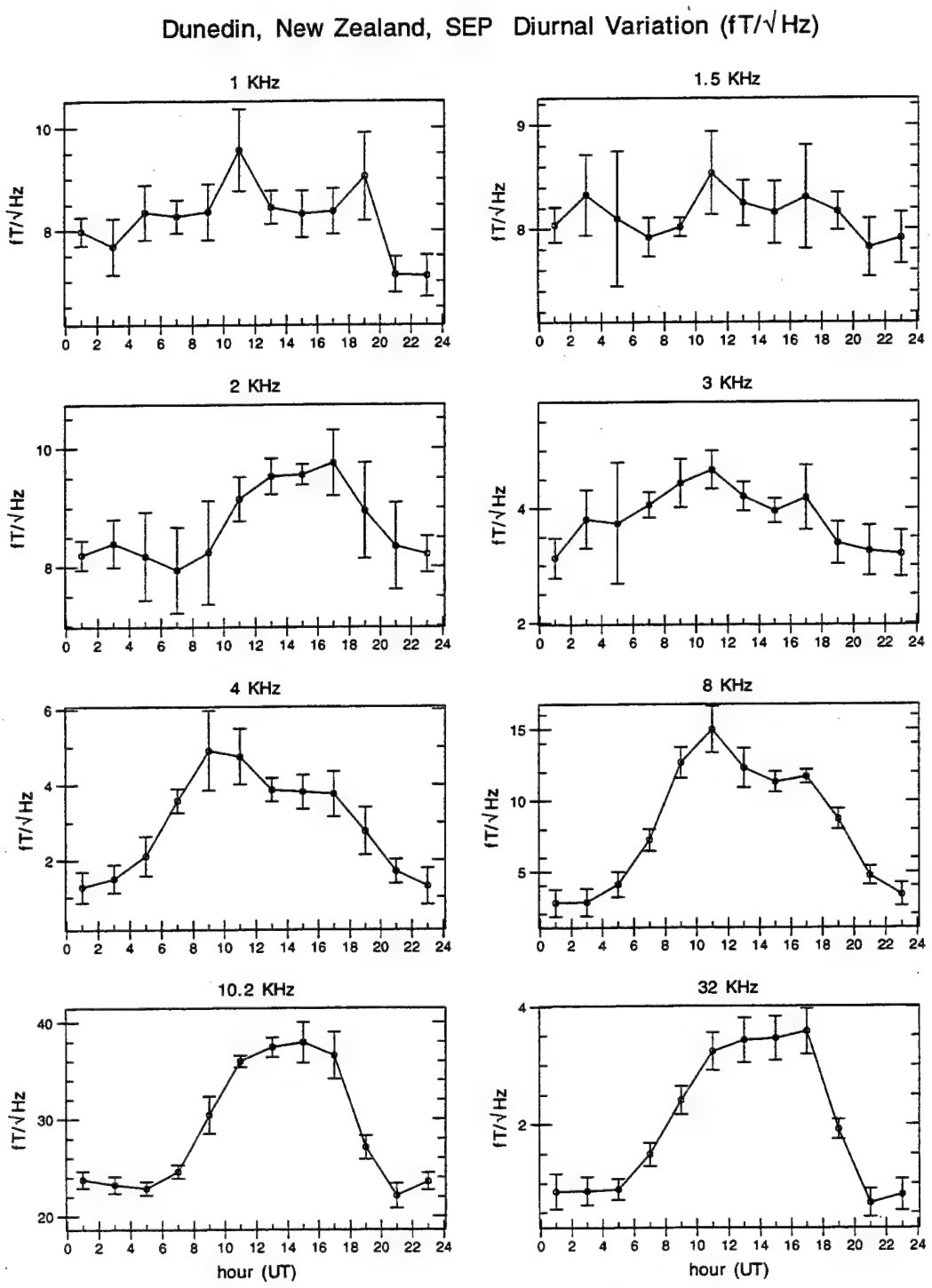

Figure 43: Diurnal variation of ELF/VLF radio noise at Dunedin, New Zealand, during the month of September for the eight highest-frequency channels. The years 1986 to 1990 are included.

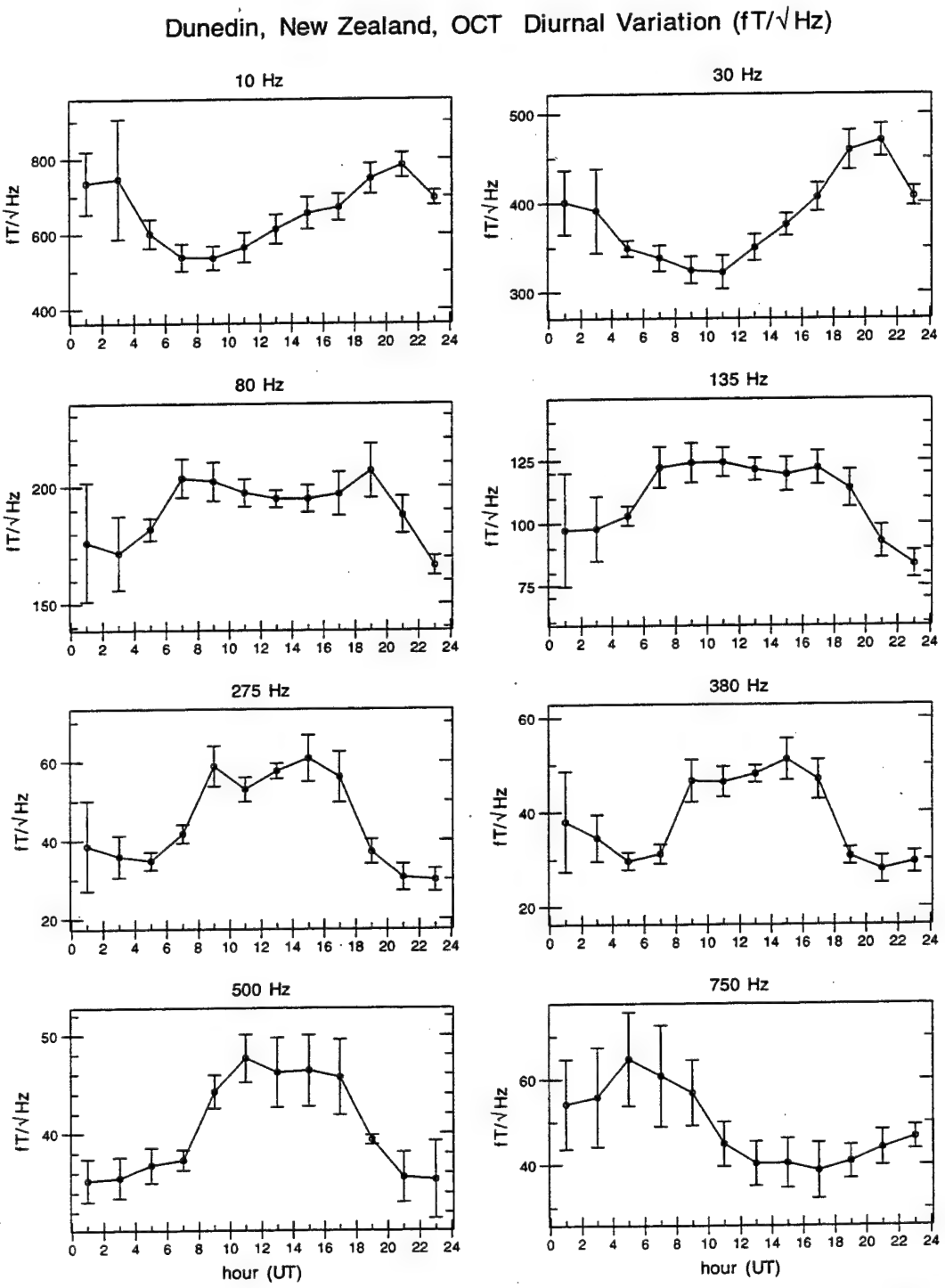

Figure 44: Diurnal variation of ELF/VLF radio noise at Dunedin, New Zealand, during the month of October for the eight lowest-frequency channels. The years 1986 to 1990 are included.

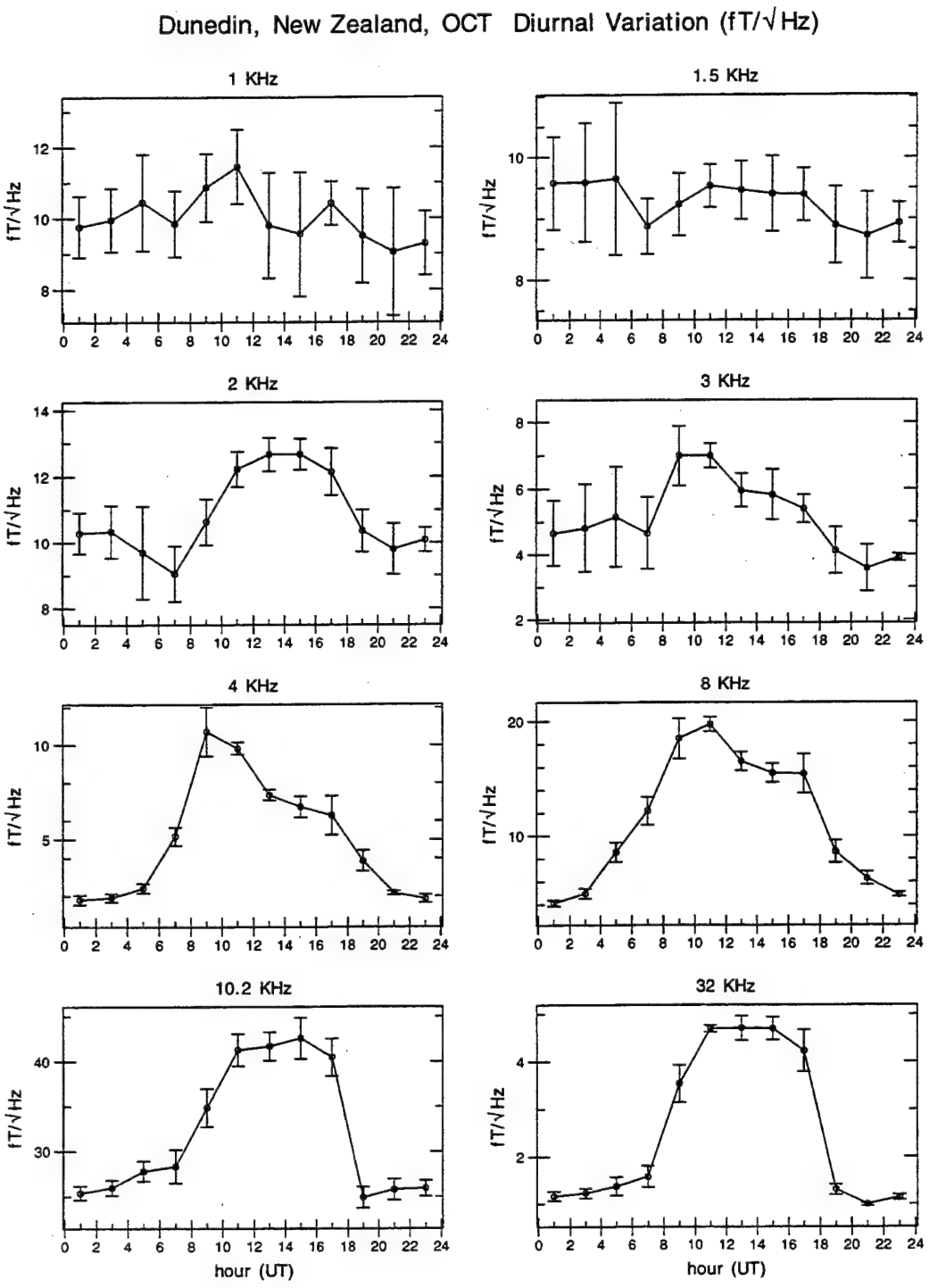

Figure 45: Diurnal variation of ELF/VLF radio noise at Dunedin, New Zealand, during the month of October for the eight highest-frequency channels. The years 1986 to 1990 are included.

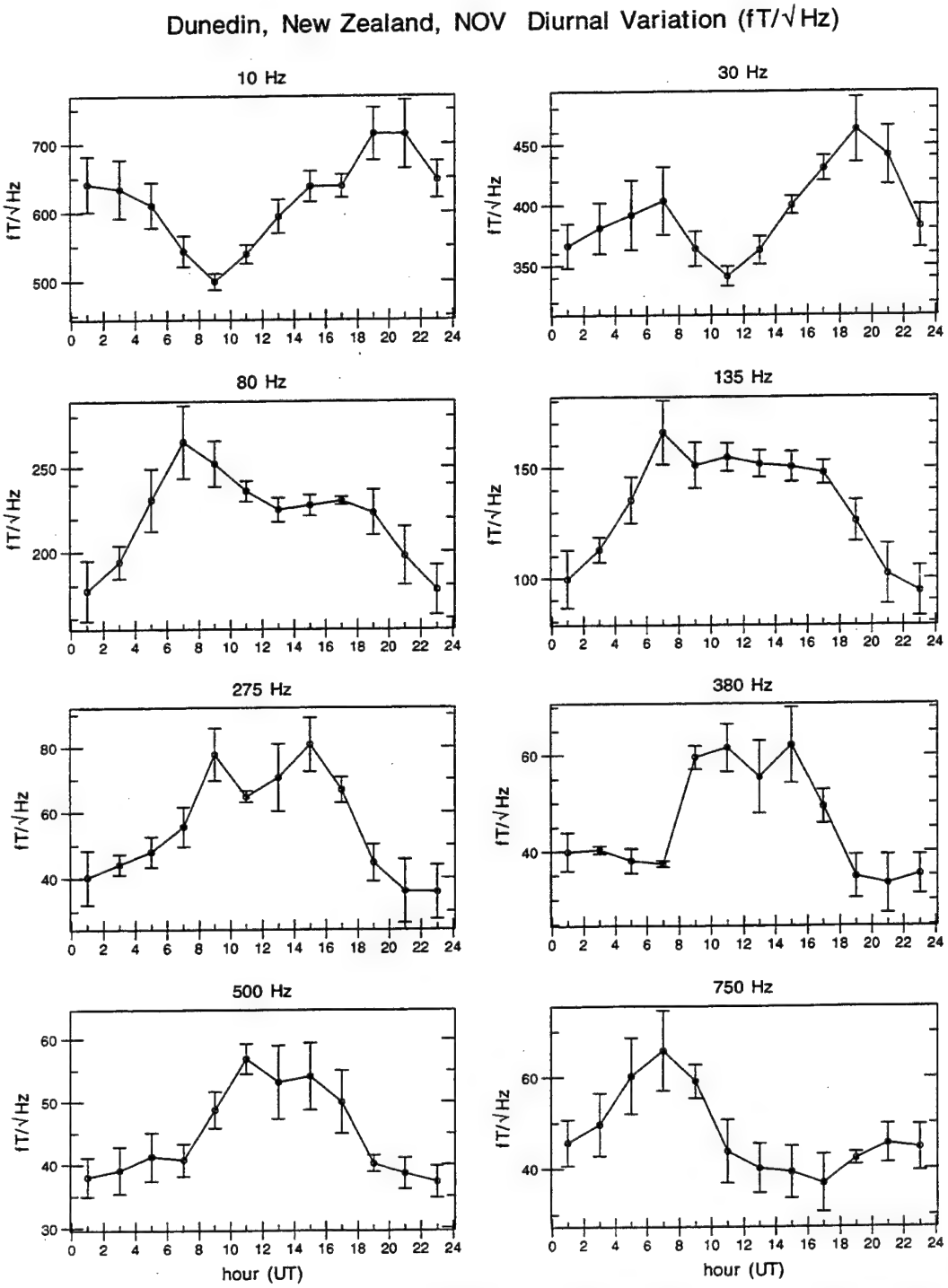

Figure 46: Diurnal variation of ELF/VLF radio noise at Dunedin, New Zealand, during the month of November for the eight lowest-frequency channels. The years 1986 to 1990 are included.

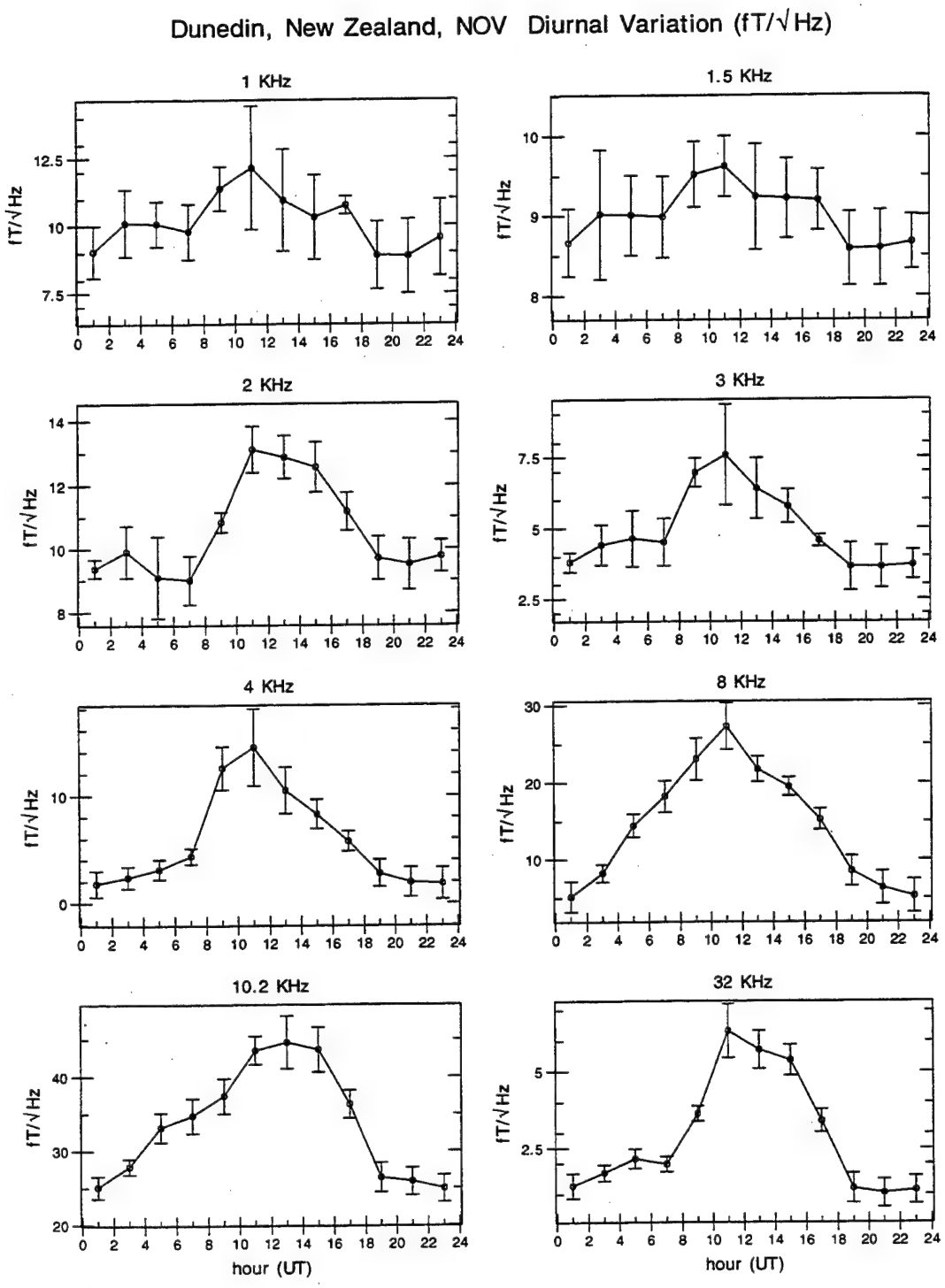

Figure 47: Diurnal variation of ELF/VLF radio noise at Dunedin, New Zealand, during the month of November for the eight highest-frequency channels. The years 1986 to 1990 are included.

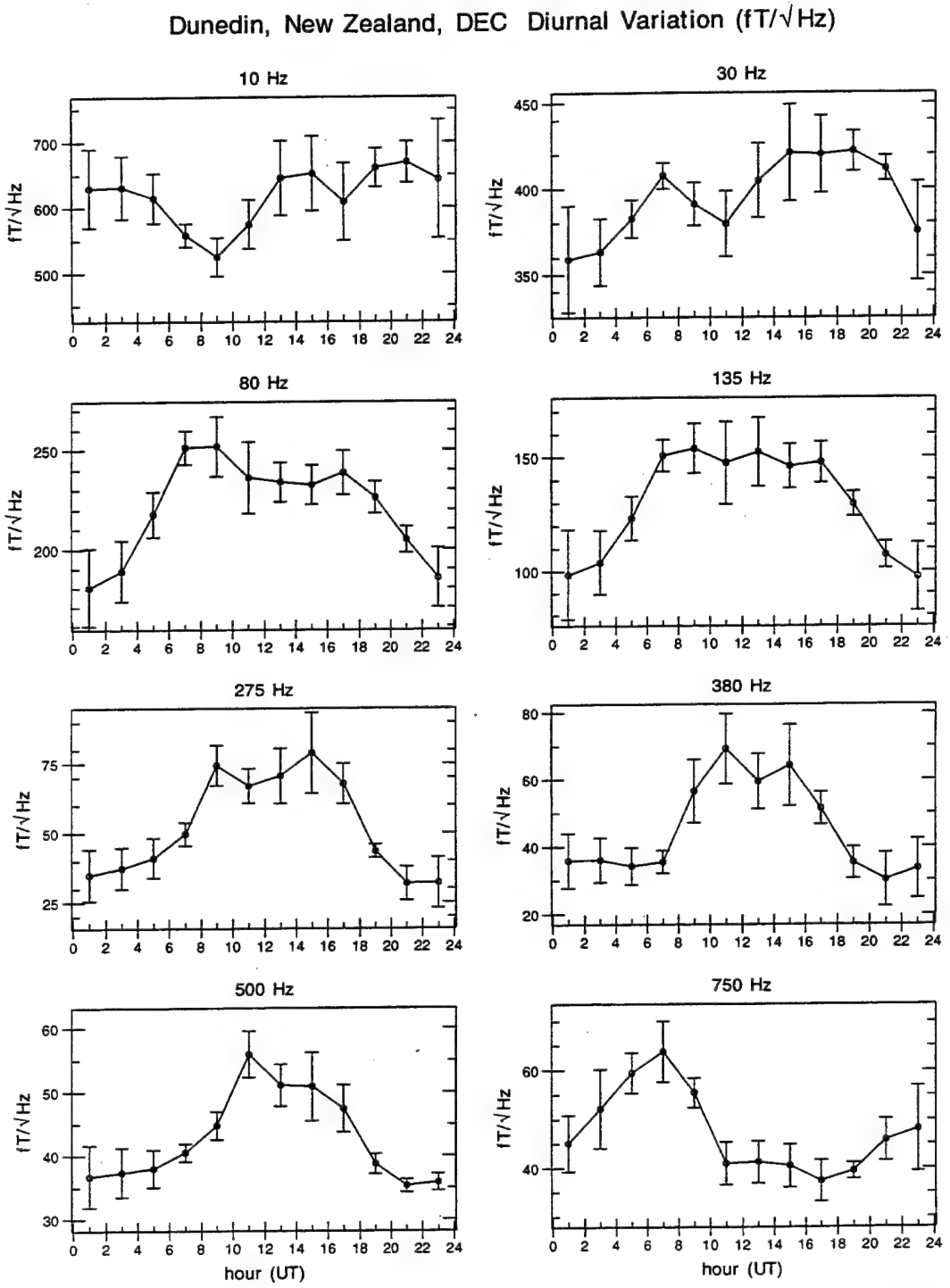

Figure 48: Diurnal variation of ELF/VLF radio noise at Dunedin, New Zealand, during the month of December for the eight lowest-frequency channels. The years 1986 to 1990 are included.

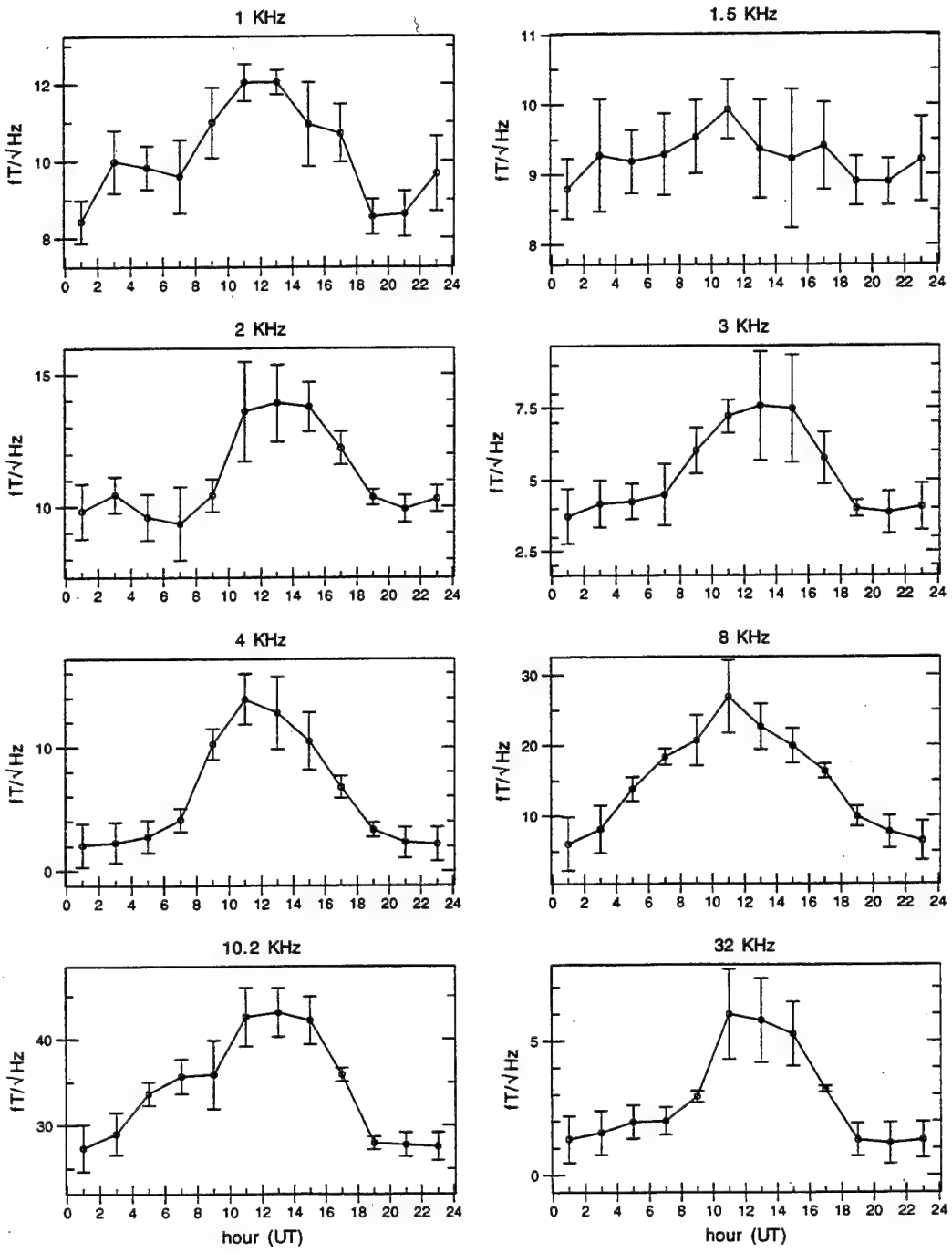

Figure 49: Diurnal variation of ELF/VLF radio noise at Dunedin, New Zealand, during the month of December for the eight highest-frequency channels. The years 1986 to 1990 are included.

10 Søndrestrøm, Greenland Diurnal Variation Figures

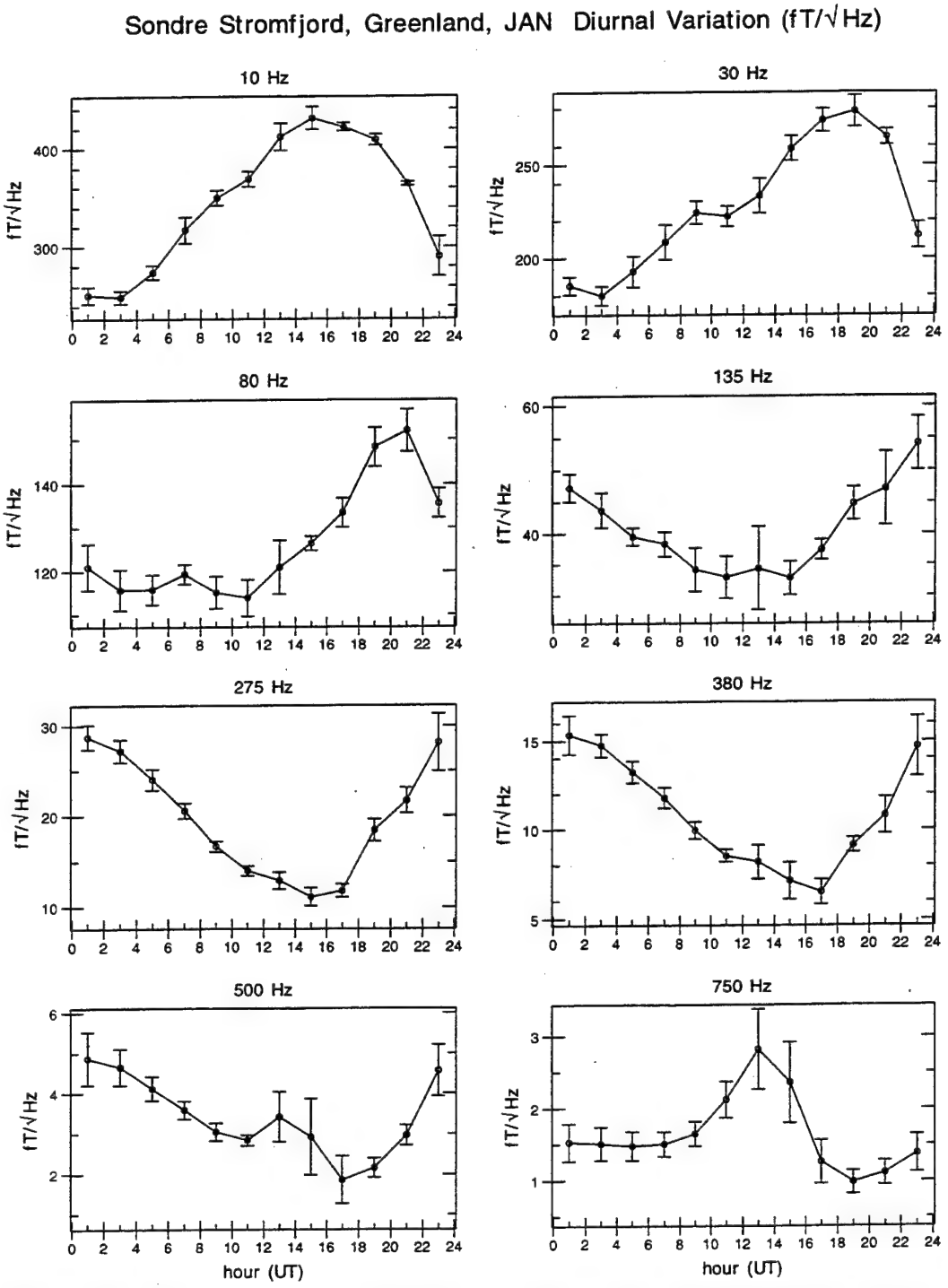

Figure 50: Diurnal variation of ELF/VLF radio noise at Søndrestrøm, Greenland, during the month of January for the eight lowest-frequency channels. The years 1986 to 1991 and the year 1993 are included.

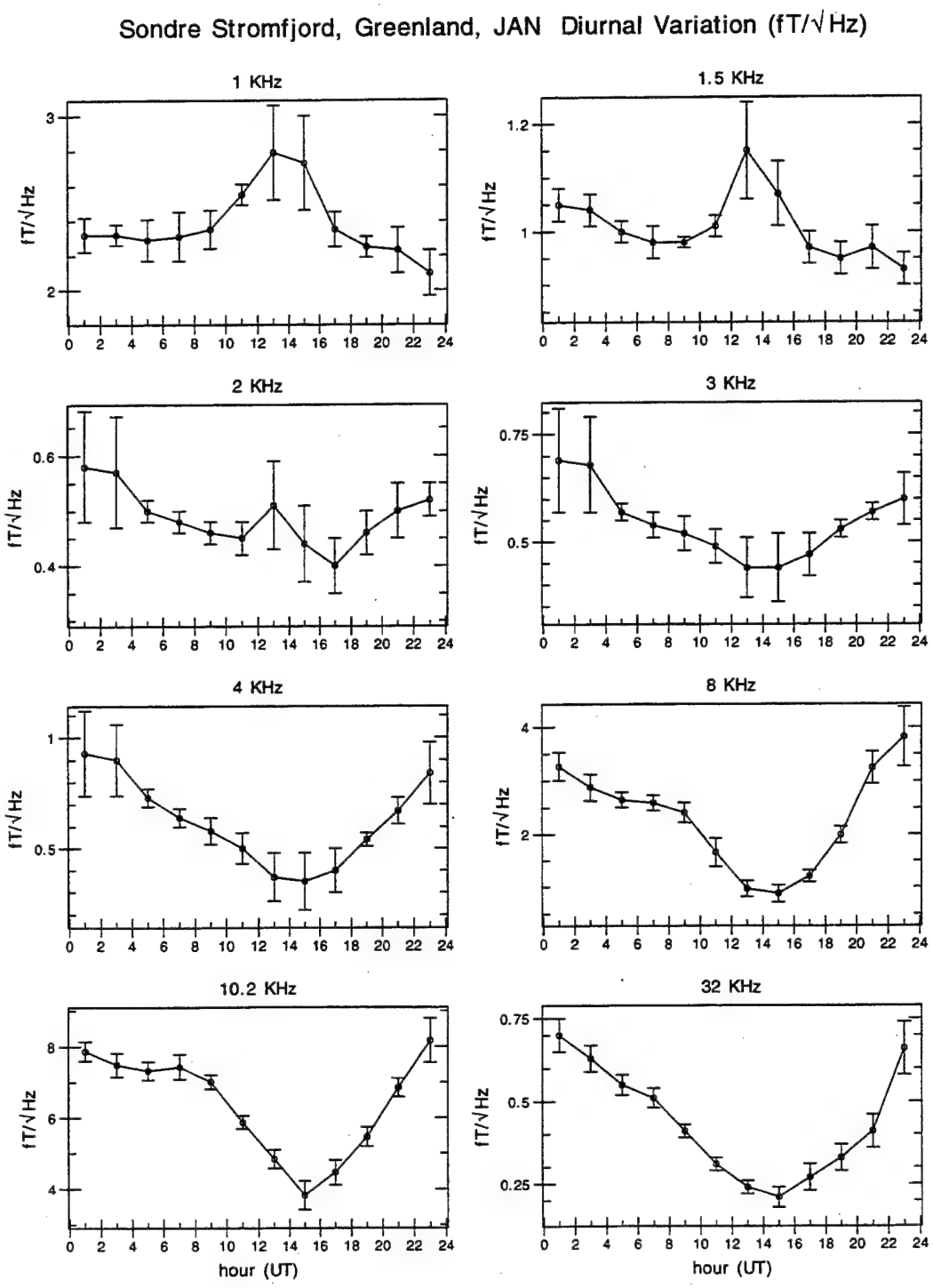

Figure 51: Diurnal variation of ELF/VLF radio noise at Søndrestrøm, Greenland, during the month of January for the eight highest-frequency channels. The years 1986 to 1991 and the year 1993 are included.

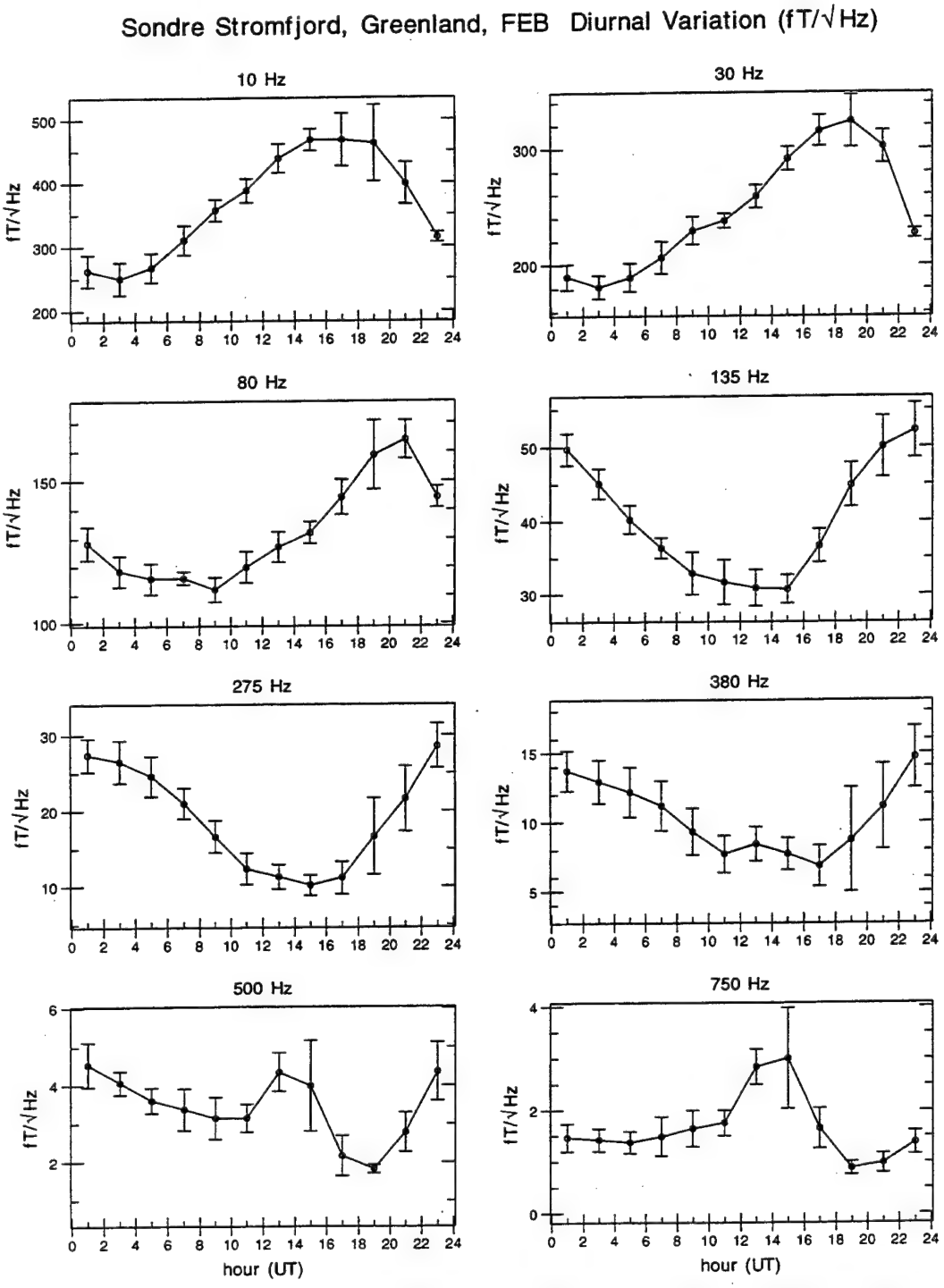

Figure 52: Diurnal variation of ELF/VLF radio noise at Søndrestrøm, Greenland, during the month of February for the eight lowest-frequency channels. The years 1986 to 1991 and the year 1993 are included.

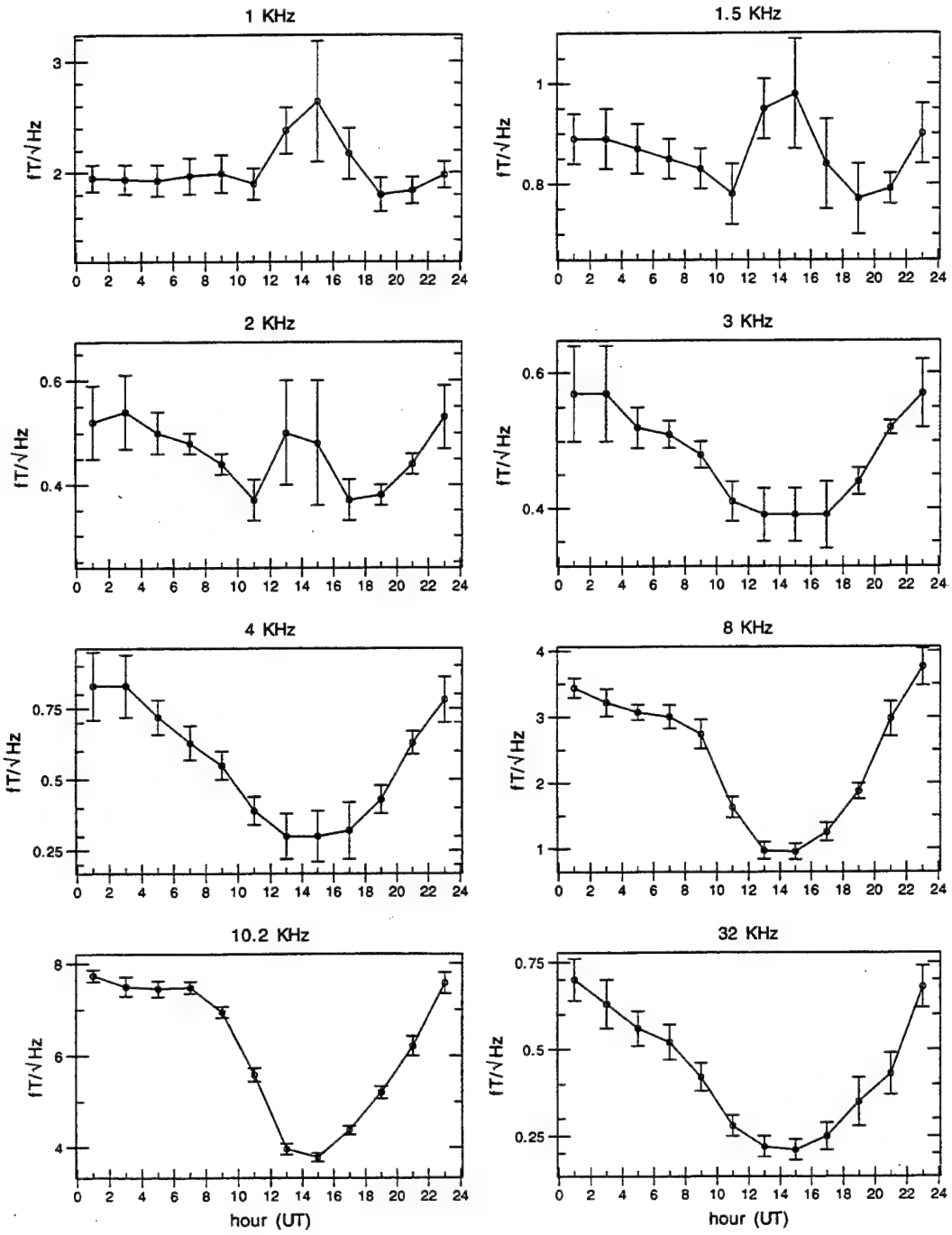

Figure 53: Diurnal variation of ELF/VLF radio noise at Søndrestrøm, Greenland, during the month of February for the eight highest-frequency channels. The years 1986 to 1991 and the year 1993 are included.

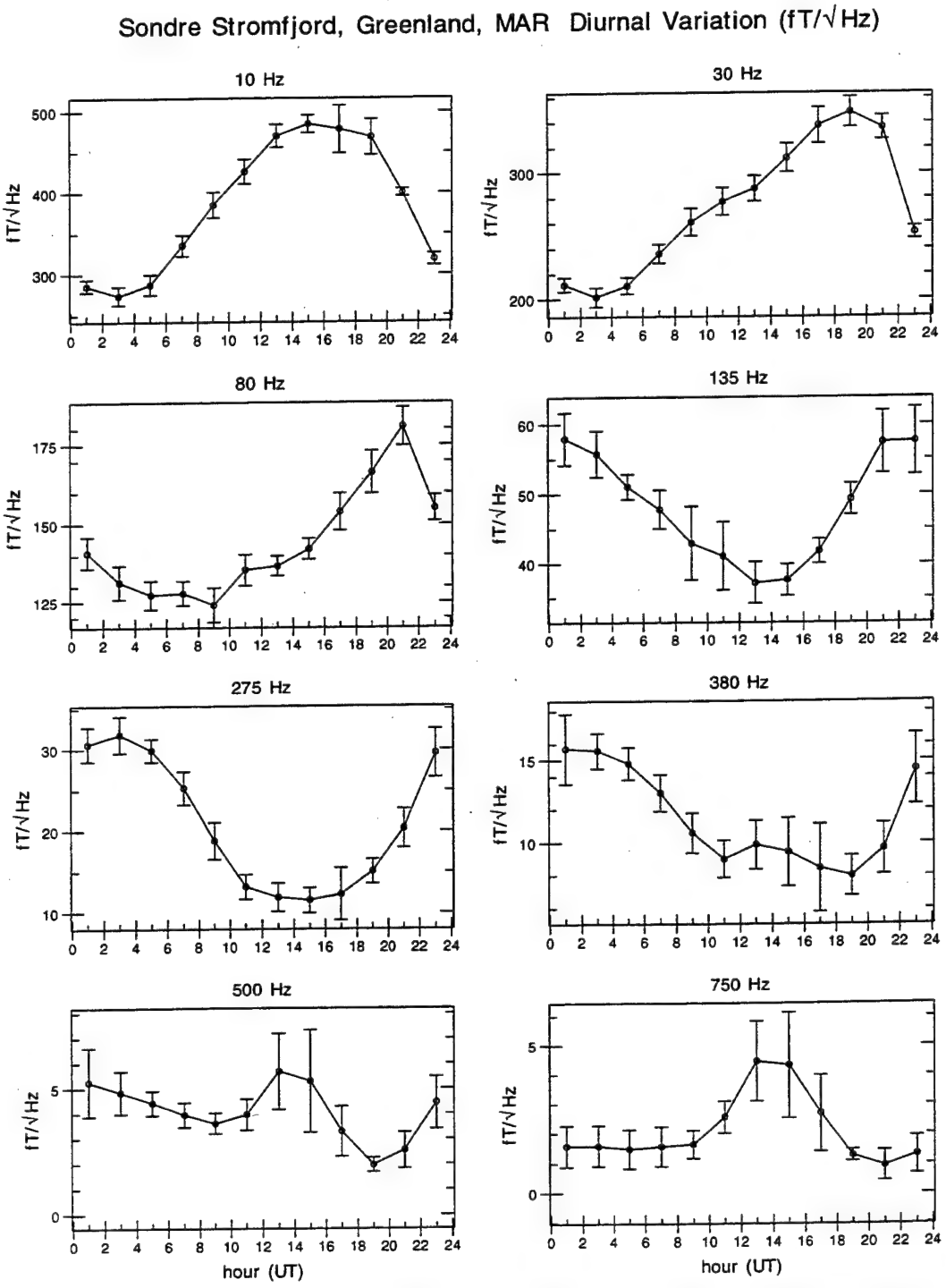

Figure 54: Diurnal variation of ELF/VLF radio noise at Søndrestrøm, Greenland, during the month of March for the eight lowest-frequency channels. The years 1986 to 1991 and the year 1993 are included.

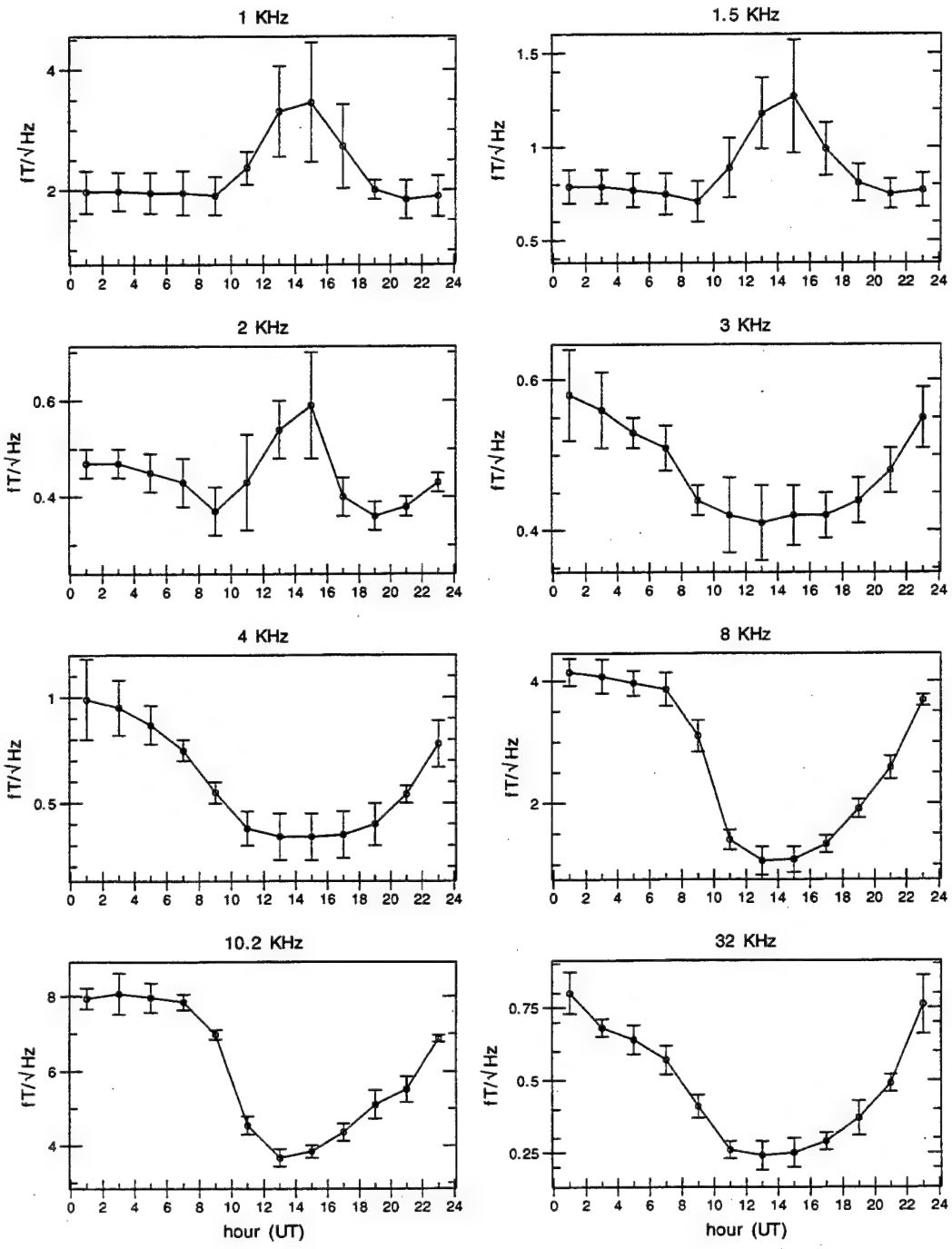

Figure 55: Diurnal variation of ELF/VLF radio noise at Søndrestrøm, Greenland, during the month of March for the eight highest-frequency channels. The years 1986 to 1991 and the year 1993 are included.

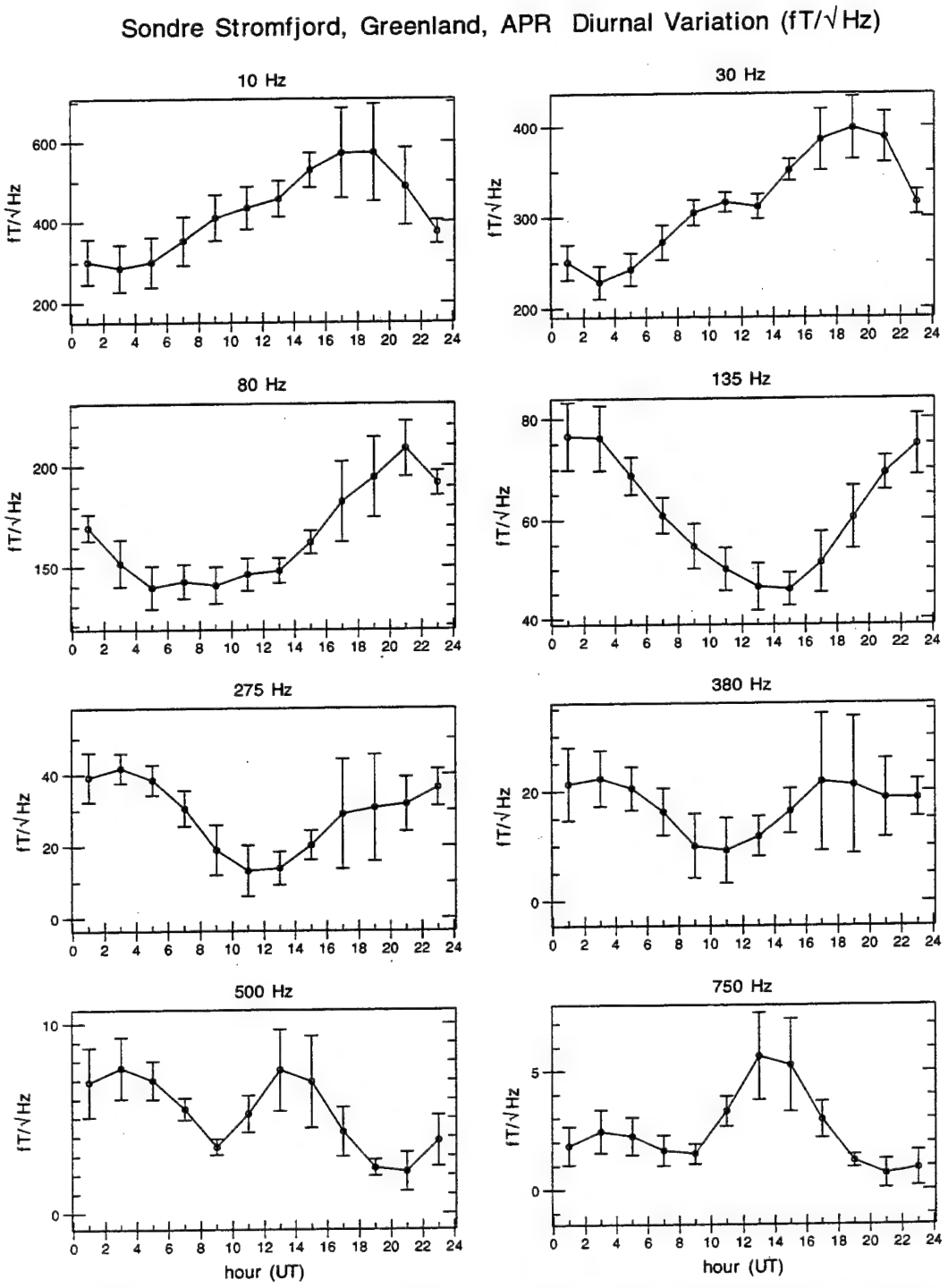

Figure 56: Diurnal variation of ELF/VLF radio noise at Søndrestrøm, Greenland, during the month of April for the eight lowest-frequency channels. The years 1986 to 1991 and the year 1993 are included.

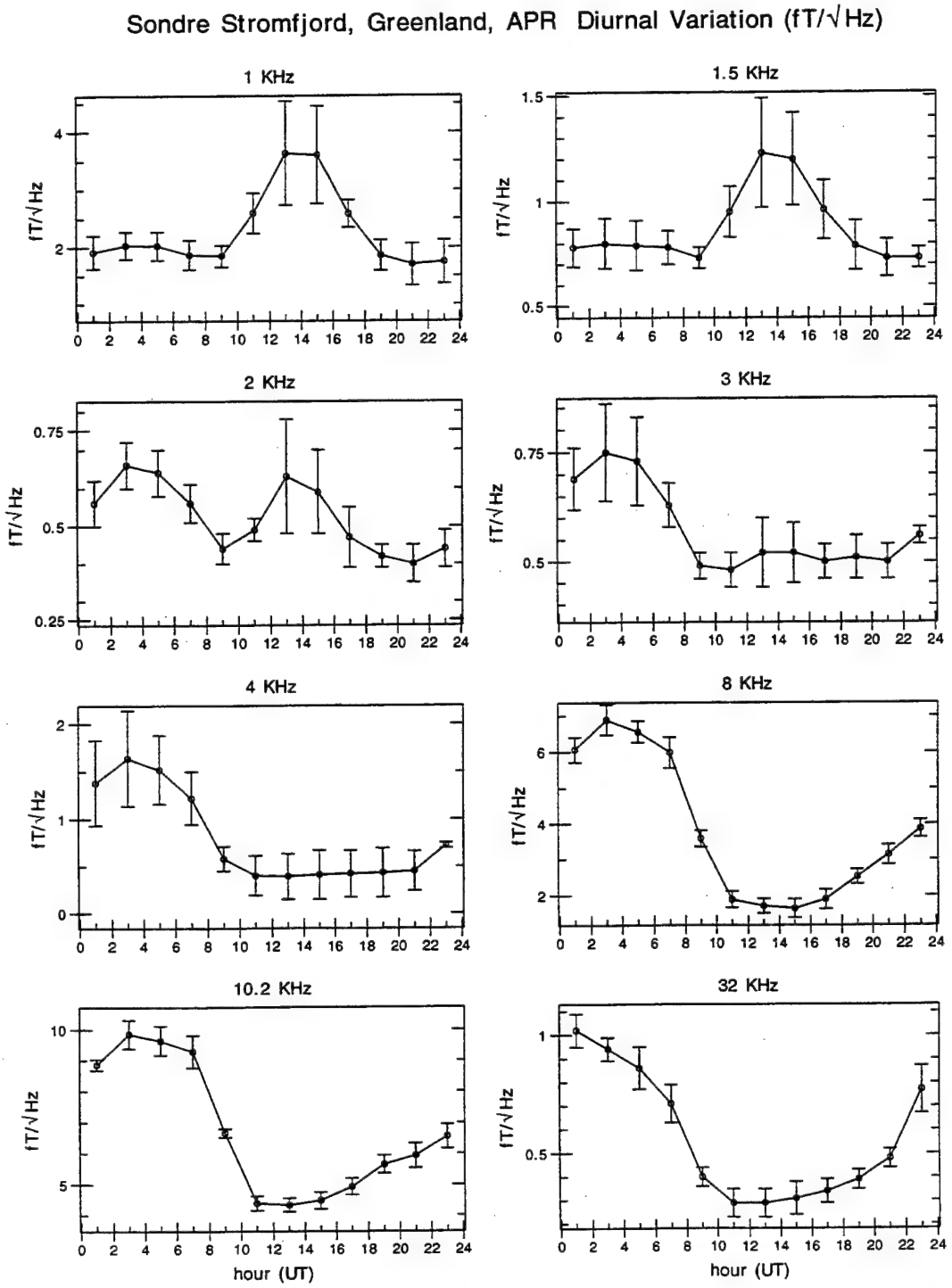

Figure 57: Diurnal variation of ELF/VLF radio noise at Søndrestrøm, Greenland, during the month of April for the eight highest-frequency channels. The years 1986 to 1991 and the year 1993 are included.

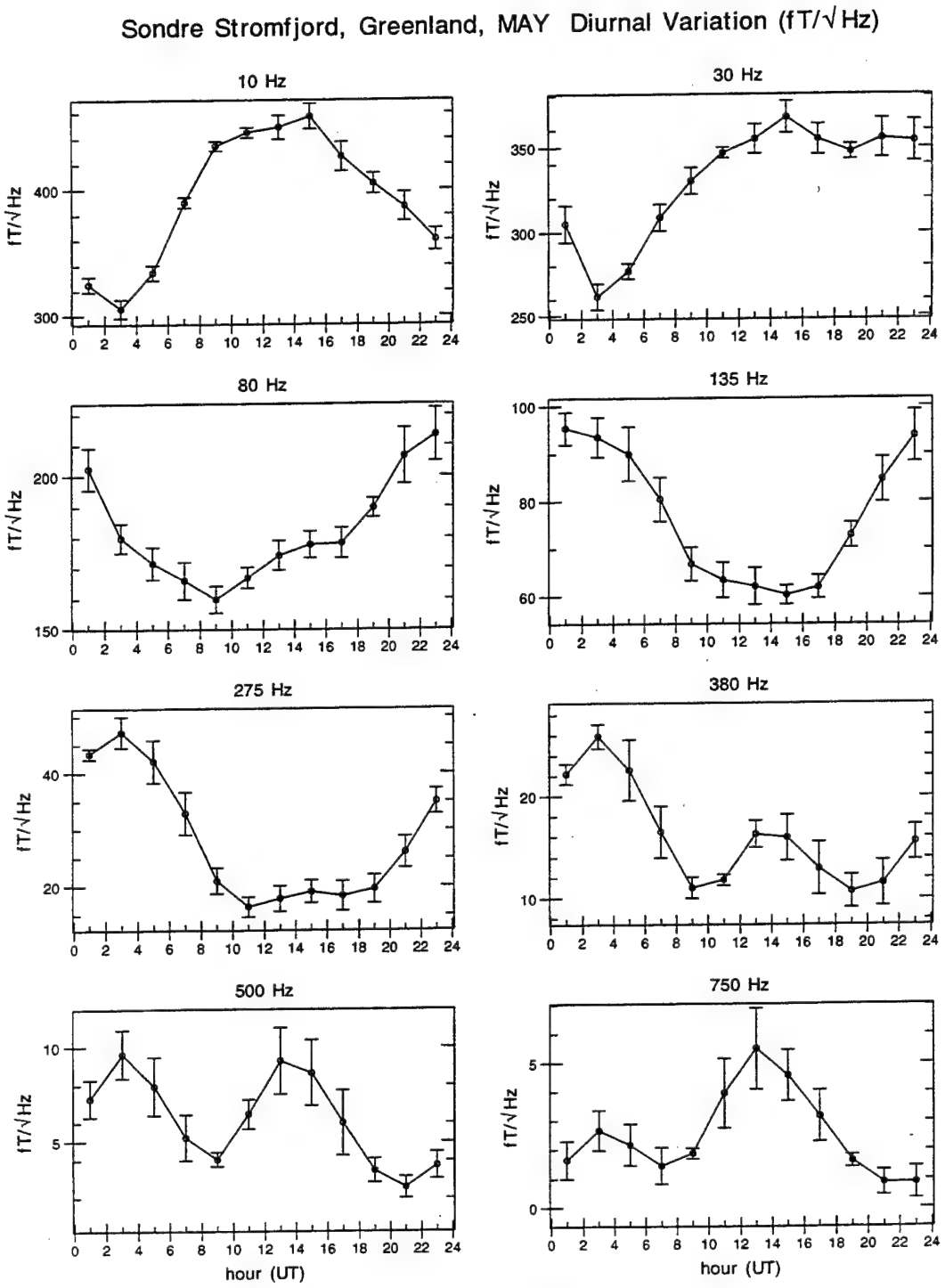

Figure 58: Diurnal variation of ELF/VLF radio noise at Søndrestrøm, Greenland, during the month of May for the eight lowest-frequency channels. The years 1986 to 1991 and the year 1993 are included.

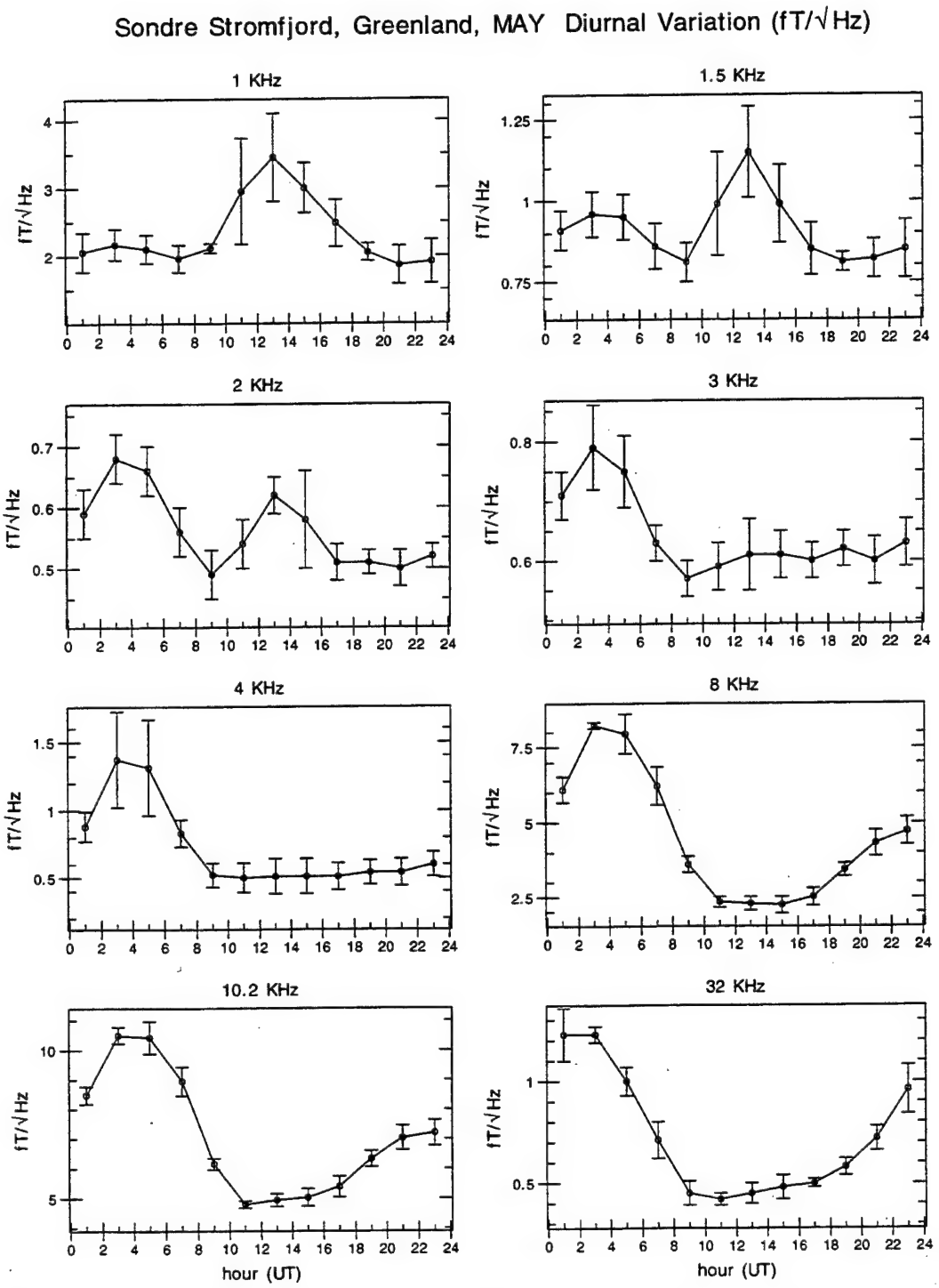

Figure 59: Diurnal variation of ELF/VLF radio noise at Søndrestrøm, Greenland, during the month of May for the eight highest-frequency channels. The years 1986 to 1991 and the year 1993 are included.

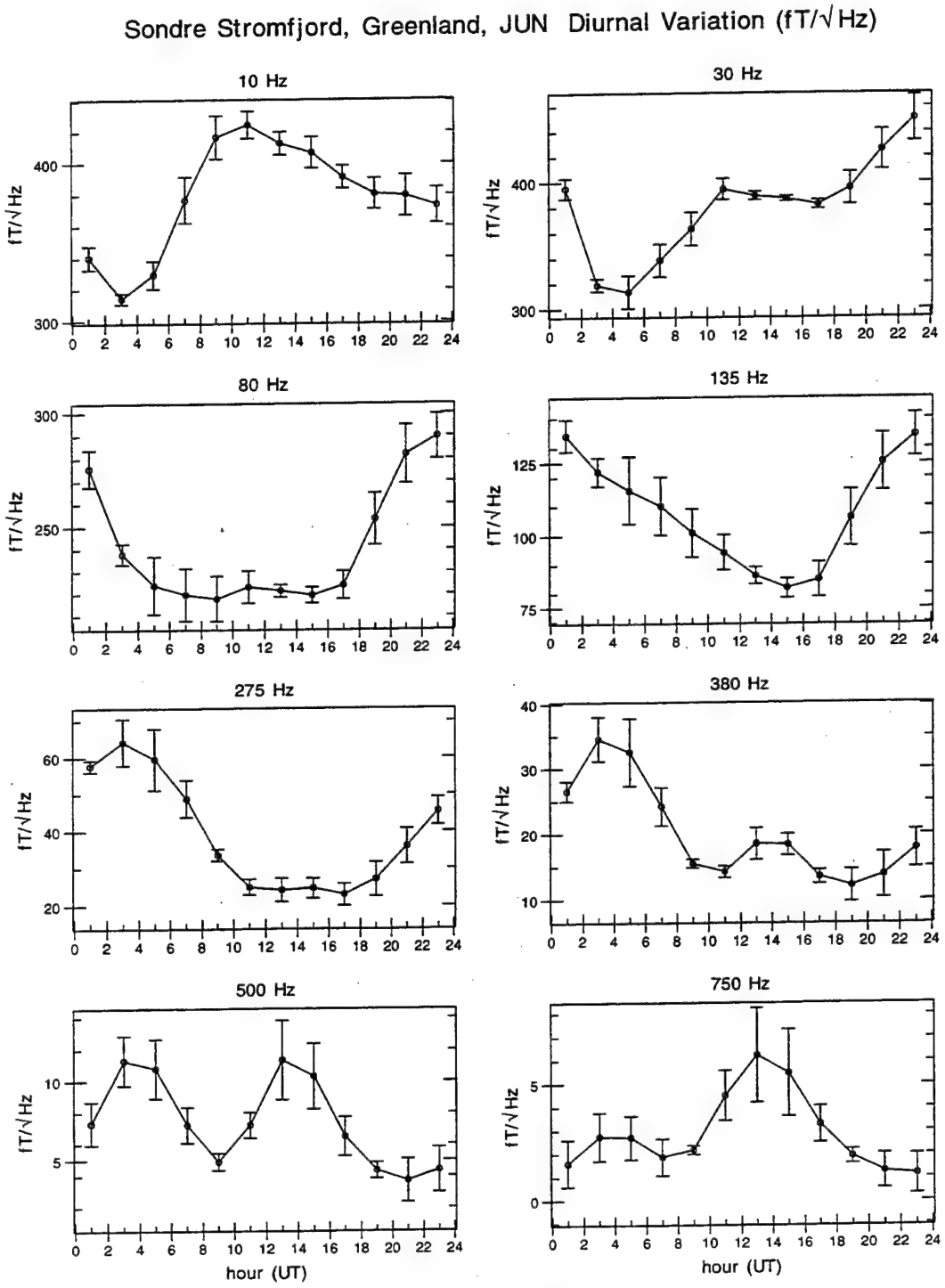

Figure 60: Diurnal variation of ELF/VLF radio noise at Søndrestrøm, Greenland, during the month of June for the eight lowest-frequency channels. The years 1986 to 1991 and the year 1993 are included.

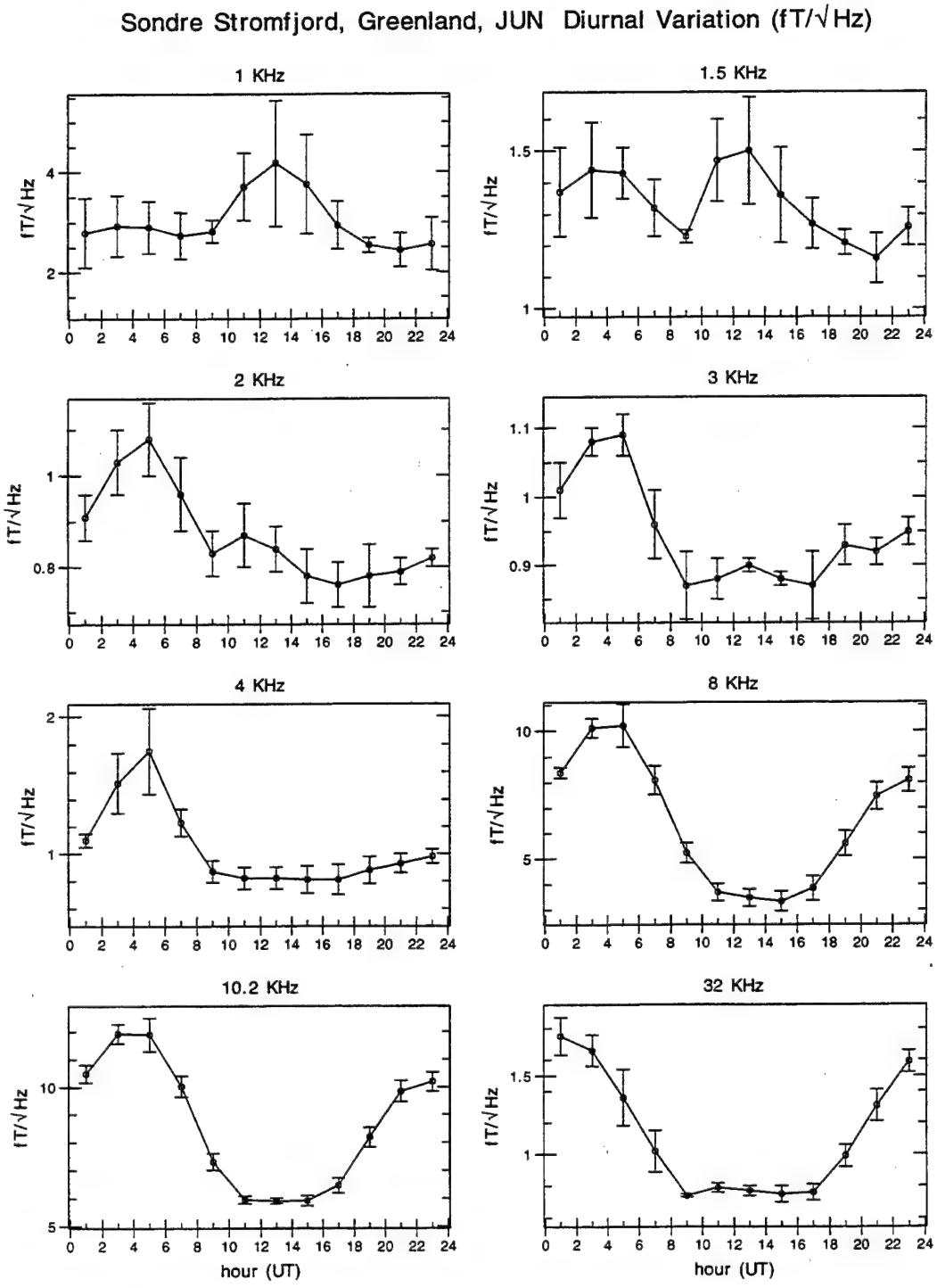

Figure 61: Diurnal variation of ELF/VLF radio noise at Søndrestrøm, Greenland, during the month of June for the eight highest-frequency channels. The years 1986 to 1991 and the year 1993 are included.

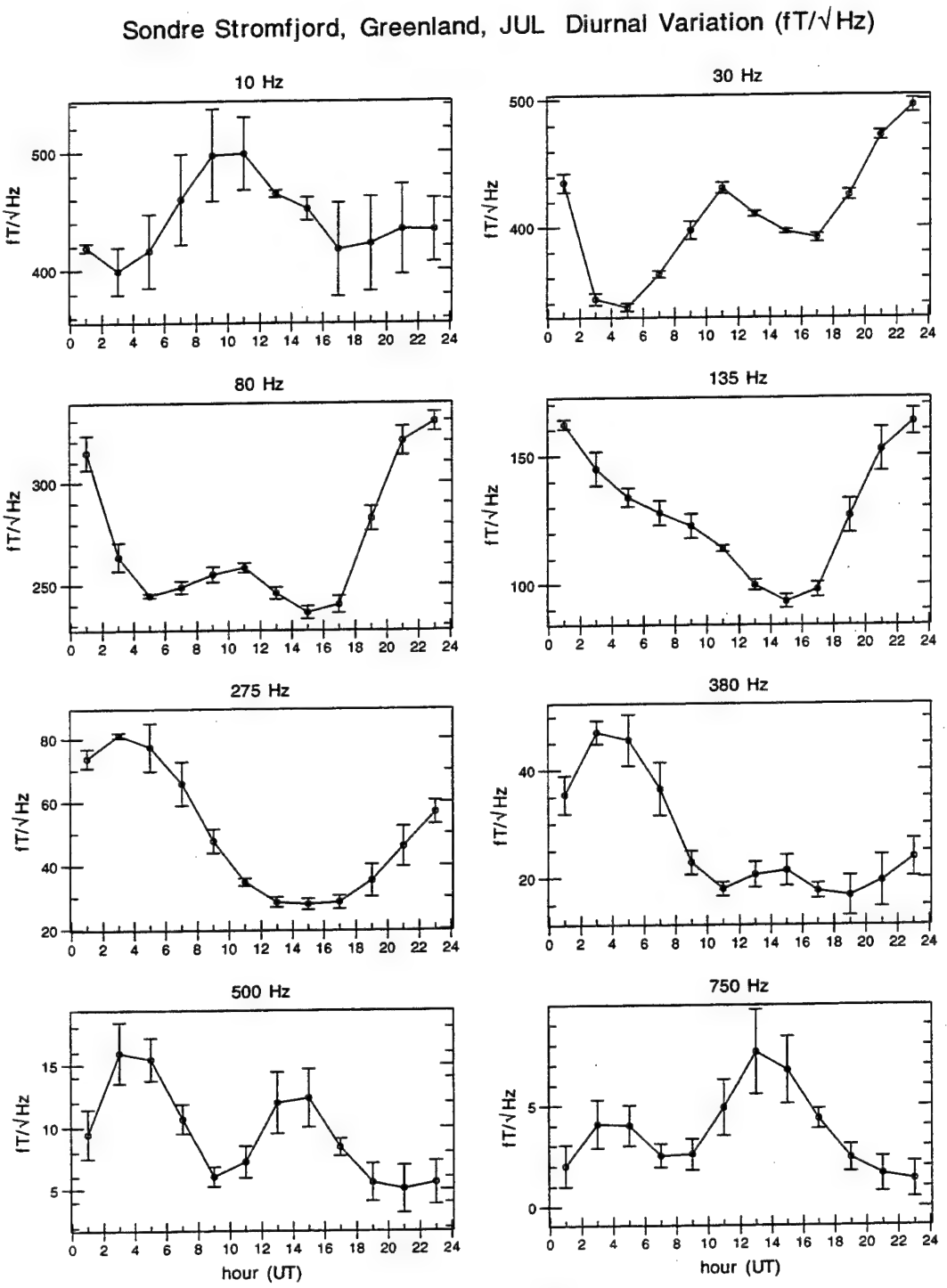

Figure 62: Diurnal variation of ELF/VLF radio noise at Søndrestrøm, Greenland, during the month of July for the eight lowest-frequency channels. The years 1986 to 1991 and the year 1993 are included.

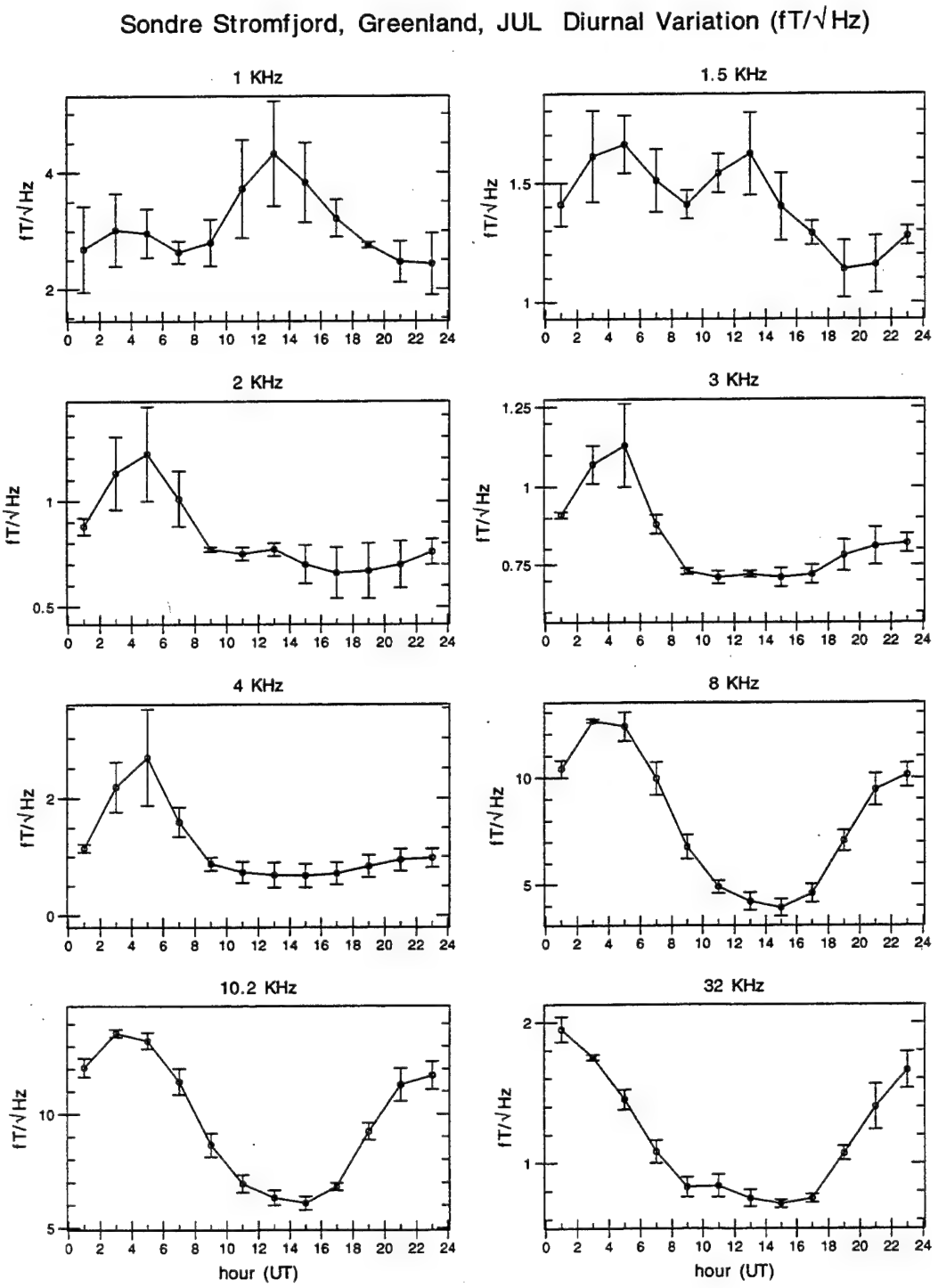

Figure 63: Diurnal variation of ELF/VLF radio noise at Søndrestrøm, Greenland, during the month of July for the eight highest-frequency channels. The years 1986 to 1991 and the year 1993 are included.

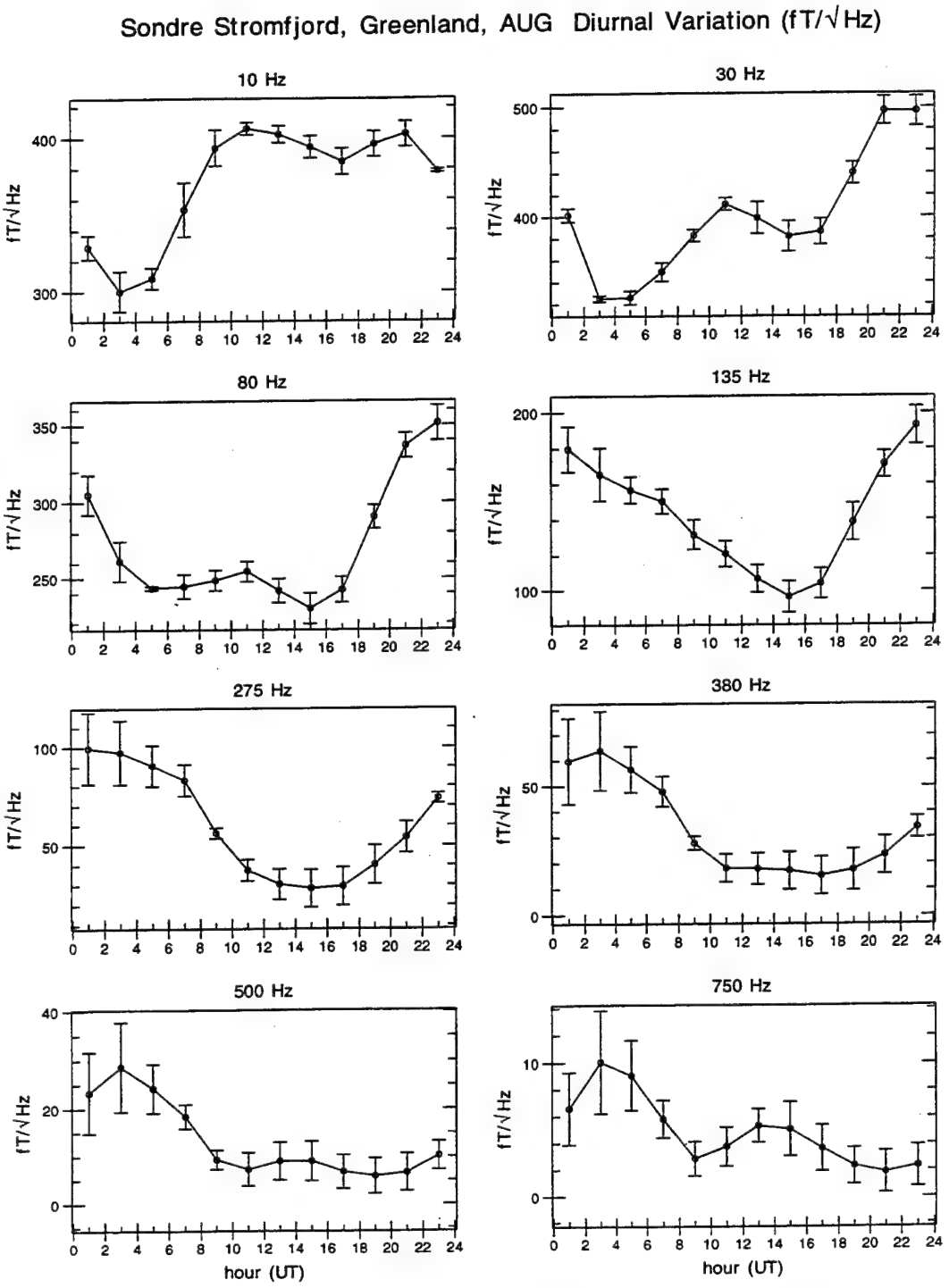

Figure 64: Diurnal variation of ELF/VLF radio noise at Søndrestrøm, Greenland, during the month of August for the eight lowest-frequency channels. The years 1986 to 1991 and the year 1993 are included.

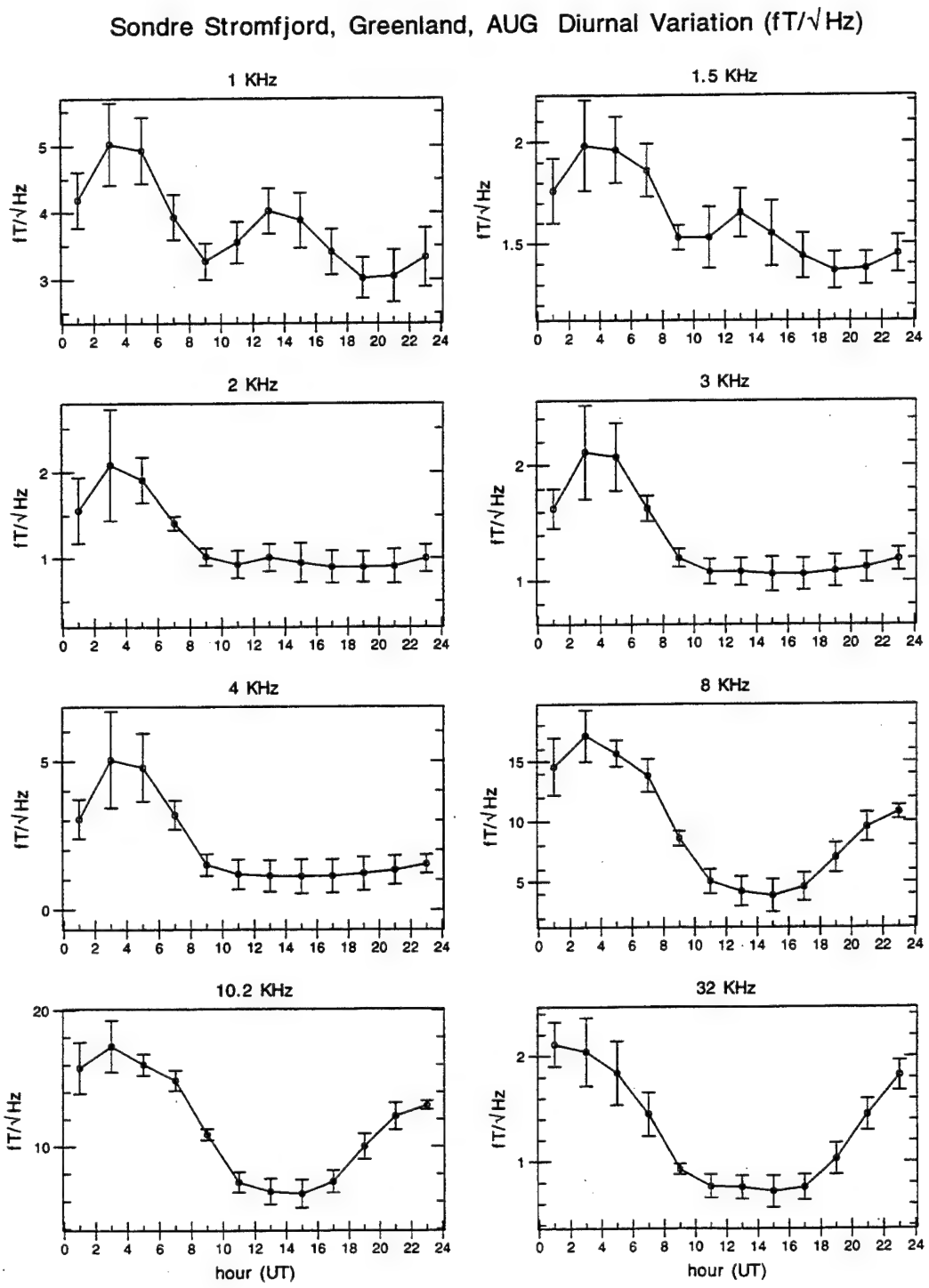

Figure 65: Diurnal variation of ELF/VLF radio noise at Søndrestrøm, Greenland, during the month of August for the eight highest-frequency channels. The years 1986 to 1991 and the year 1993 are included.

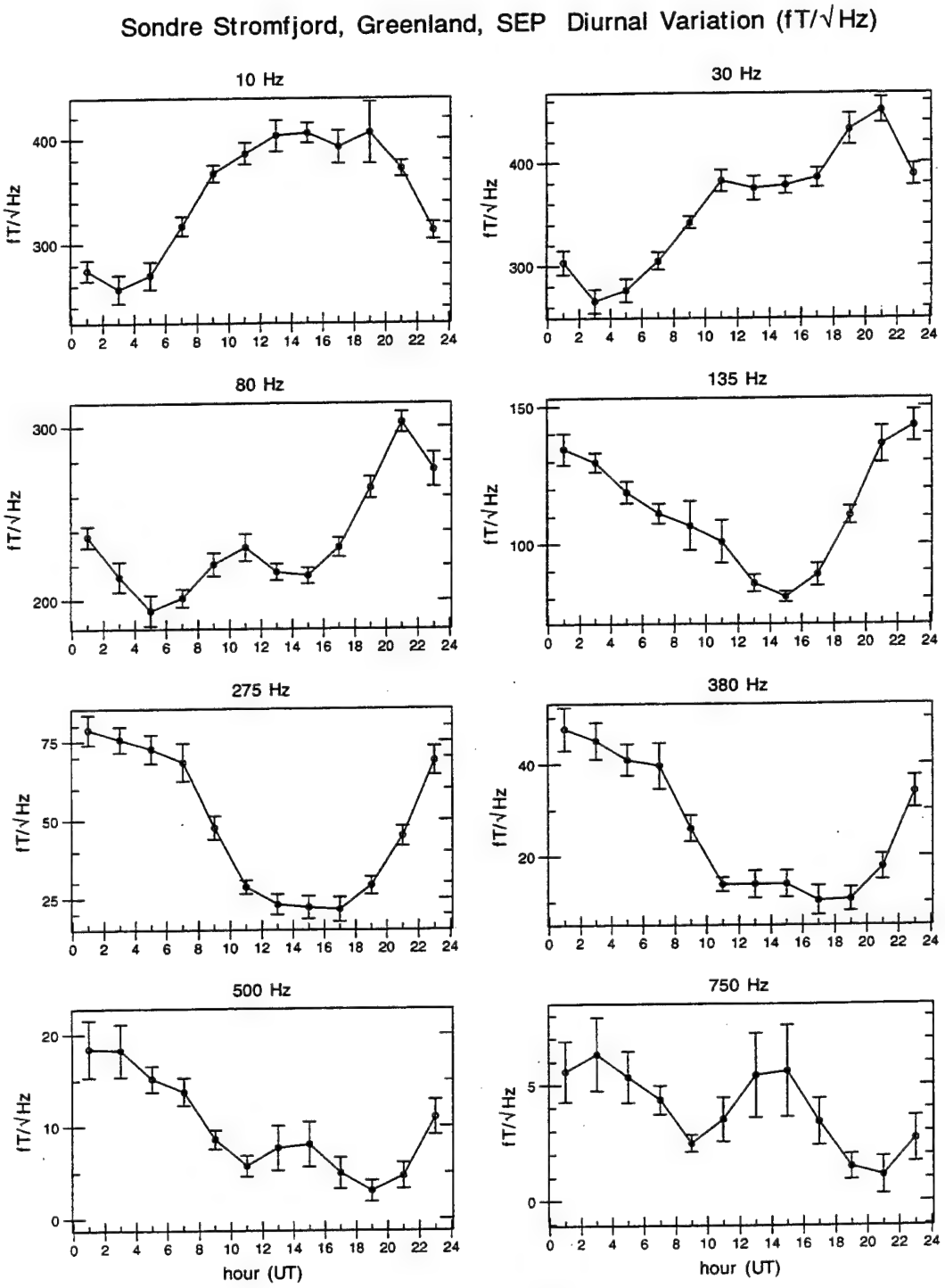

Figure 66: Diurnal variation of ELF/VLF radio noise at Søndrestrøm, Greenland, during the month of September for the eight lowest-frequency channels. The years 1986 to 1991 and the year 1993 are included.

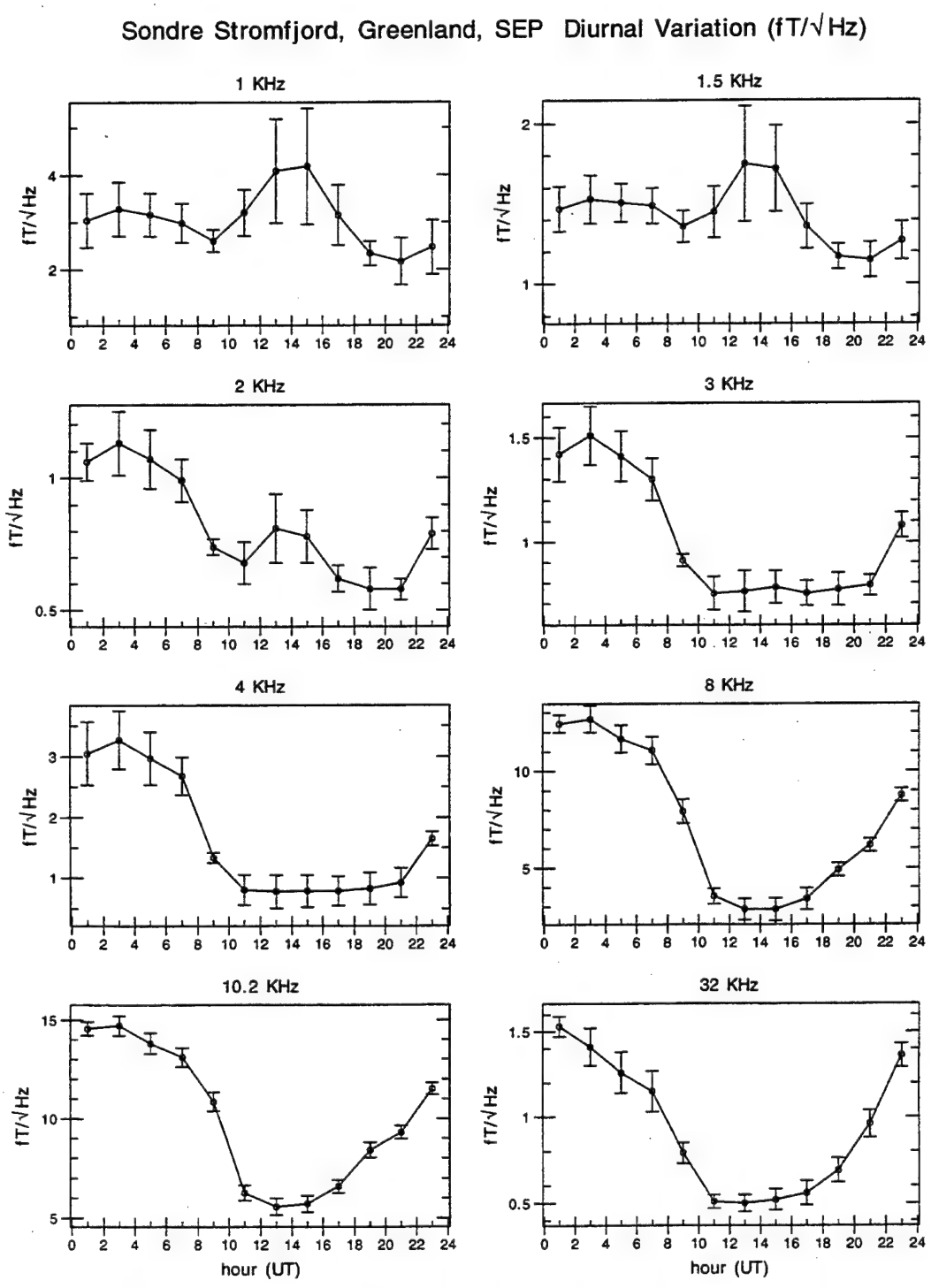

Figure 67: Diurnal variation of ELF/VLF radio noise at Søndrestrøm, Greenland, during the month of September for the eight highest-frequency channels. The years 1986 to 1991 and the year 1993 are included.

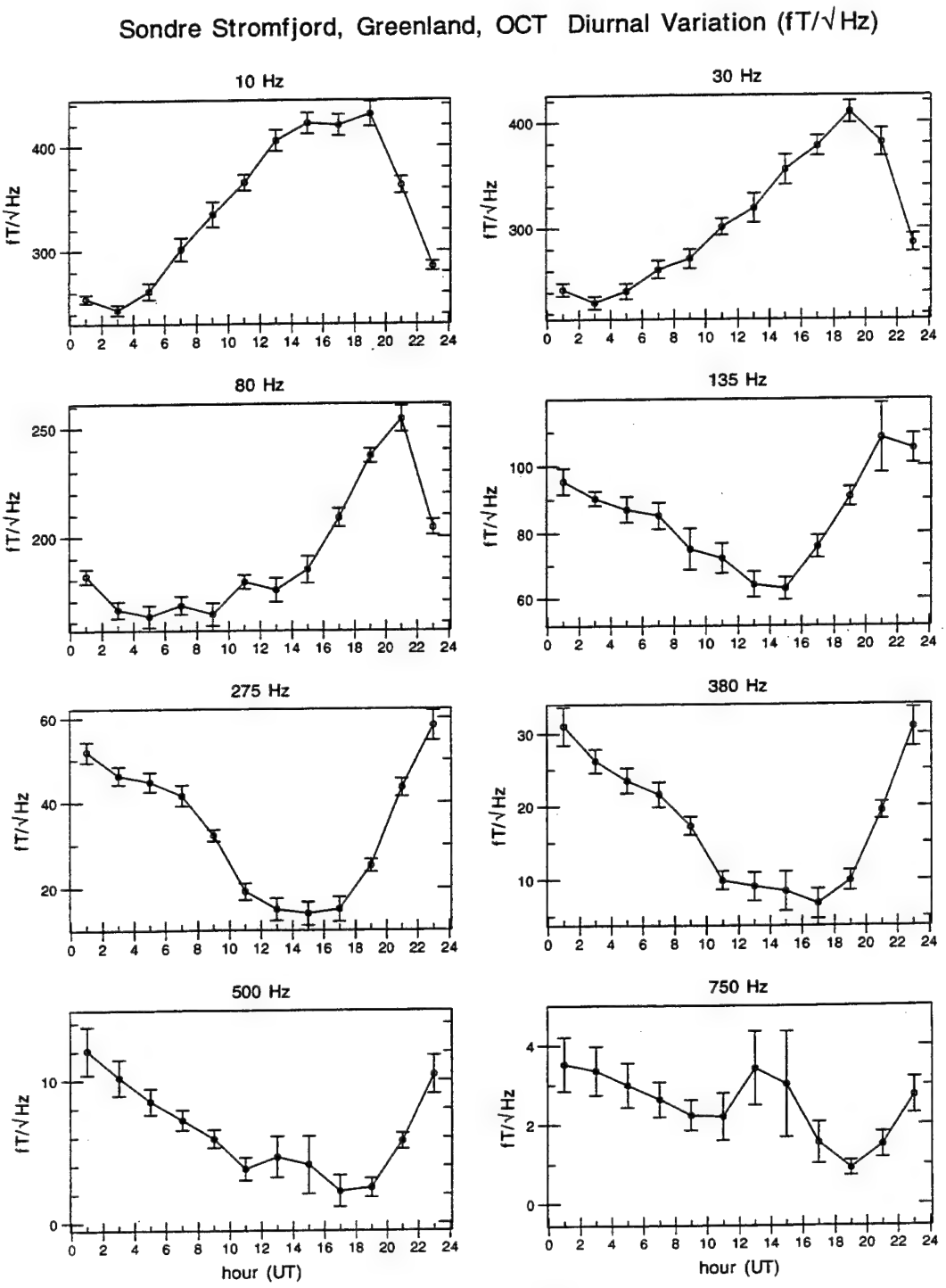

Figure 68: Diurnal variation of ELF/VLF radio noise at Søndrestrøm, Greenland, during the month of October for the eight lowest-frequency channels. The years 1986 to 1991 and the year 1993 are included.

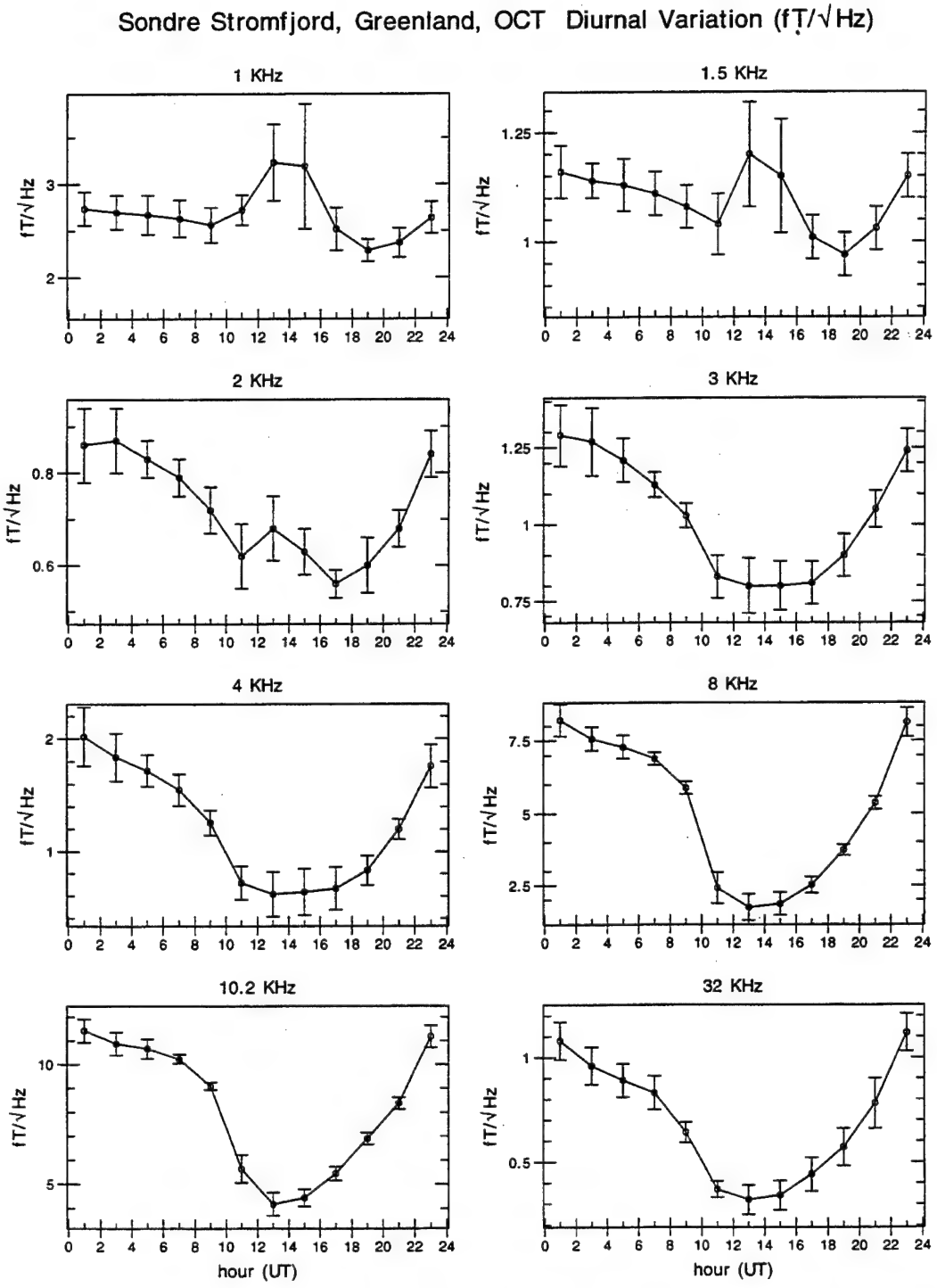

Figure 69: Diurnal variation of ELF/VLF radio noise at Søndrestrøm, Greenland, during the month of October for the eight highest-frequency channels. The years 1986 to 1991 and the year 1993 are included.

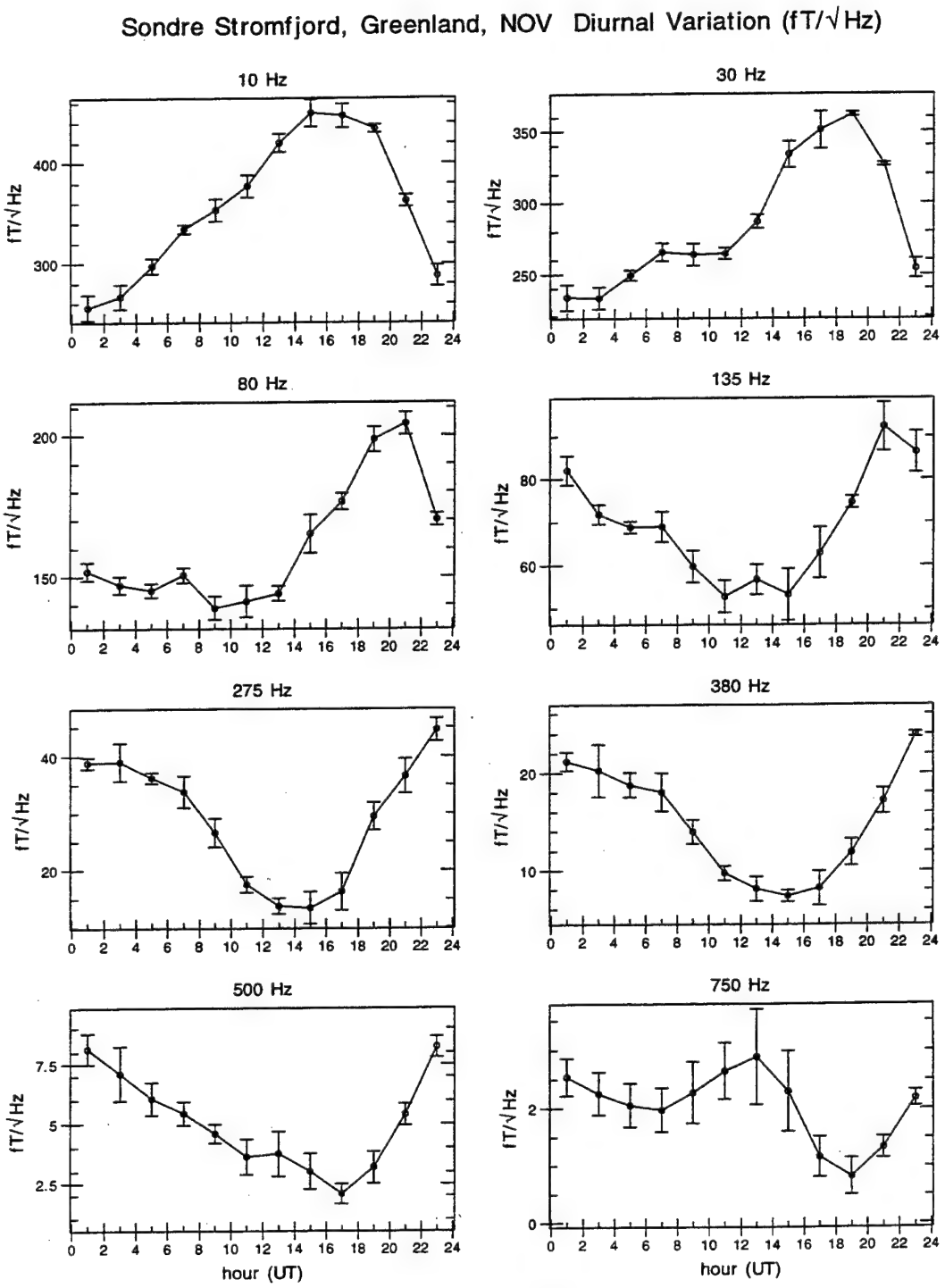

Figure 70: Diurnal variation of ELF/VLF radio noise at Søndrestrøm, Greenland, during the month of November for the eight lowest-frequency channels. The years 1986 to 1991 and the year 1993 are included.

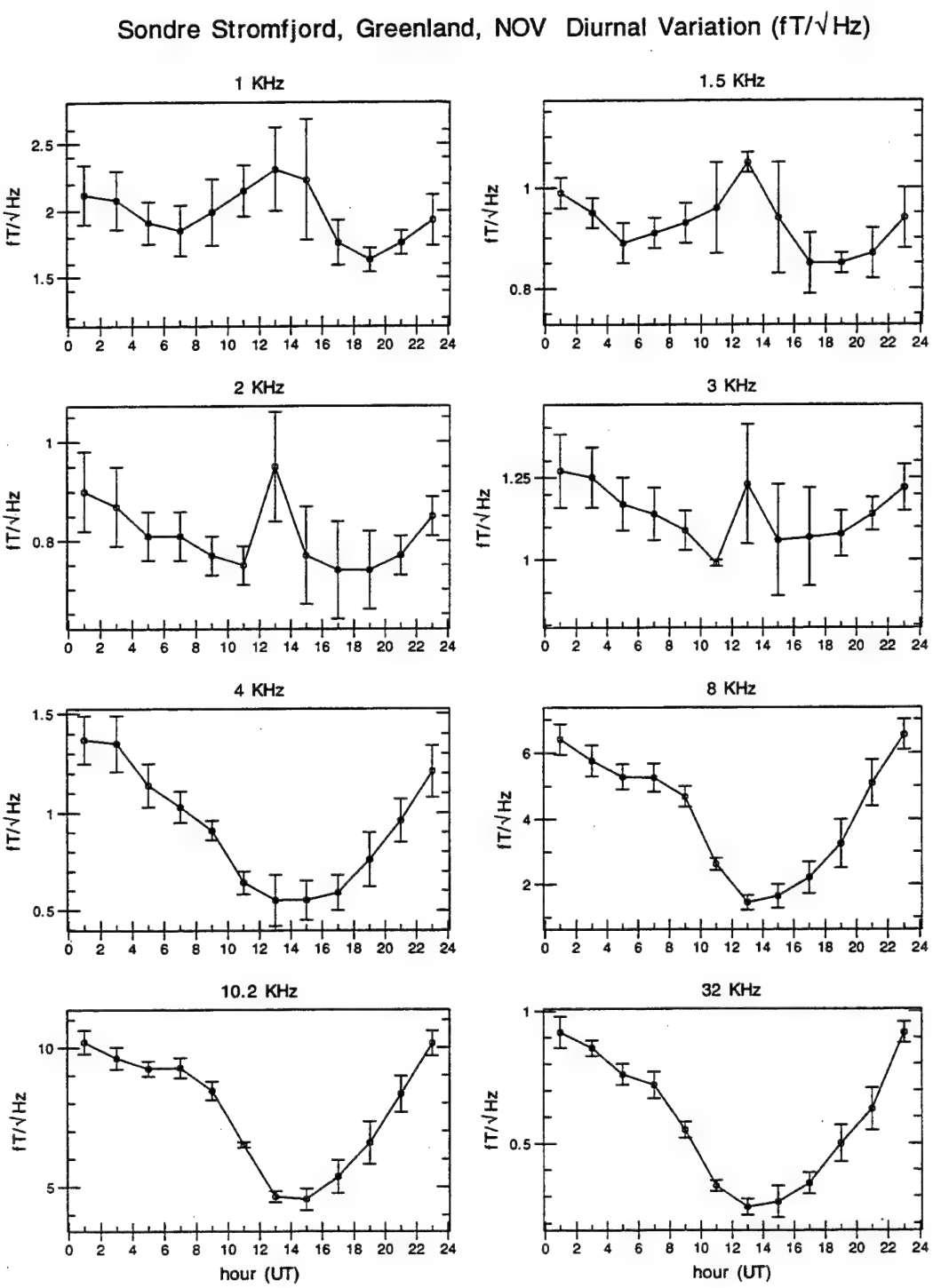

Figure 71: Diurnal variation of ELF/VLF radio noise at Søndrestrøm, Greenland, during the month of November for the eight highest-frequency channels. The years 1986 to 1991 and the year 1993 are included.

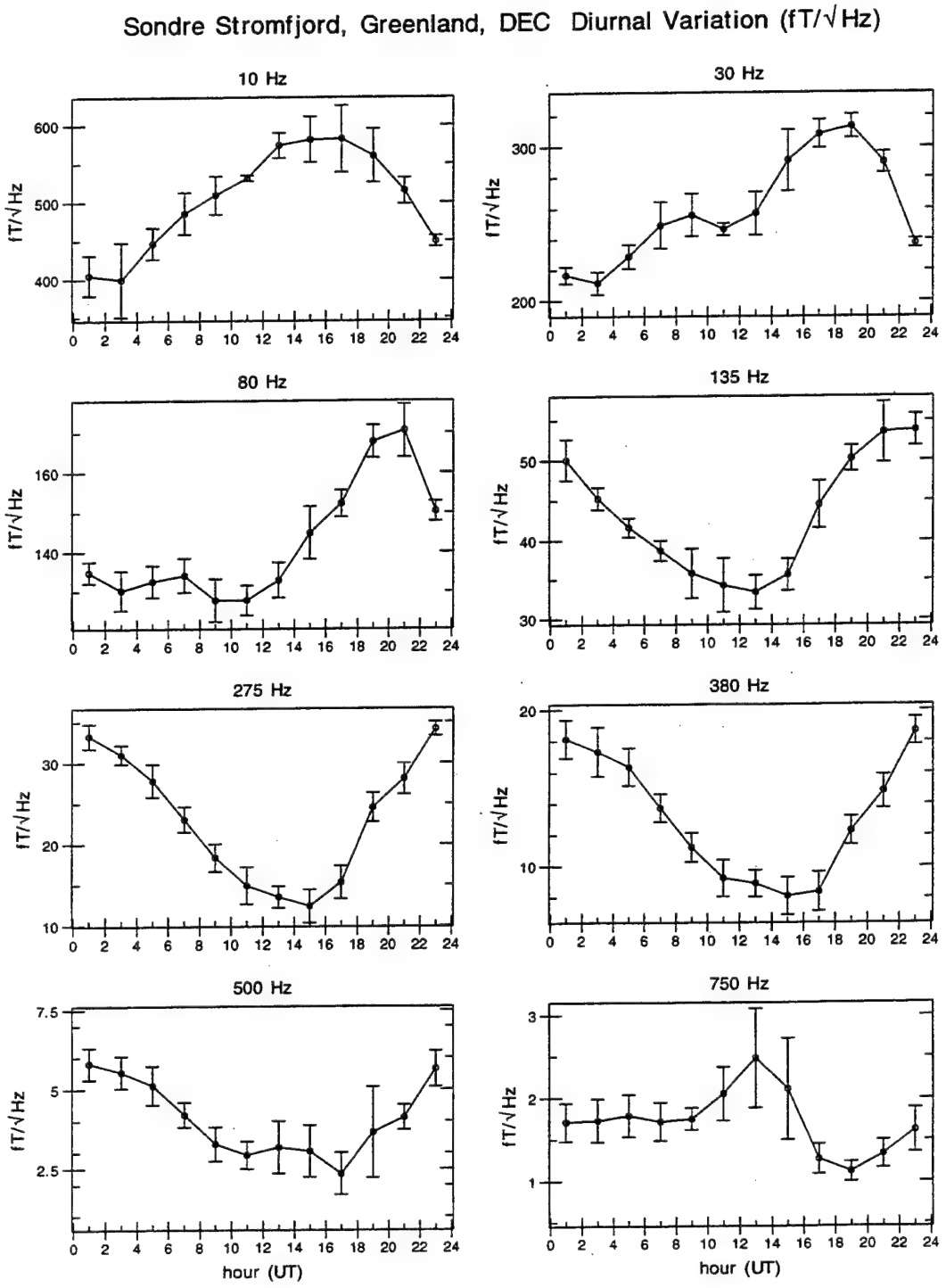

Figure 72: Diurnal variation of ELF/VLF radio noise at Søndrestrøm, Greenland, during the month of December for the eight lowest-frequency channels. The years 1986 to 1991 and the year 1993 are included.

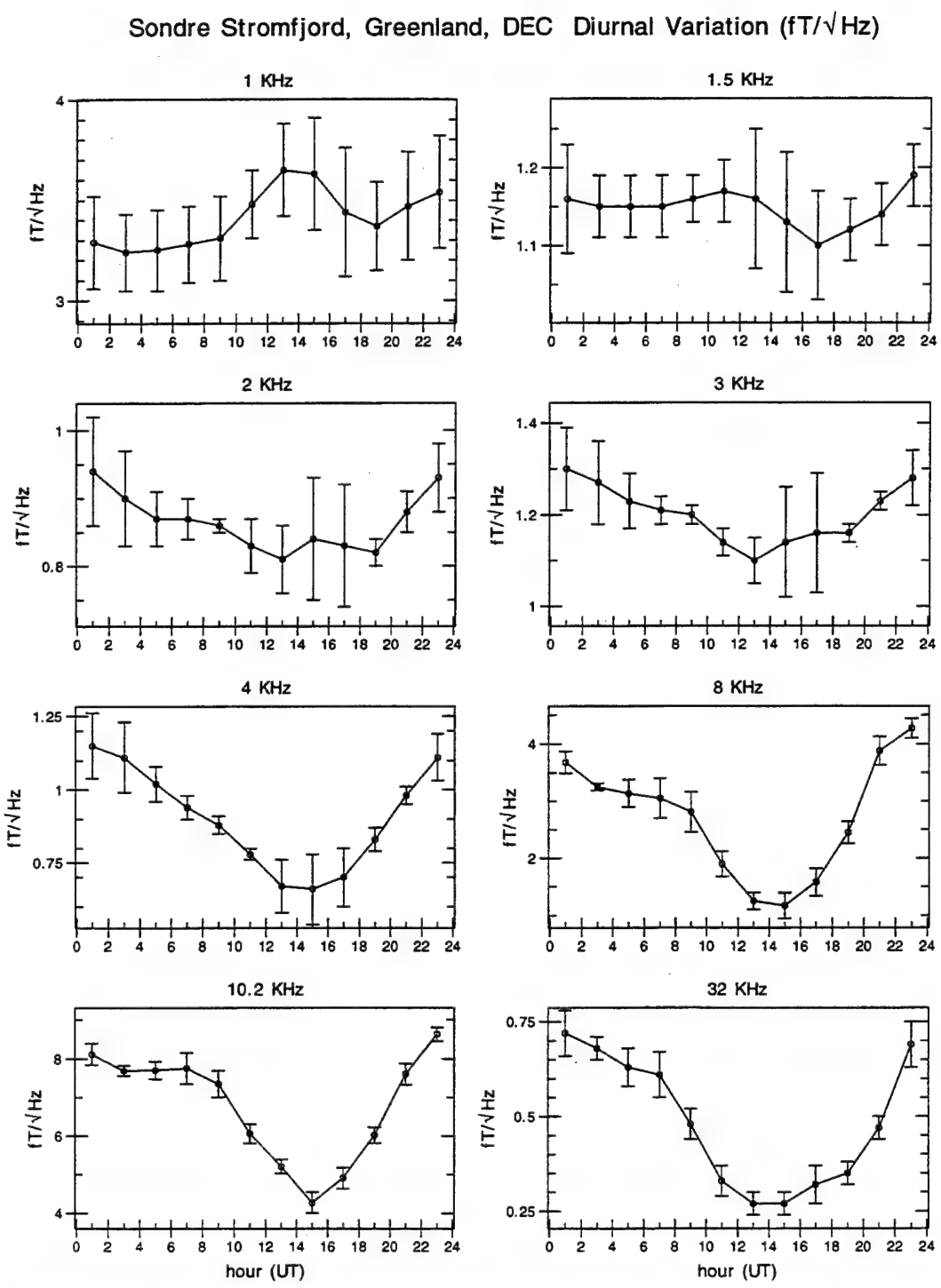

Figure 73: Diurnal variation of ELF/VLF radio noise at Søndrestrøm, Greenland, during the month of December for the eight highest-frequency channels. The years 1986 to 1991 and the year 1993 are included.

11 Stanford, California Diurnal Variation Figures

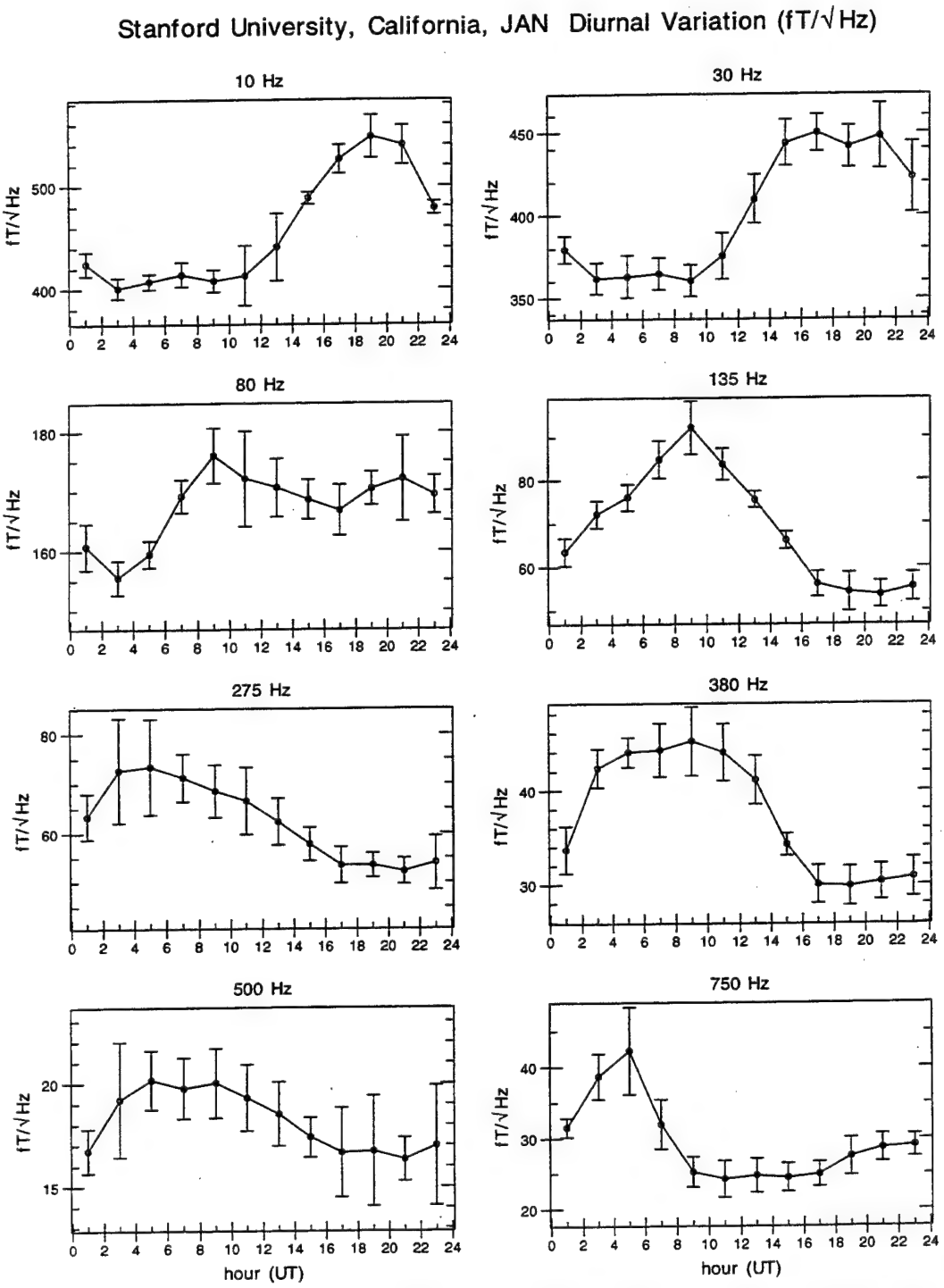

Figure 74: Diurnal variation of ELF/VLF radio noise at Stanford, California, during the month of January for the eight lowest-frequency channels. The years 1986 to 1993 are included.

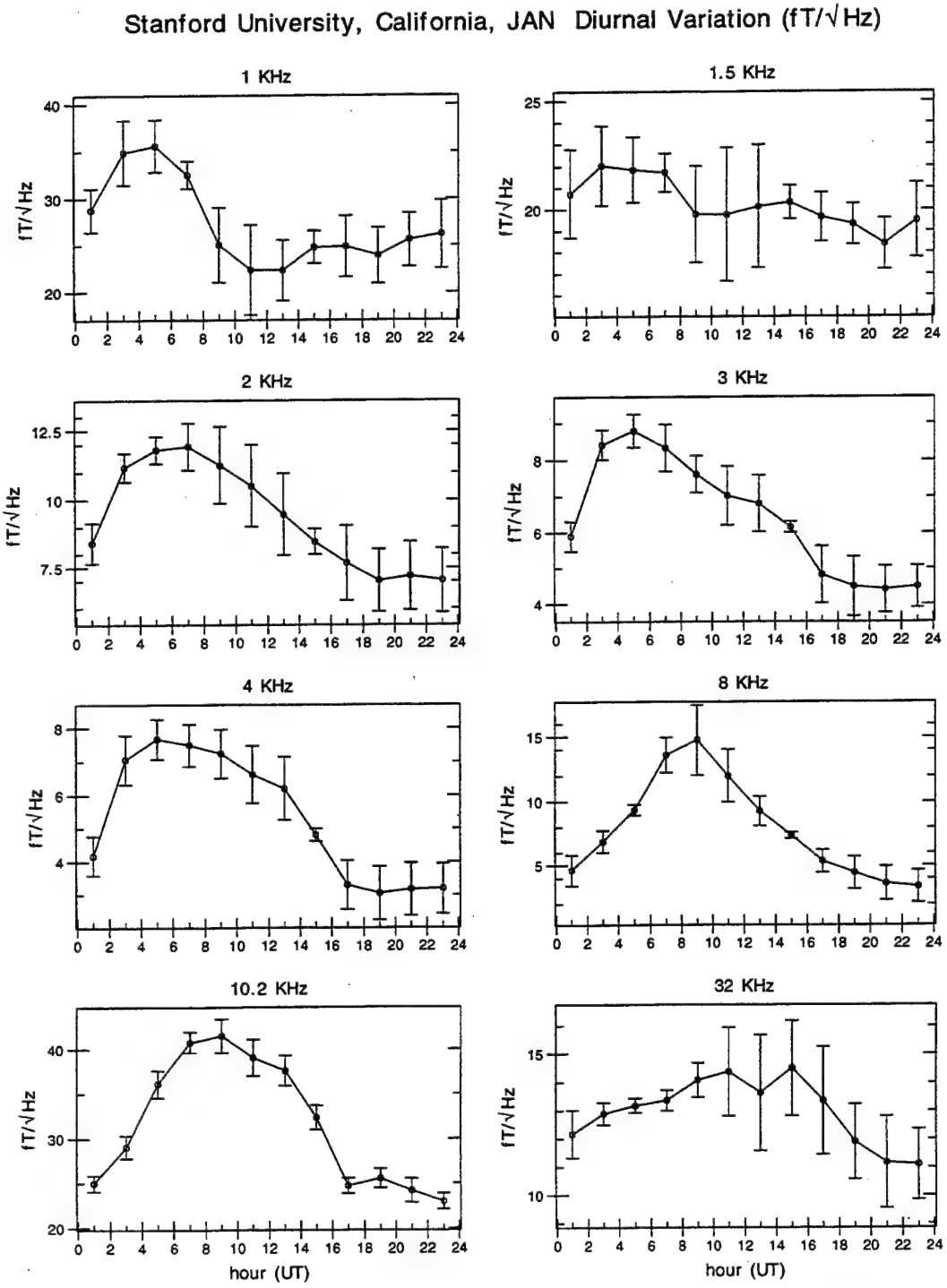

Figure 75: Diurnal variation of ELF/VLF radio noise at Stanford, California, during the month of January for the eight highest-frequency channels. The years 1986 to 1993 are included.

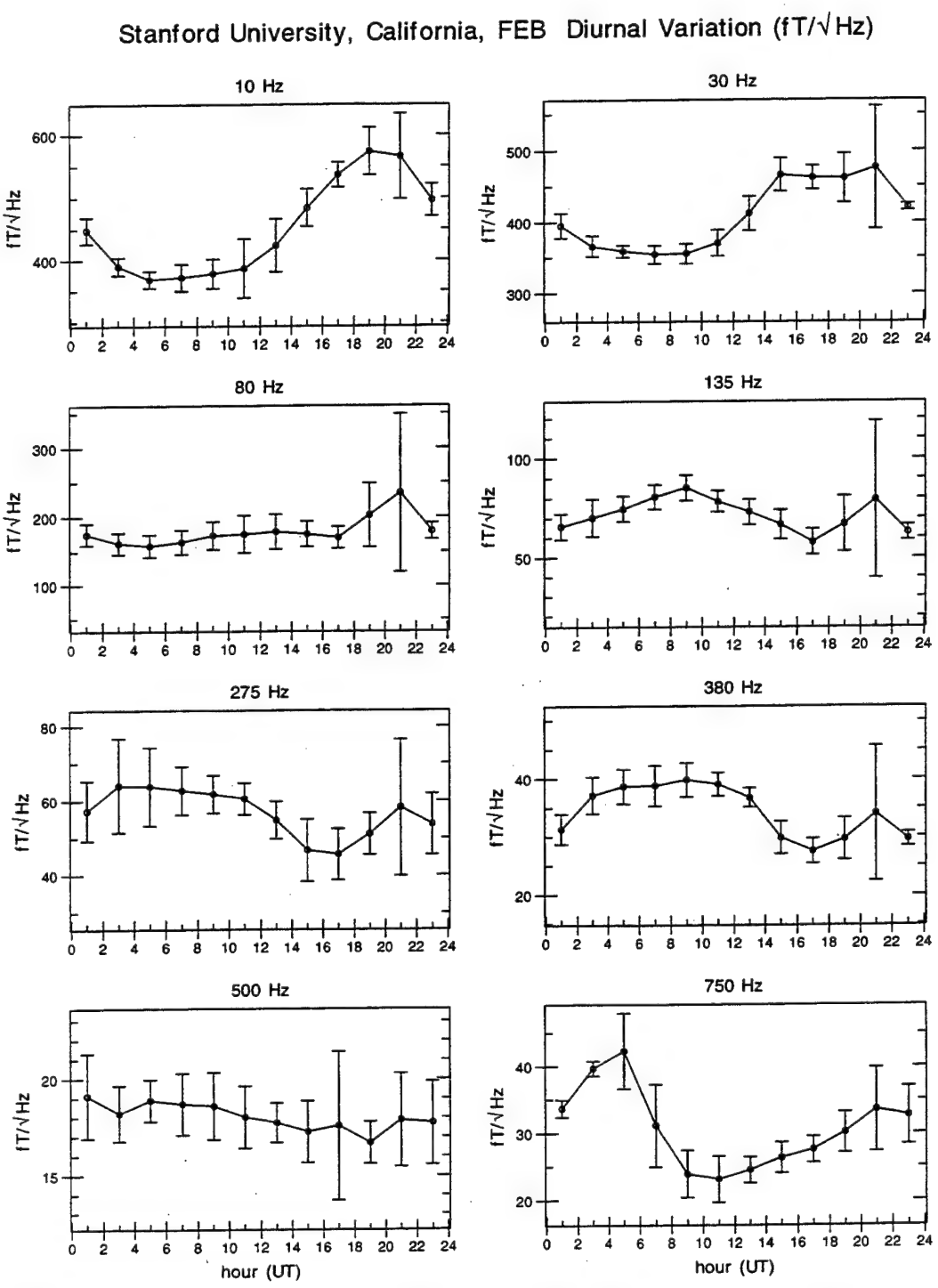

Figure 76: Diurnal variation of ELF/VLF radio noise at Stanford, California, during the month of February for the eight lowest-frequency channels. The years 1986 to 1993 are included.

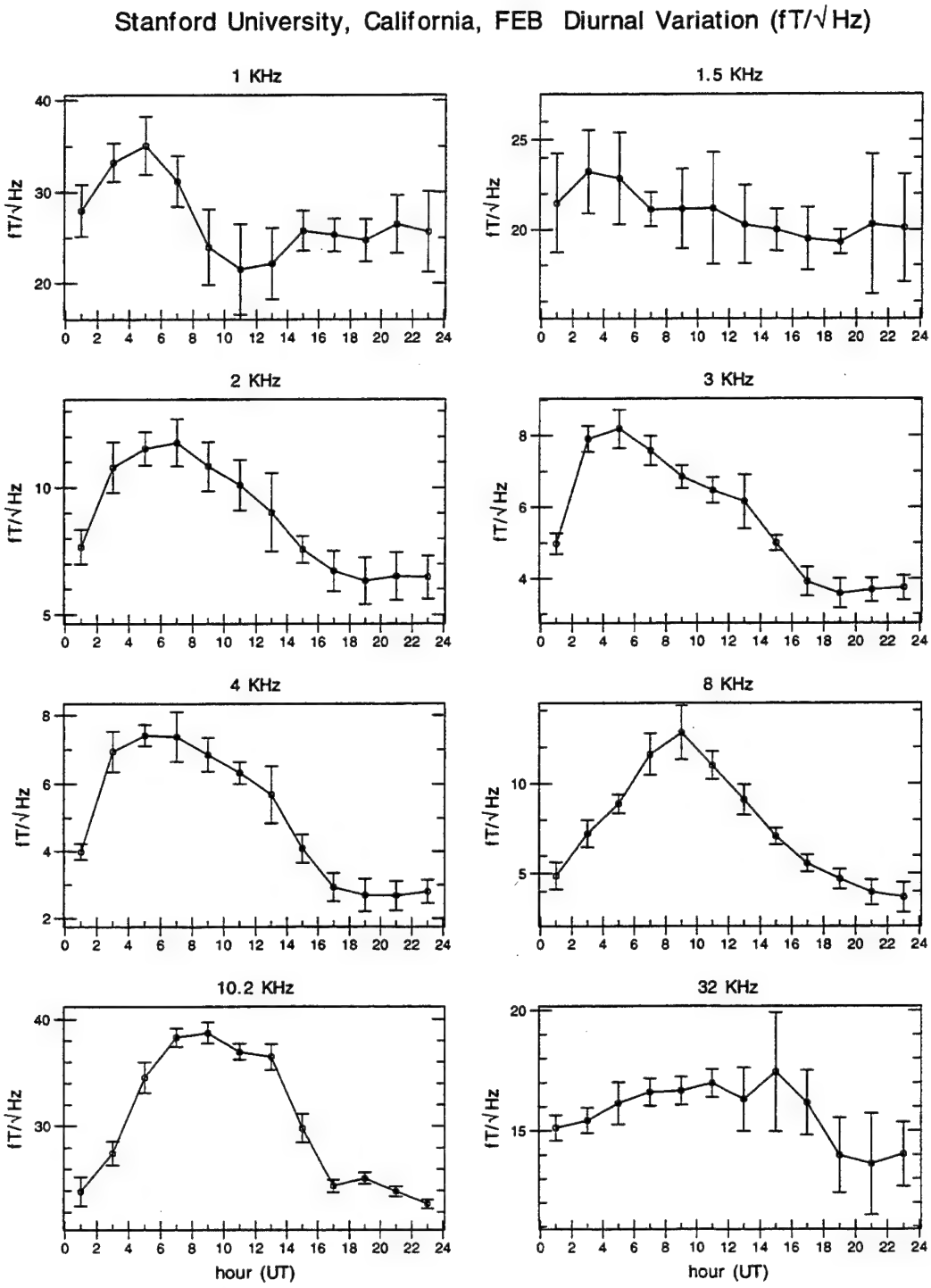

Figure 77: Diurnal variation of ELF/VLF radio noise at Stanford, California, during the month of February for the eight highest-frequency channels. The years 1986 to 1993 are included.

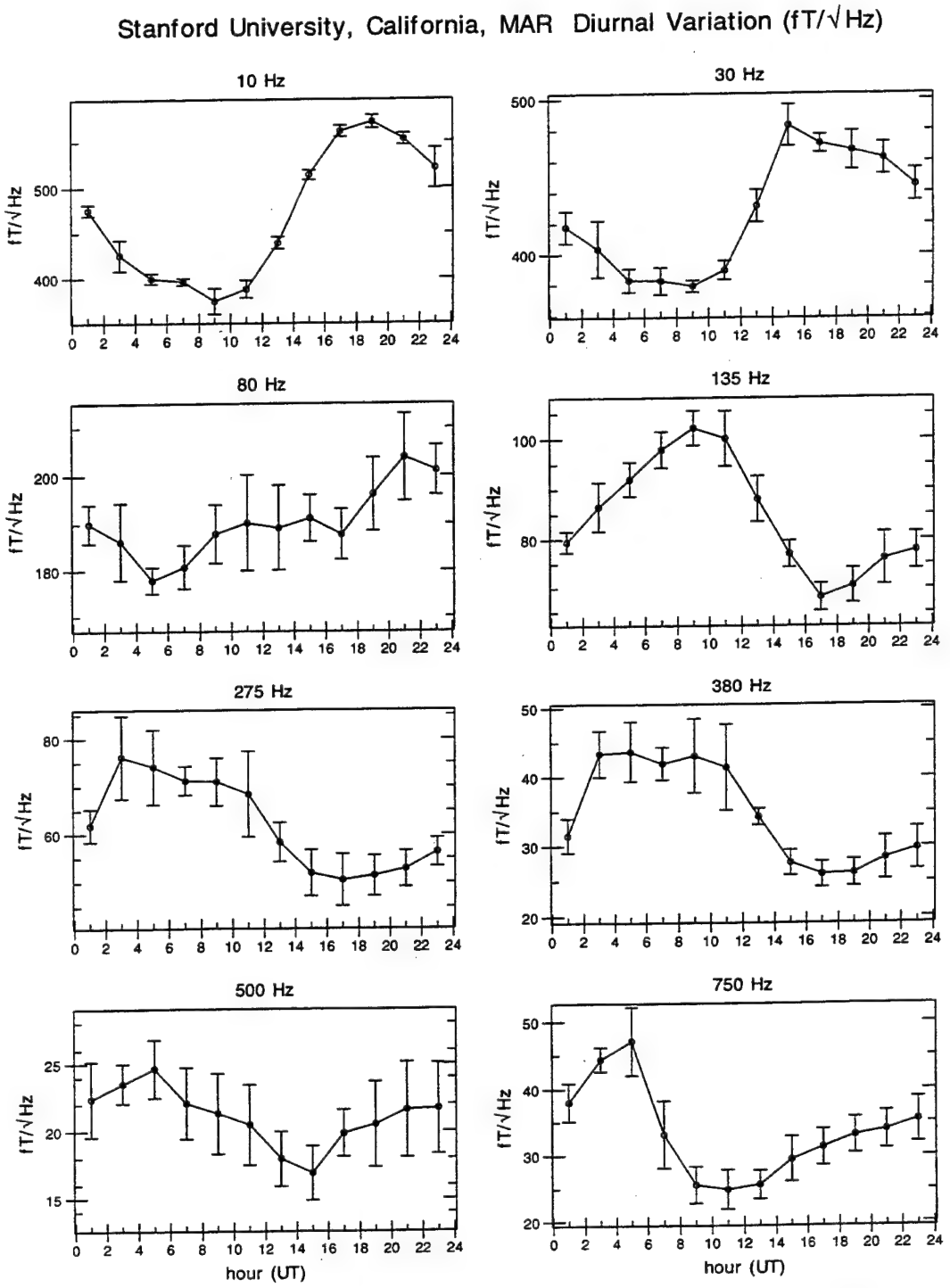

Figure 78: Diurnal variation of ELF/VLF radio noise at Stanford, California, during the month of March for the eight lowest-frequency channels. The years 1986 to 1993 are included.

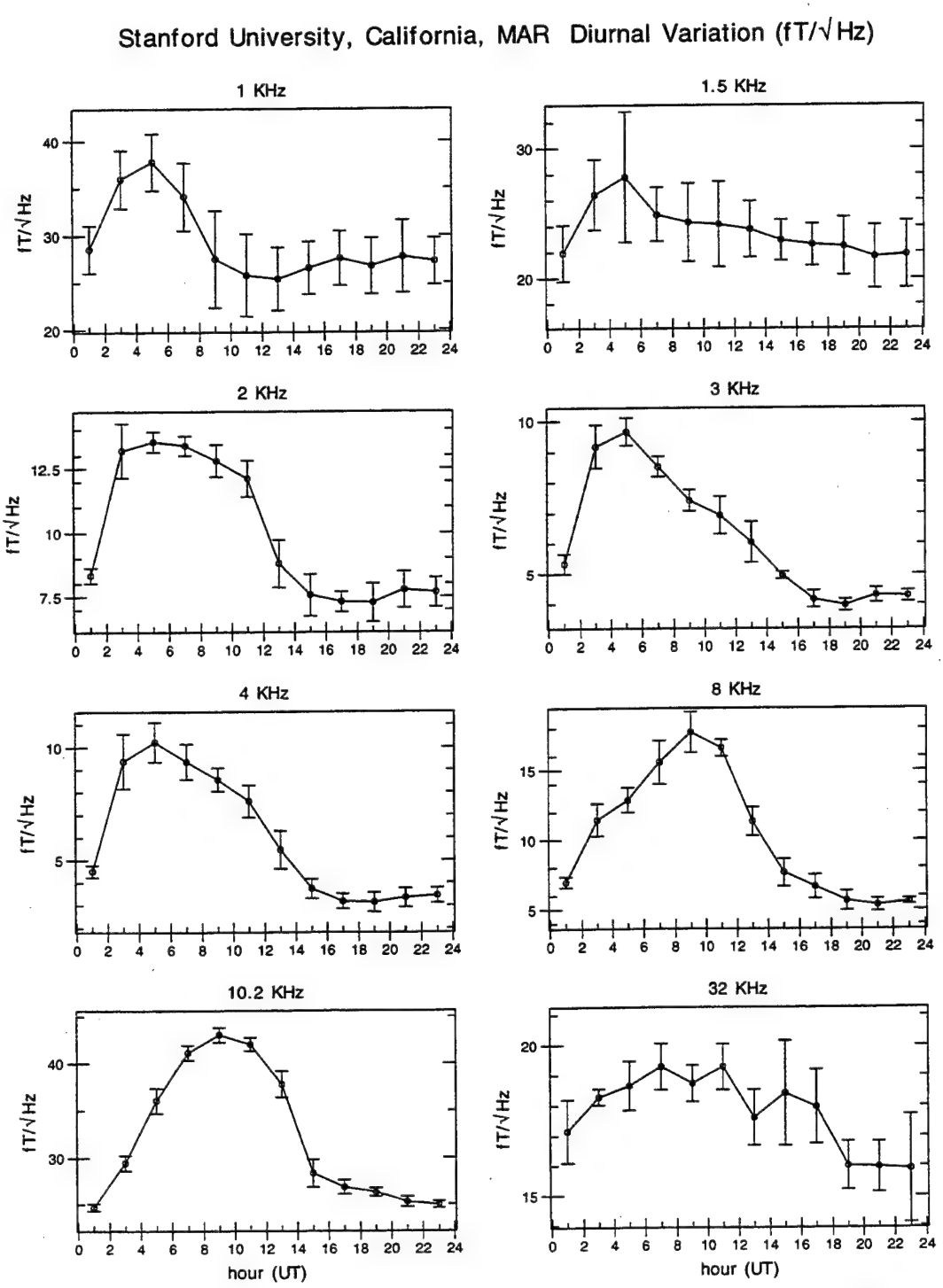

Figure 79: Diurnal variation of ELF/VLF radio noise at Stanford, California, during the month of March for the eight highest-frequency channels. The years 1986 to 1993 are included.

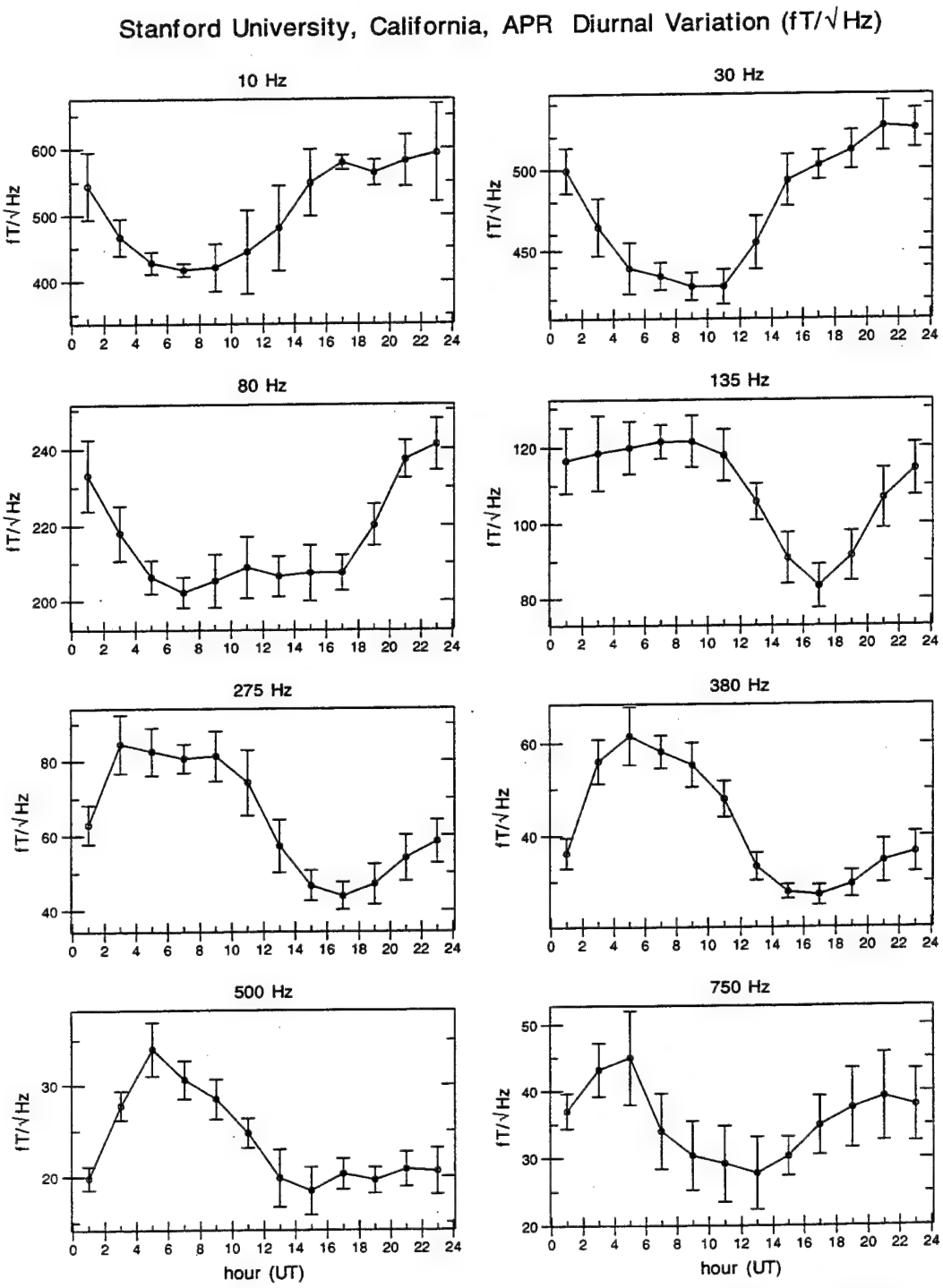

Figure 80: Diurnal variation of ELF/VLF radio noise at Stanford, California, during the month of April for the eight lowest-frequency channels. The years 1986 to 1993 are included.

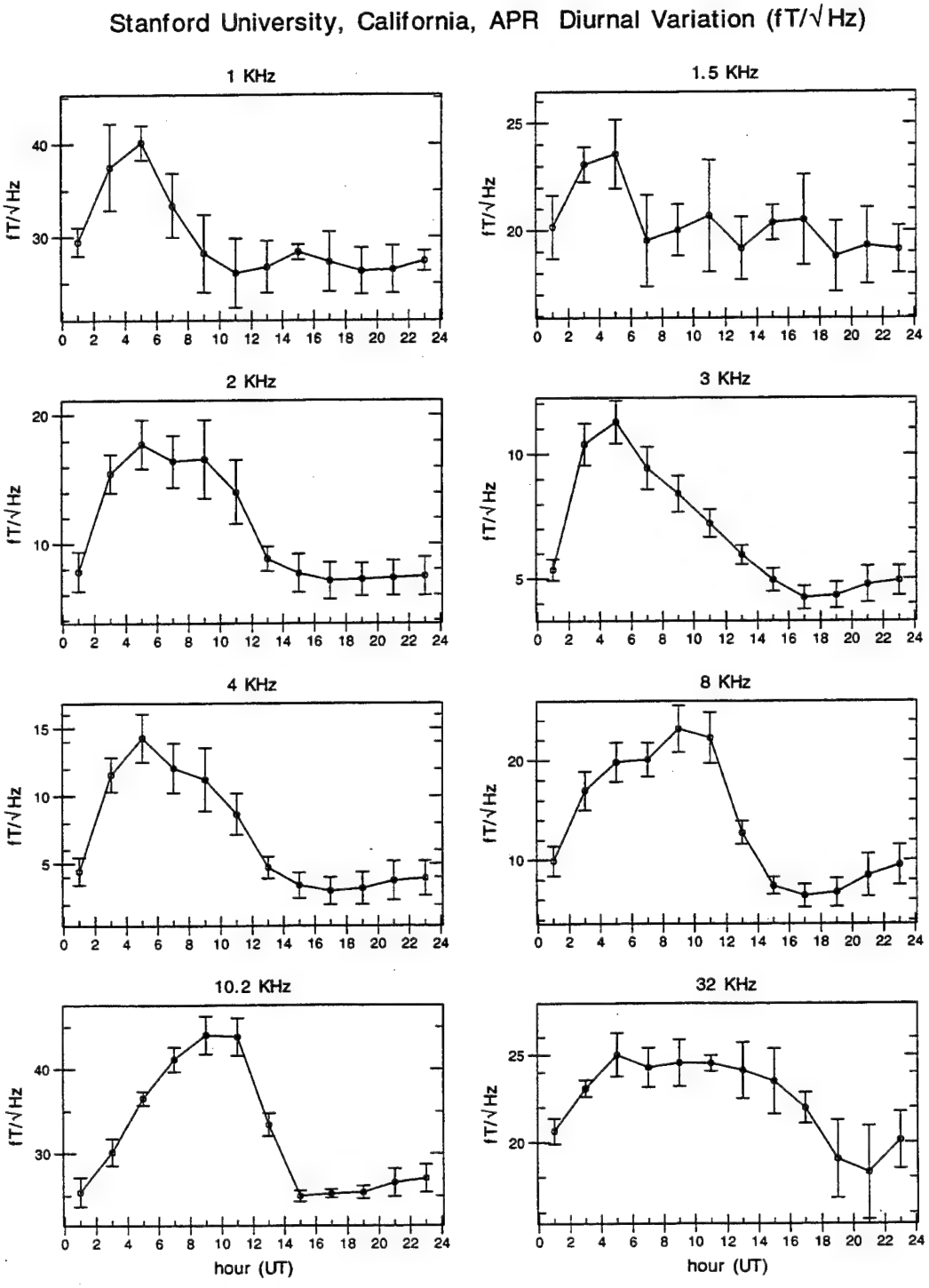

Figure 81: Diurnal variation of ELF/VLF radio noise at Stanford, California, during the month of April for the eight highest-frequency channels. The years 1986 to 1993 are included.

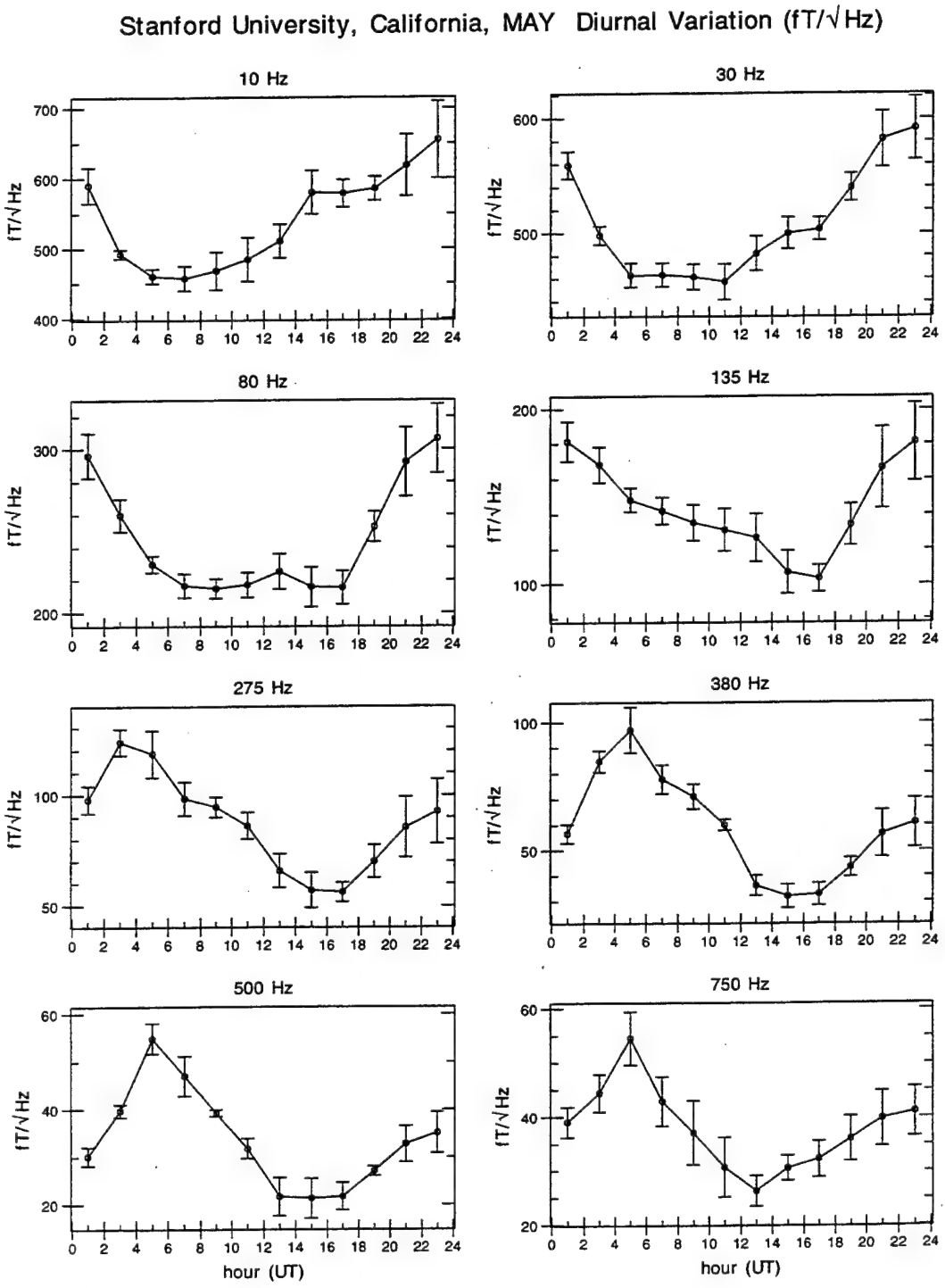

Figure 82: Diurnal variation of ELF/VLF radio noise at Stanford, California, during the month of May for the eight lowest-frequency channels. The years 1986 to 1993 are included.

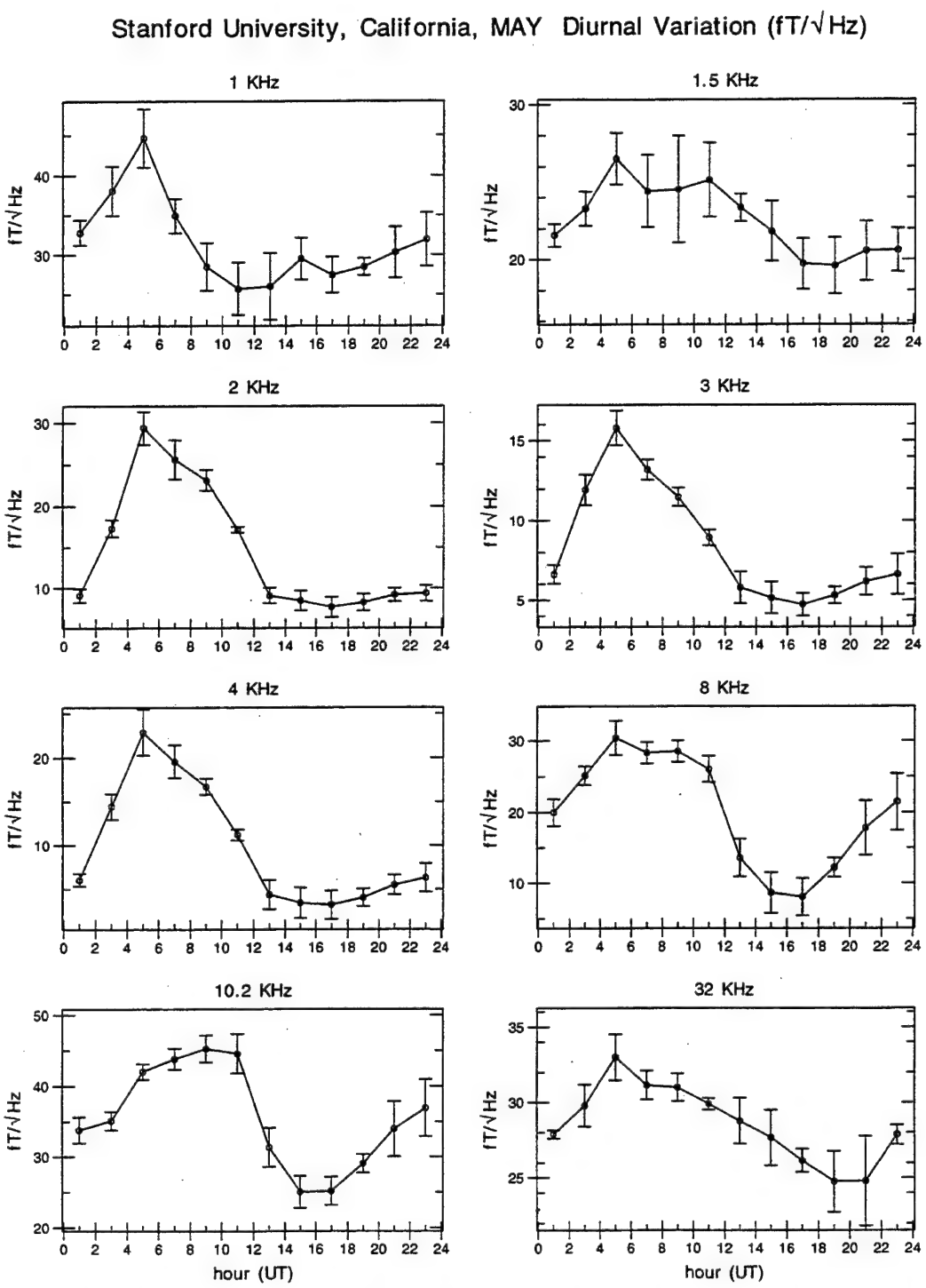

Figure 83: Diurnal variation of ELF/VLF radio noise at Stanford, California, during the month of May for the eight highest-frequency channels. The years 1986 to 1993 are included.

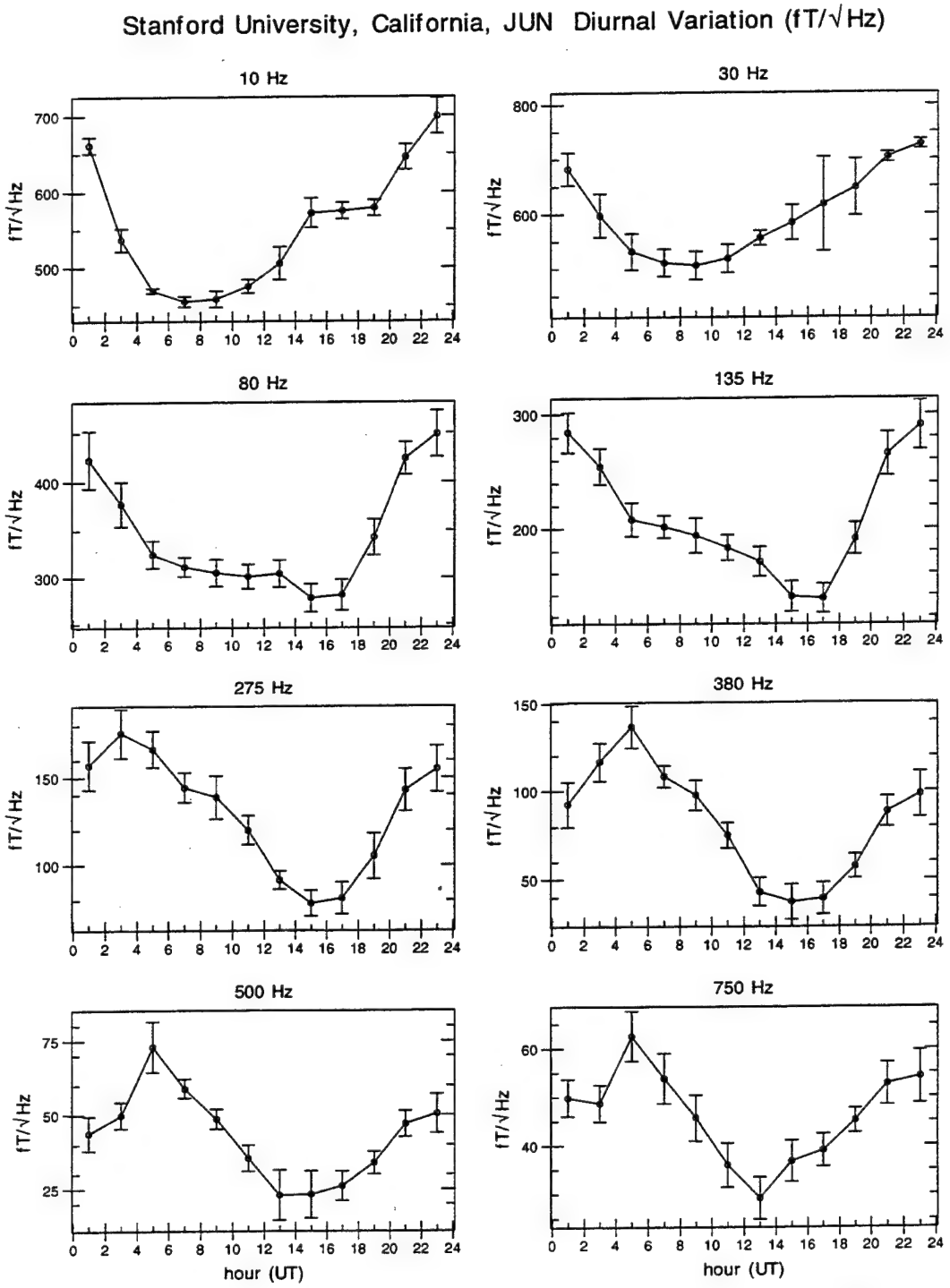

Figure 84: Diurnal variation of ELF/VLF radio noise at Stanford, California, during the month of June for the eight lowest-frequency channels. The years 1986 to 1993 are included.

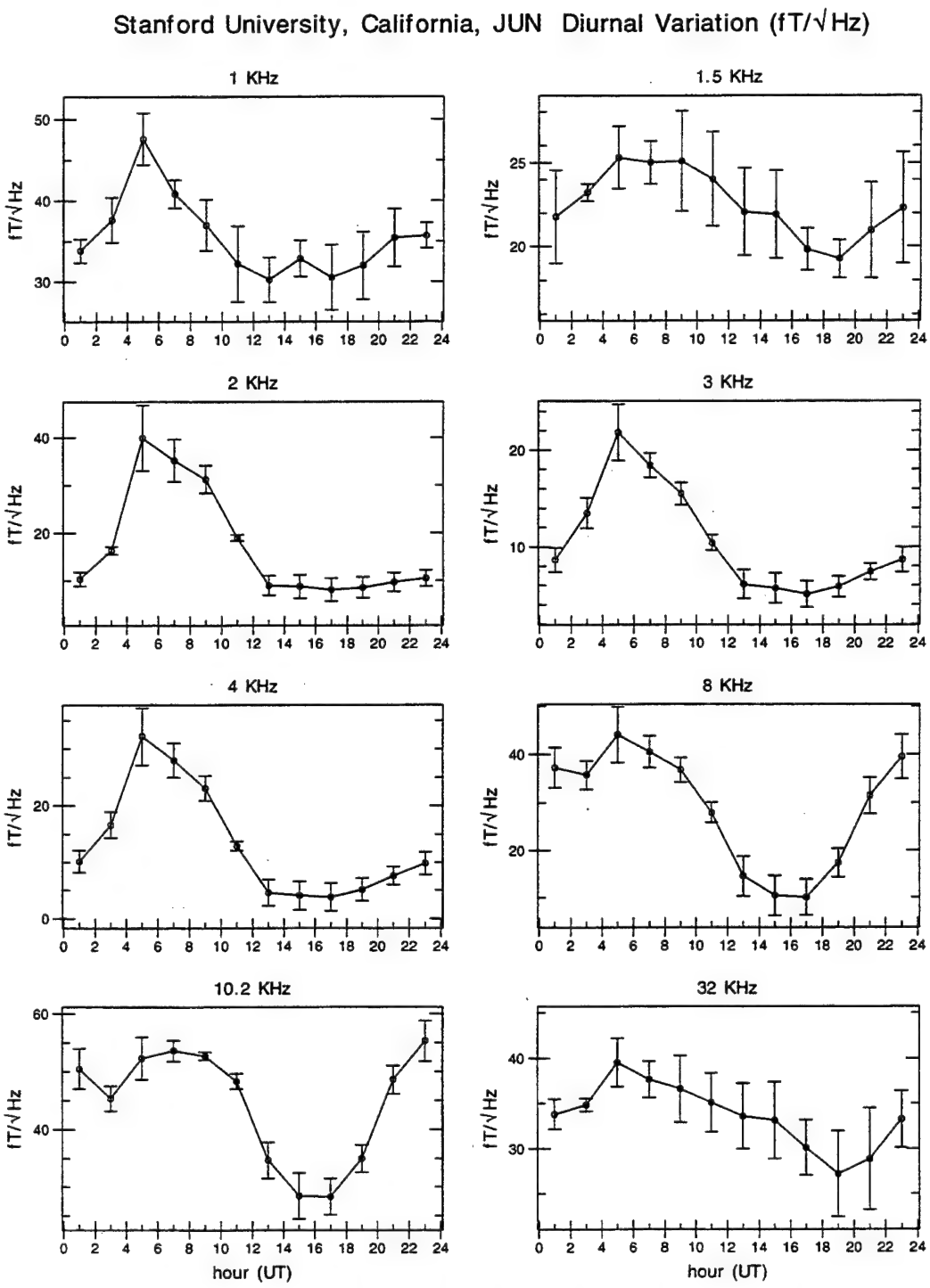

Figure 85: Diurnal variation of ELF/VLF radio noise at Stanford, California, during the month of June for the eight highest-frequency channels. The years 1986 to 1993 are included.

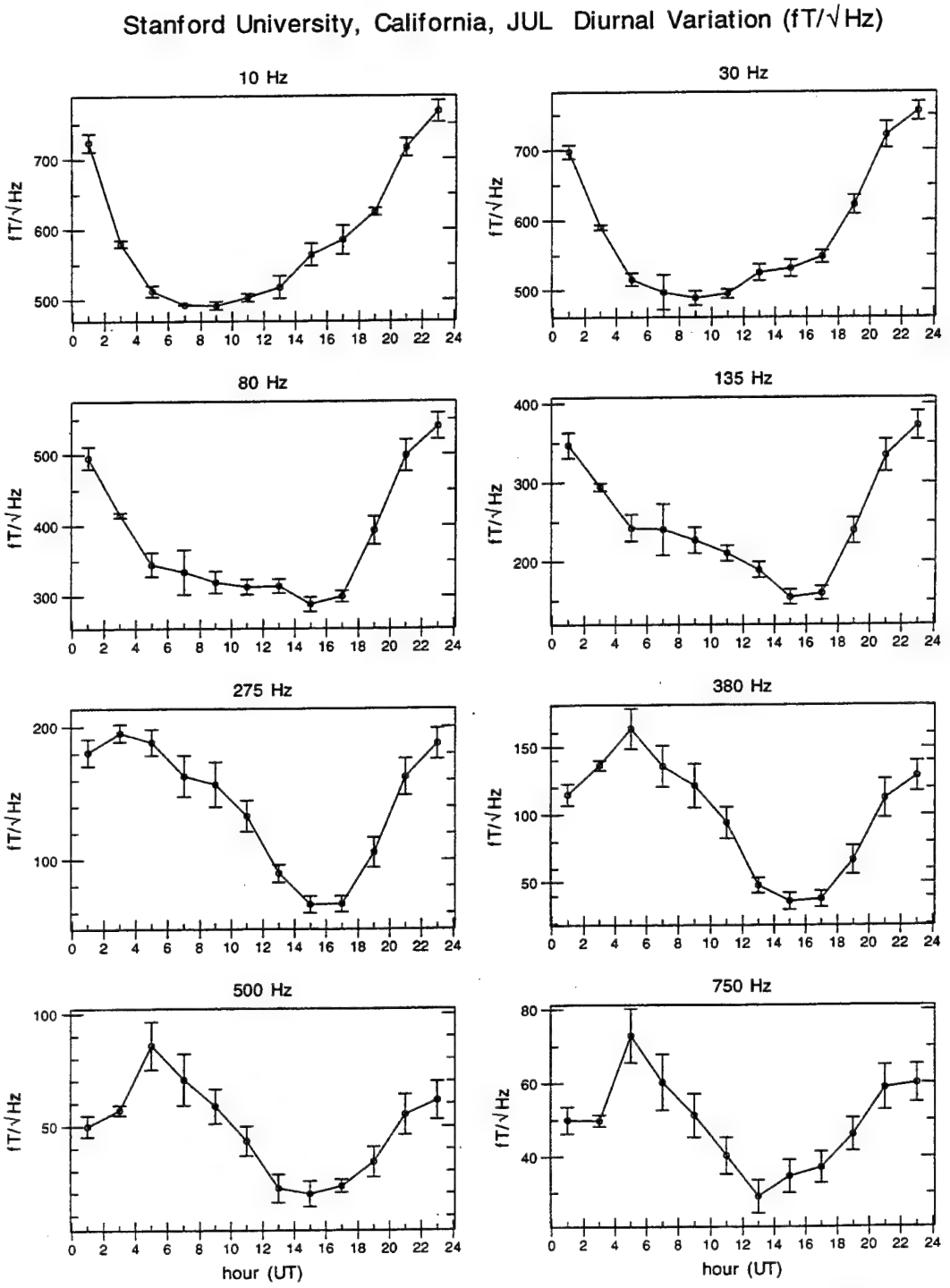

Figure 86: Diurnal variation of ELF/VLF radio noise at Stanford, California, during the month of July for the eight lowest-frequency channels. The years 1986 to 1993 are included.

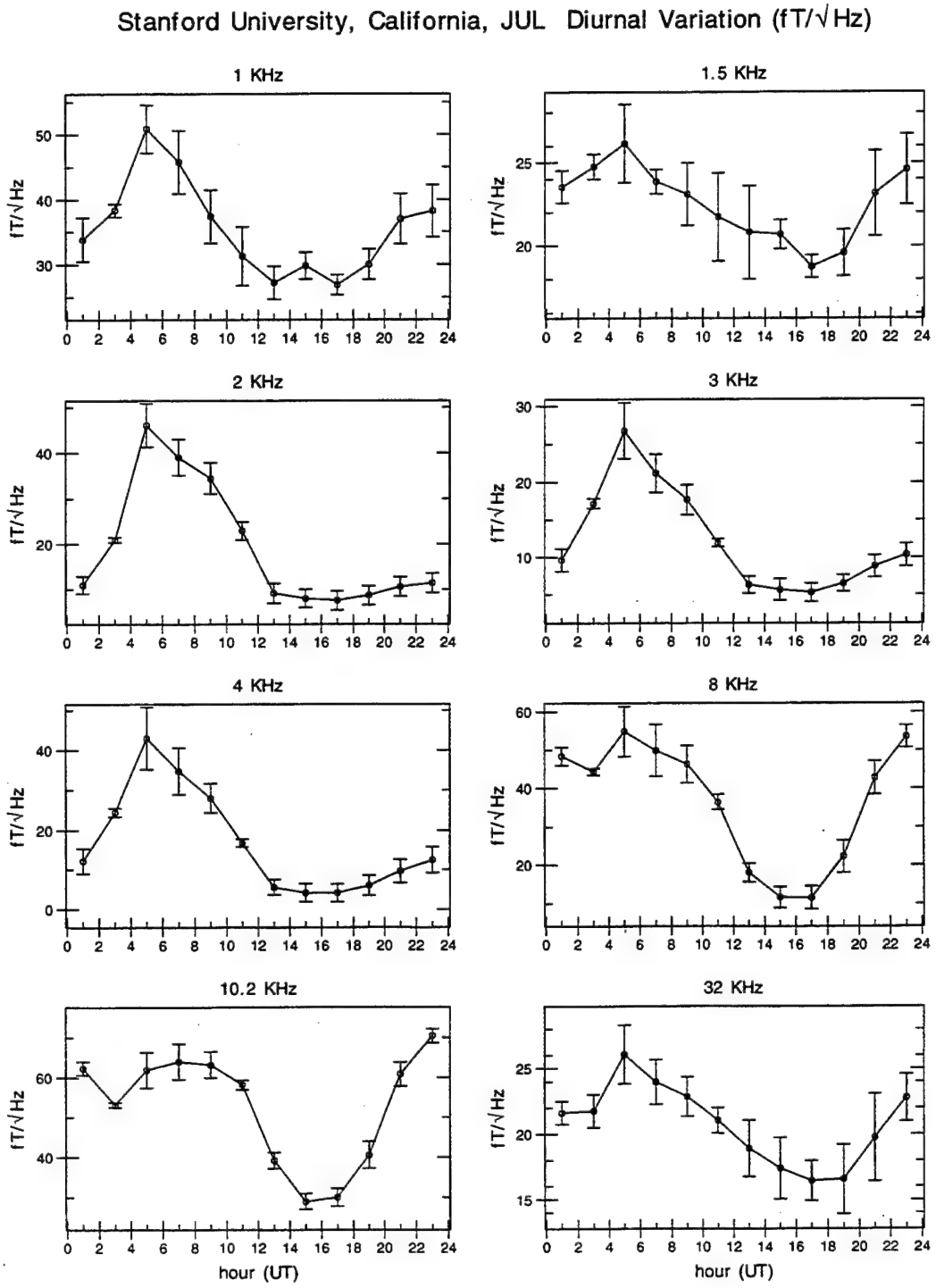

Figure 87: Diurnal variation of ELF/VLF radio noise at Stanford, California, during the month of July for the eight highest-frequency channels. The years 1986 to 1993 are included.

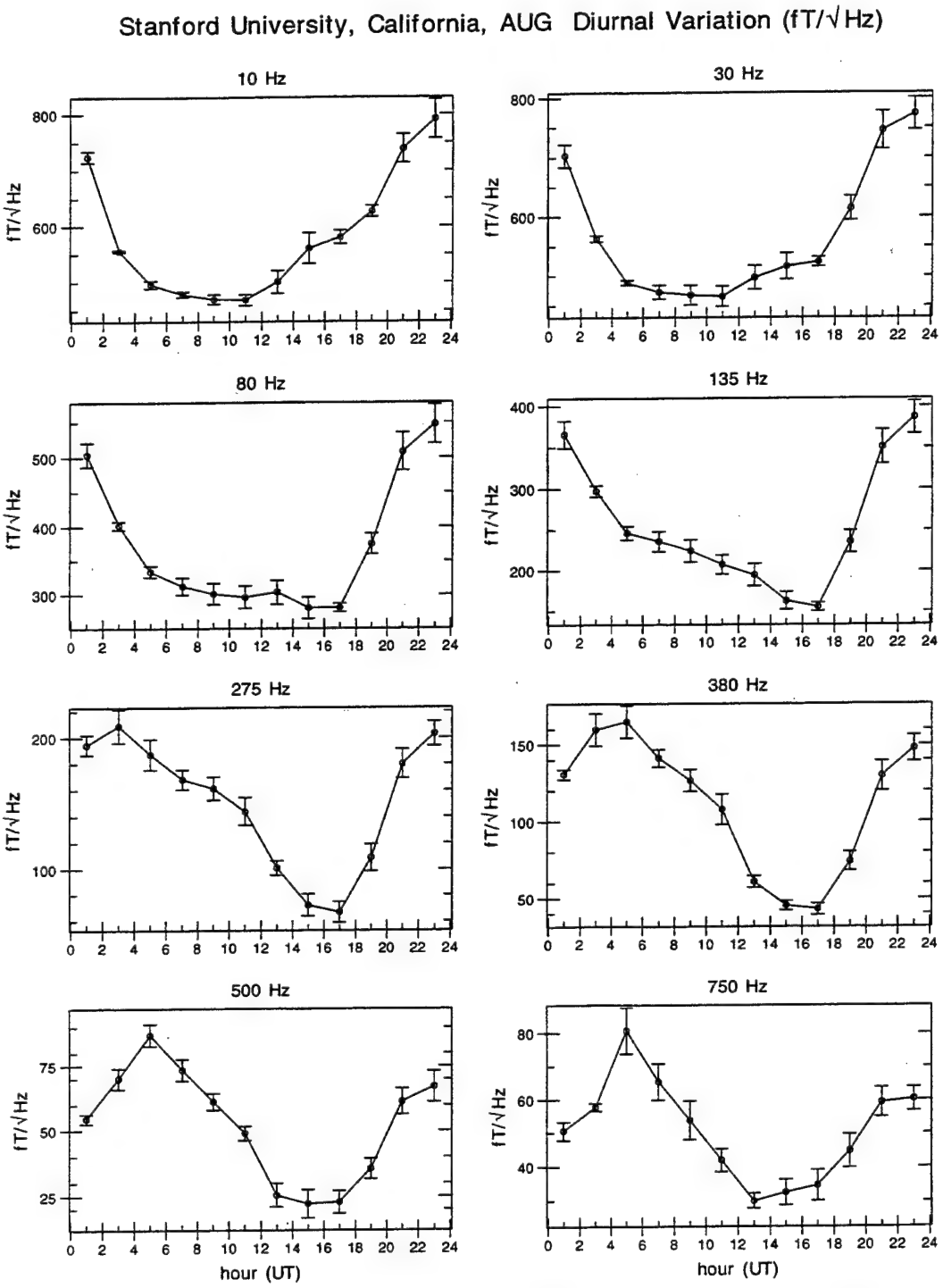

Figure 88: Diurnal variation of ELF/VLF radio noise at Stanford, California, during the month of August for the eight lowest-frequency channels. The years 1986 to 1993 are included.

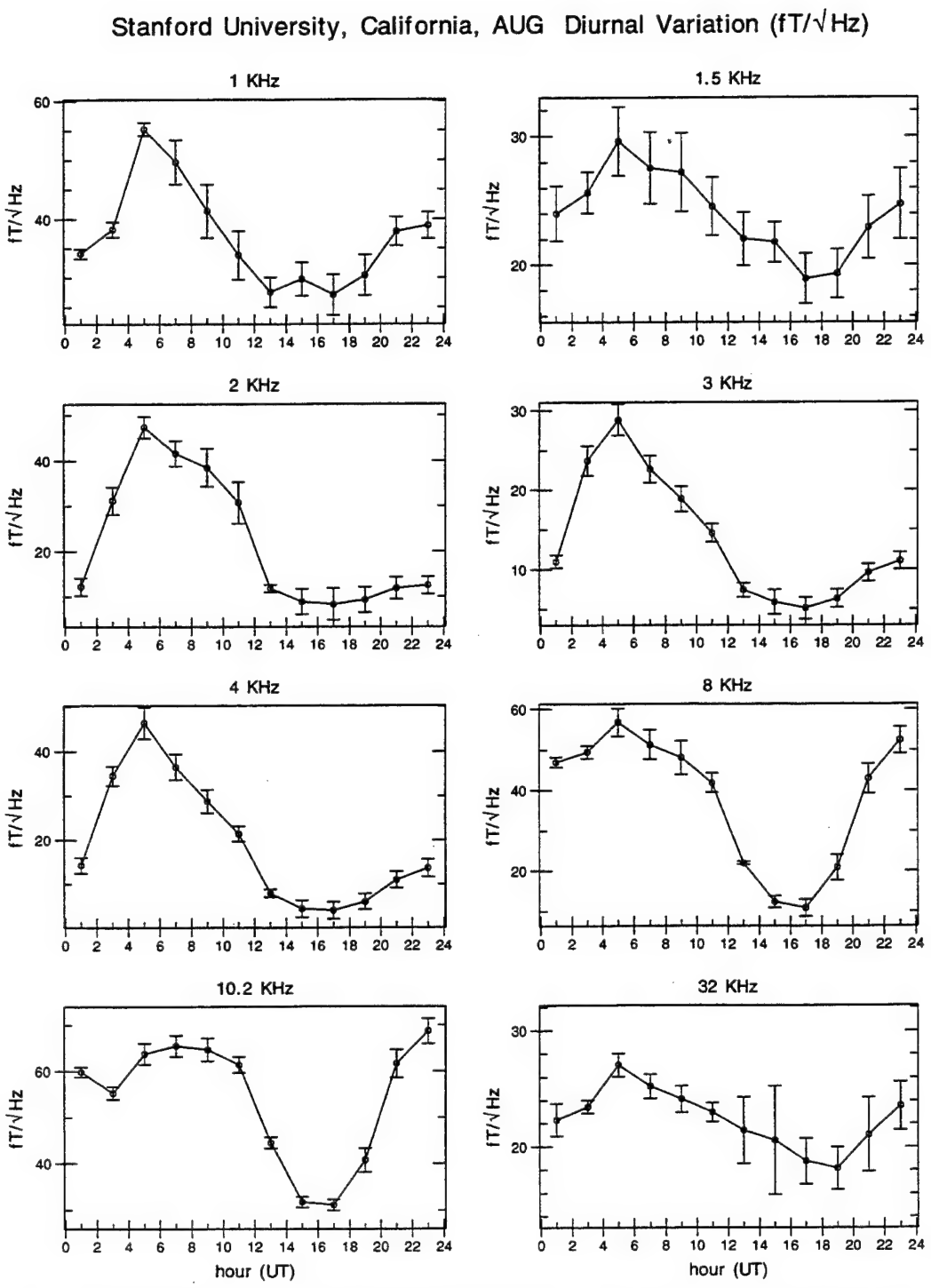

Figure 89: Diurnal variation of ELF/VLF radio noise at Stanford, California, during the month of August for the eight highest-frequency channels. The years 1986 to 1993 are included.

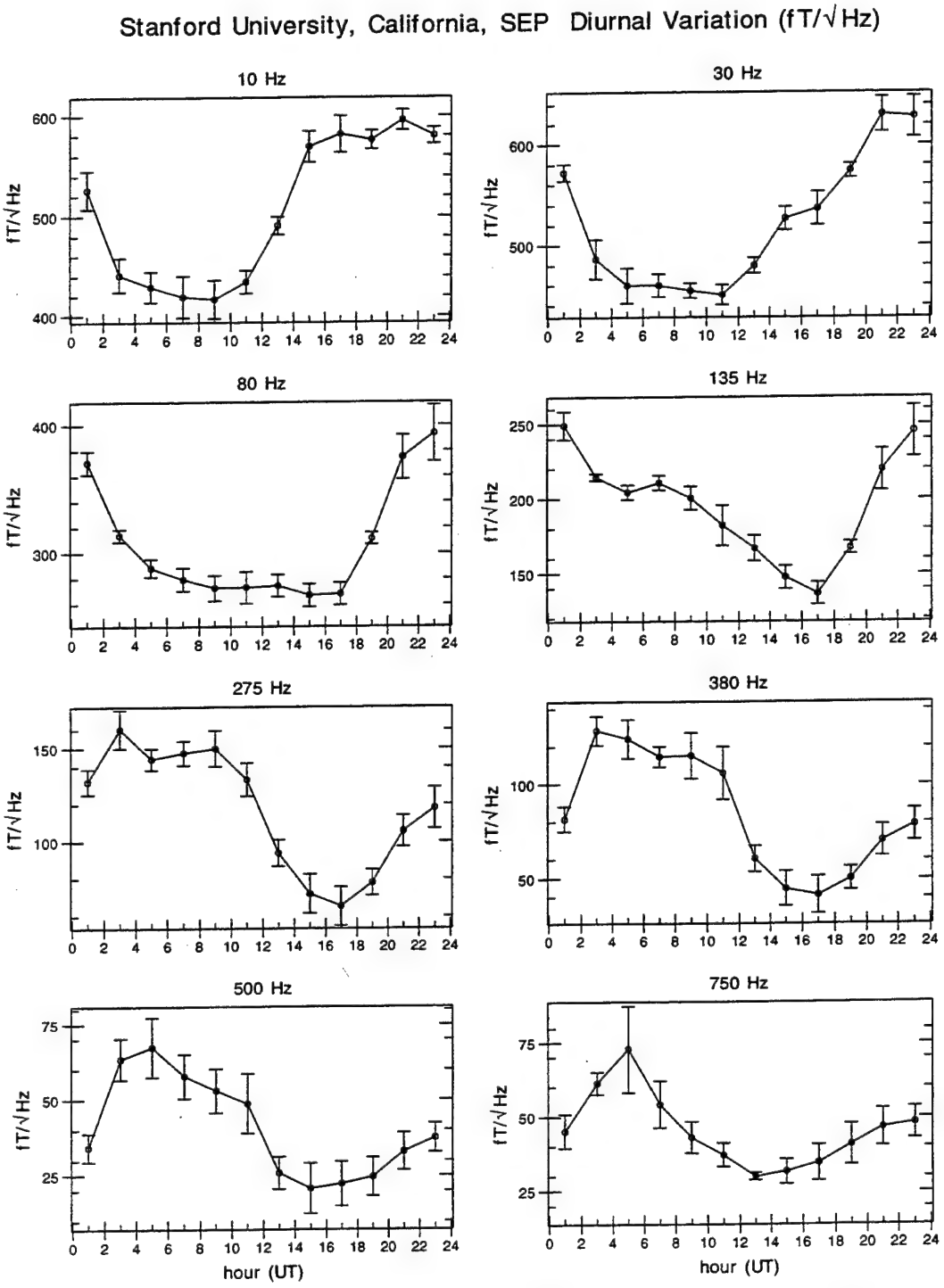

Figure 90: Diurnal variation of ELF/VLF radio noise at Stanford, California, during the month of September for the eight lowest-frequency channels. The years 1986 to 1993 are included.

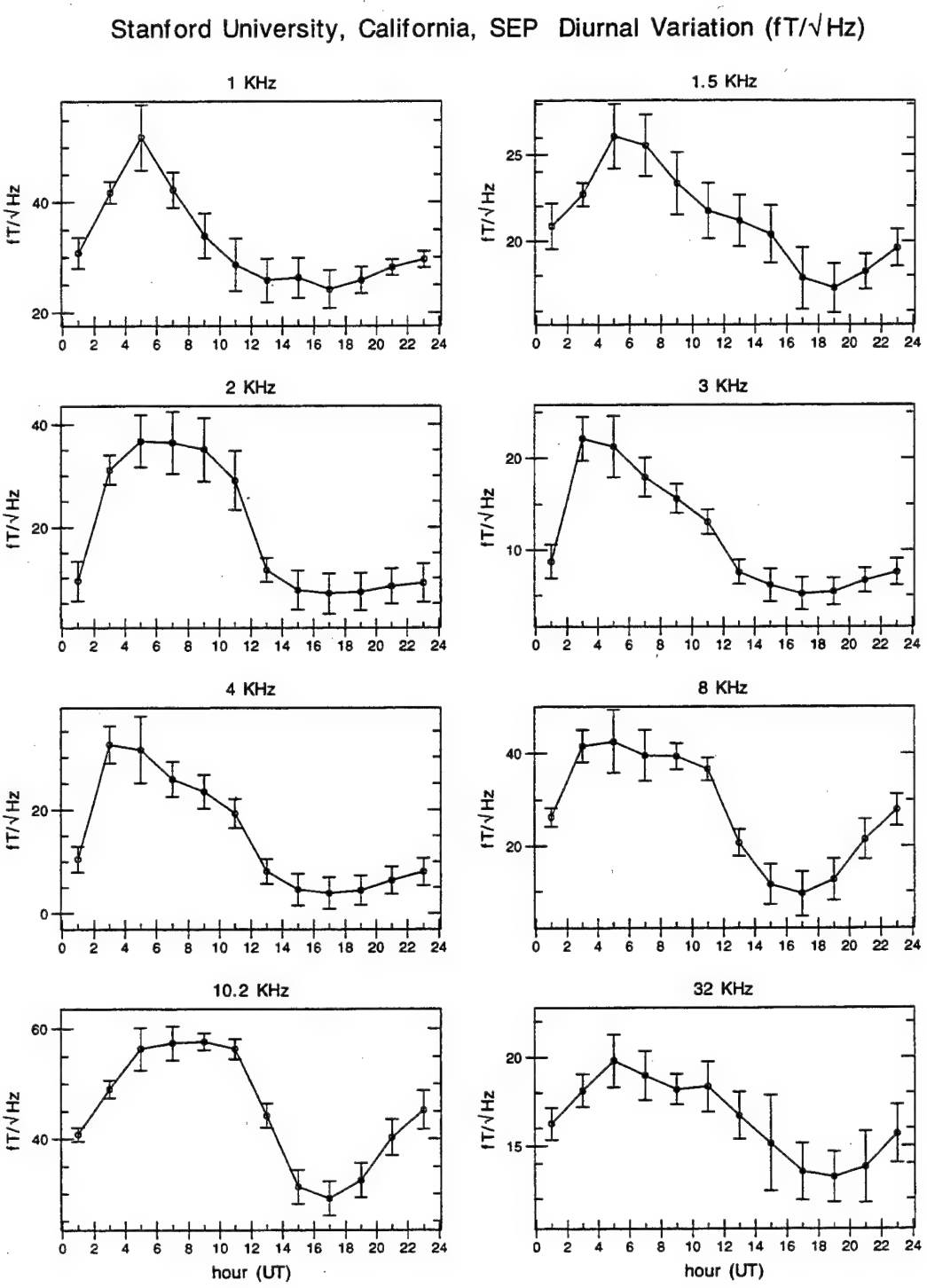

Figure 91: Diurnal variation of ELF/VLF radio noise at Stanford, California, during the month of September for the eight highest-frequency channels. The years 1986 to 1993 are included.

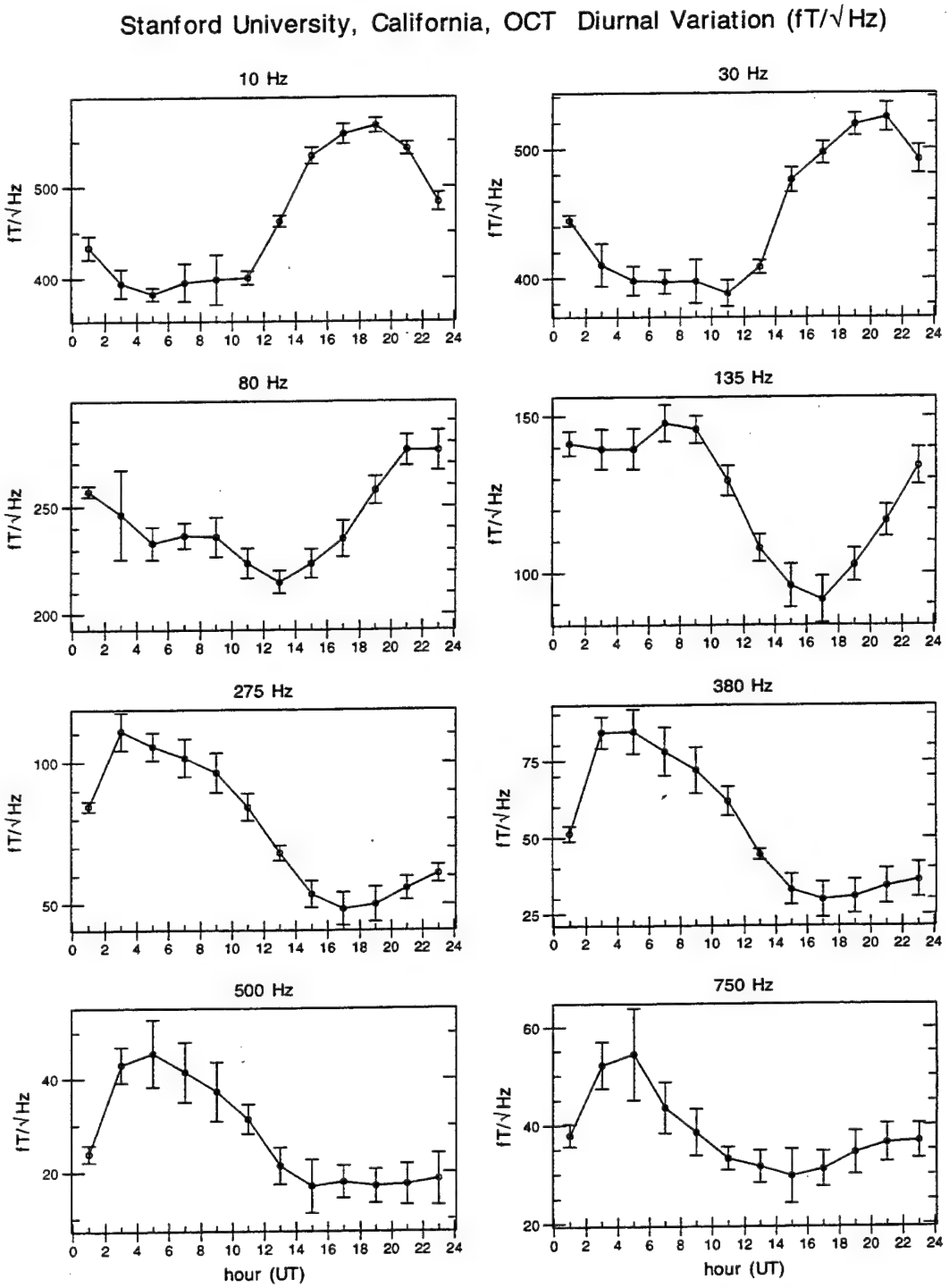

Figure 92: Diurnal variation of ELF/VLF radio noise at Stanford, California, during the month of October for the eight lowest-frequency channels. The years 1986 to 1993 are included.

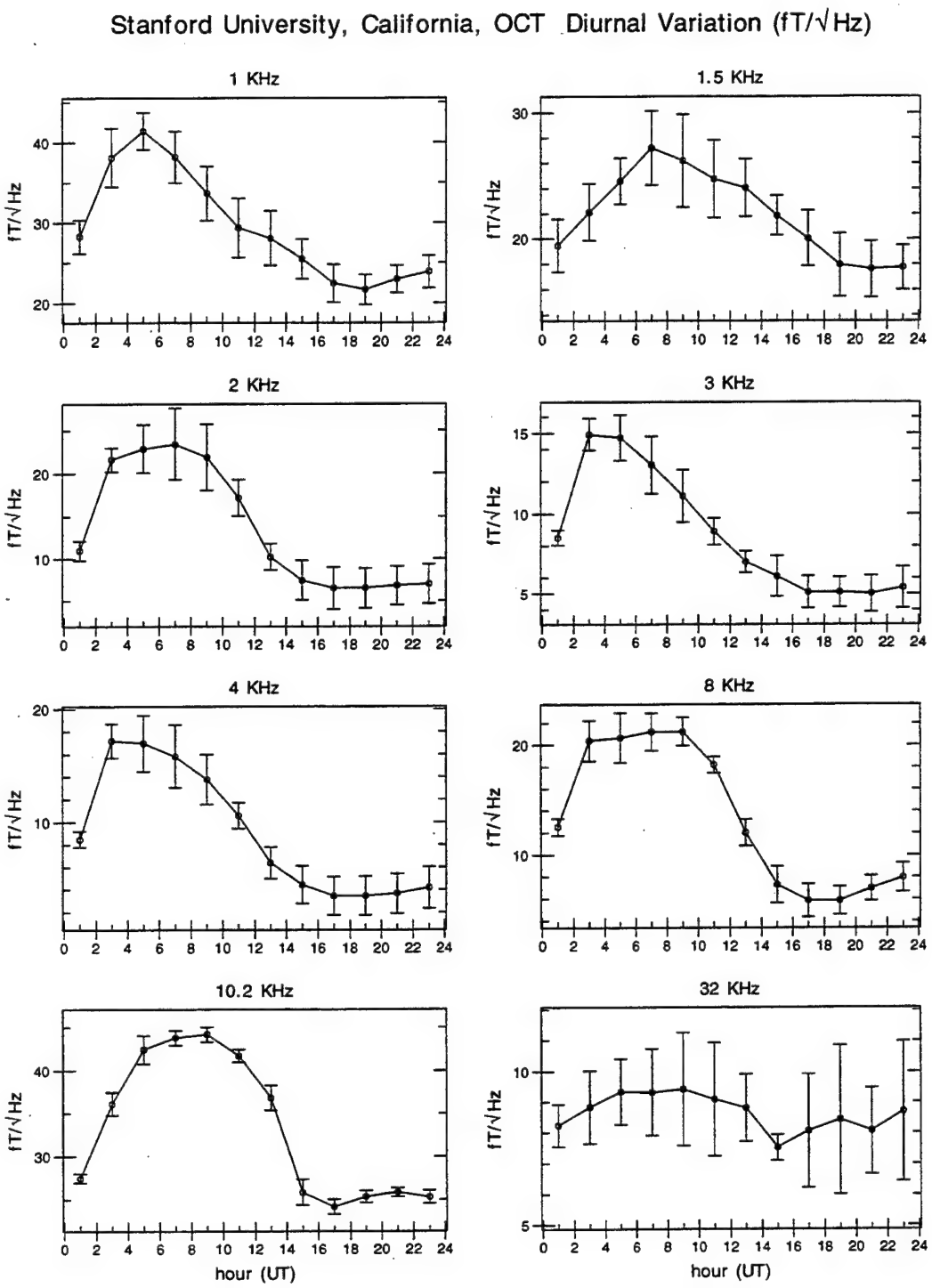

Figure 93: Diurnal variation of ELF/VLF radio noise at Stanford, California, during the month of October for the eight highest-frequency channels. The years 1986 to 1993 are included.

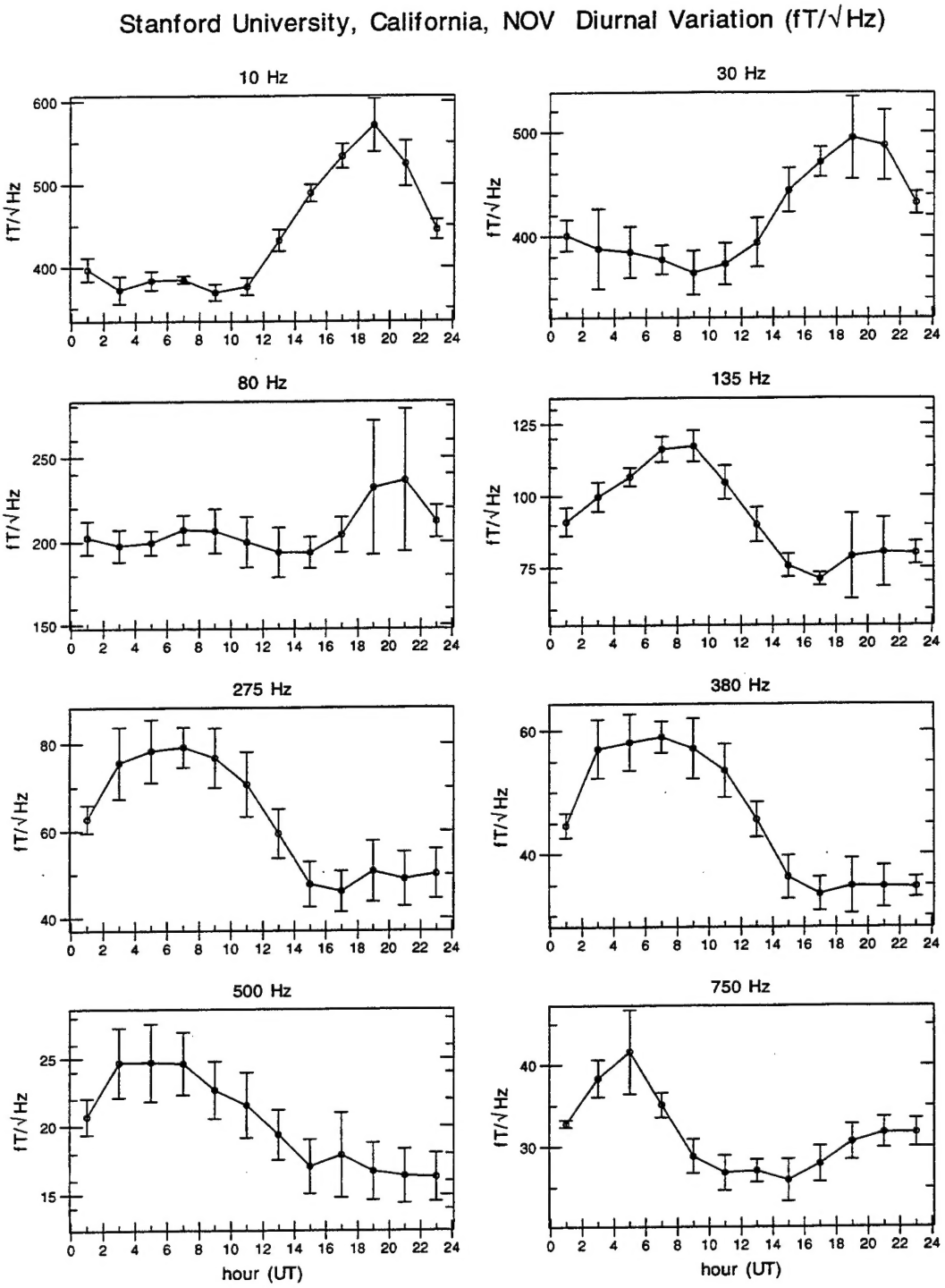

Figure 94: Diurnal variation of ELF/VLF radio noise at Stanford, California, during the month of November for the eight lowest-frequency channels. The years 1986 to 1993 are included.

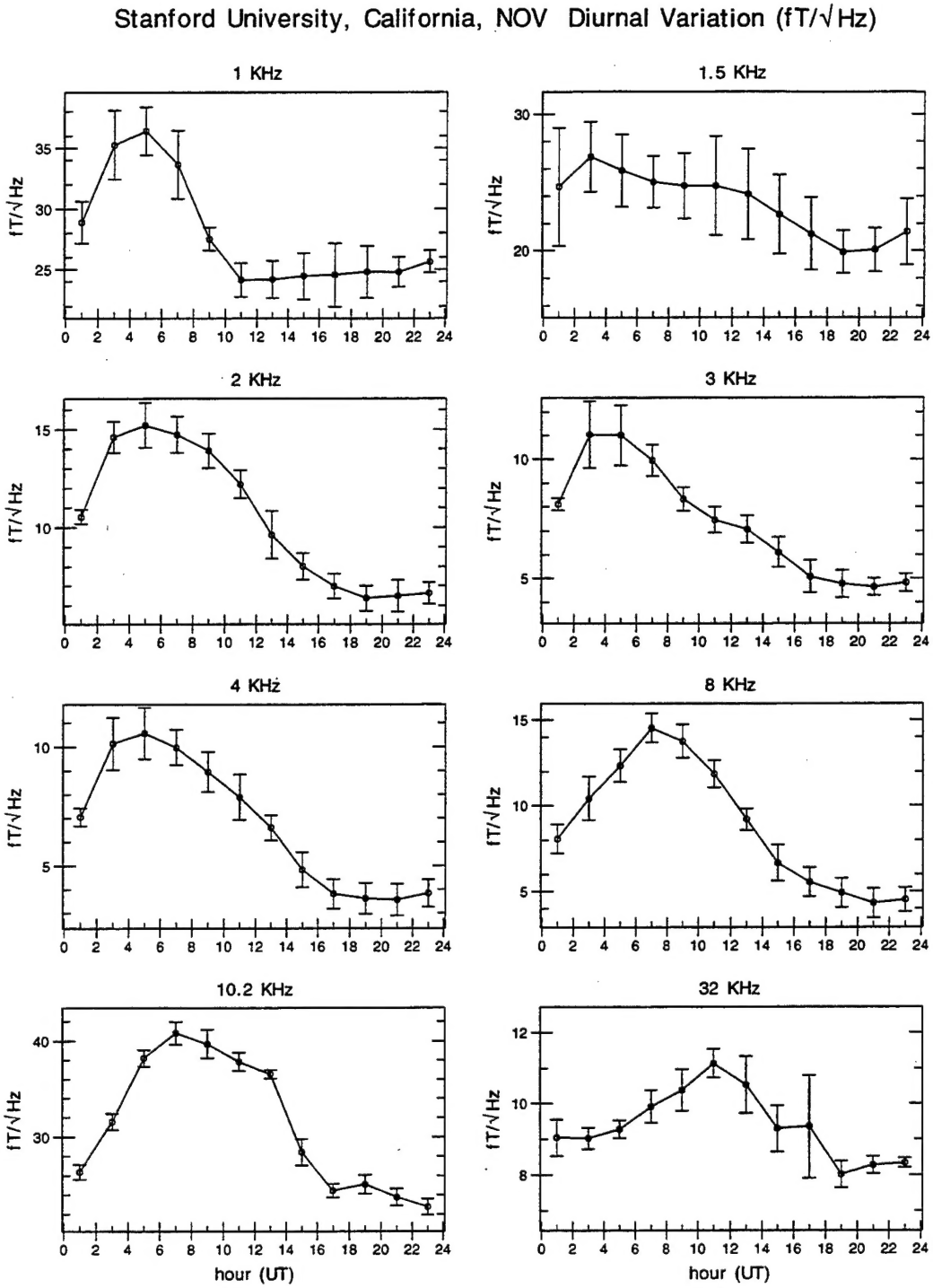

Figure 95: Diurnal variation of ELF/VLF radio noise at Stanford, California, during the month of November for the eight highest-frequency channels. The years 1986 to 1993 are included.

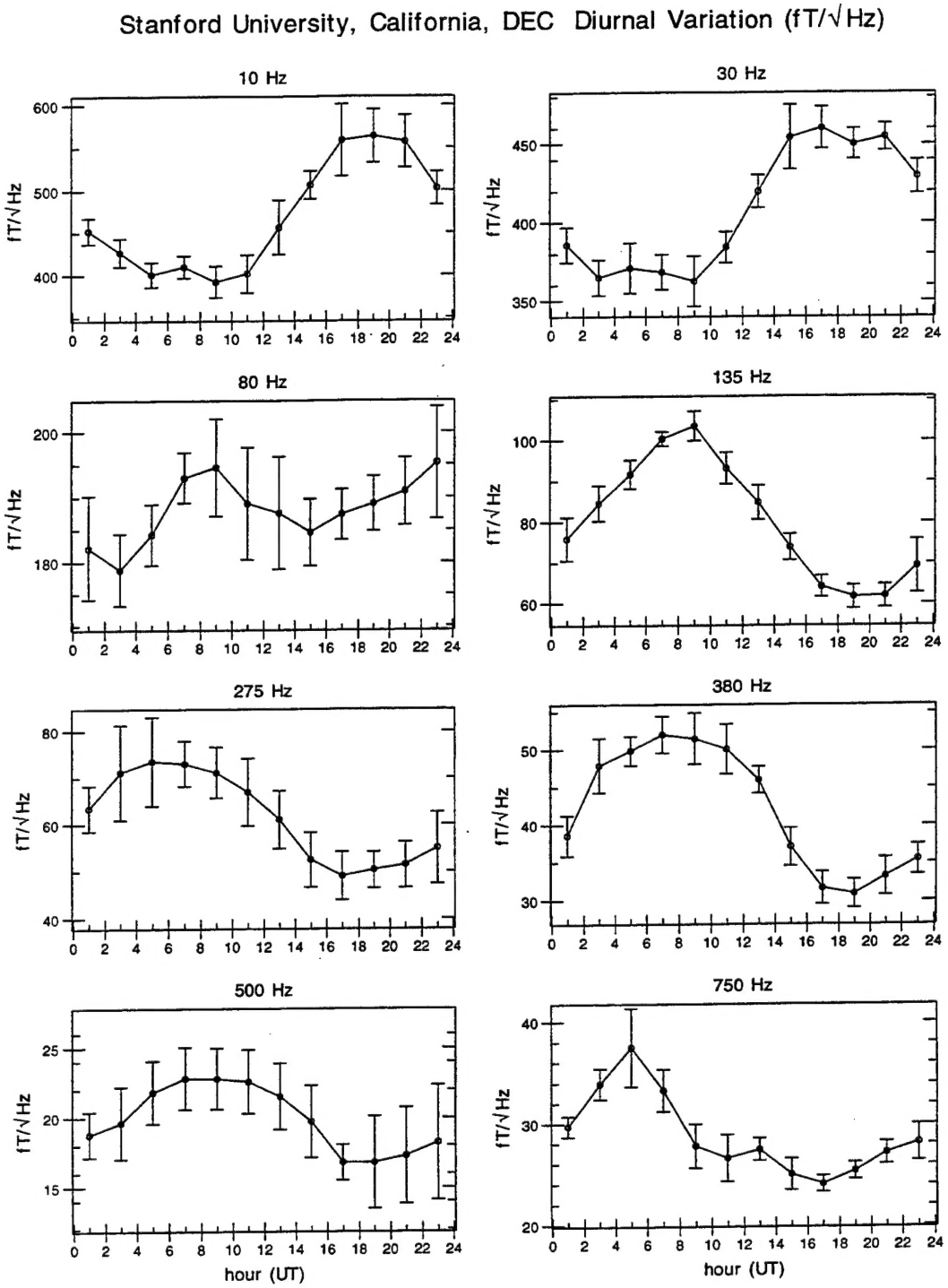

Figure 96: Diurnal variation of ELF/VLF radio noise at Stanford, California, during the month of December for the eight lowest-frequency channels. The years 1986 to 1993 are included.

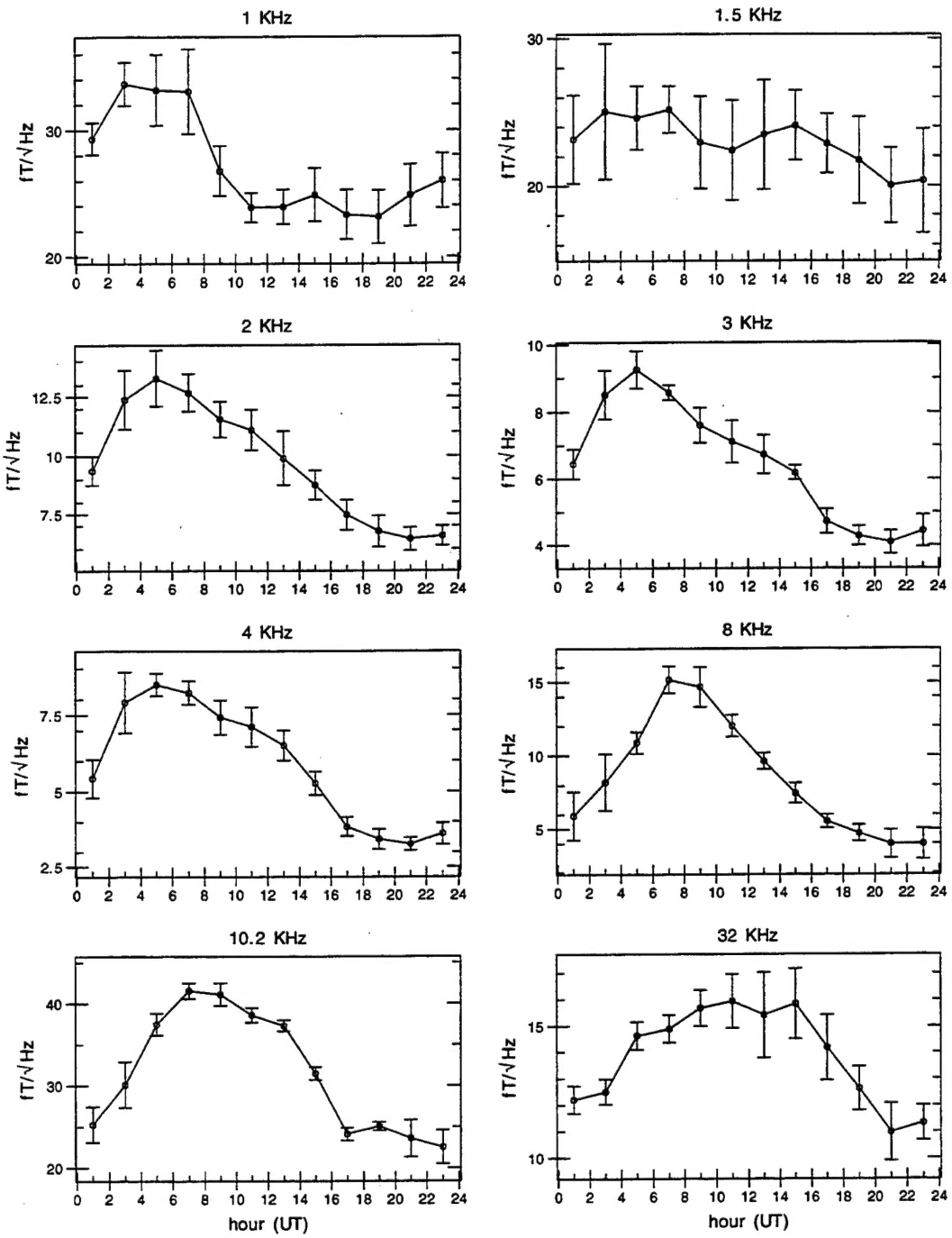

Figure 97: Diurnal variation of ELF/VLF radio noise at Stanford, California, during the month of December for the eight highest-frequency channels. The years 1986 to 1993 are included.